

# Engineered Carbon-Nanomaterial-Based Electrochemical Sensors for Biomolecules

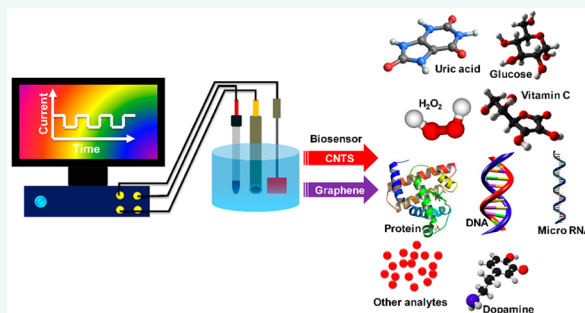
Jitendra N. Tiwari,\* Varun Vij, K. Christian Kemp, and Kwang S. Kim\*

Center for Superfunctional Materials, Department of Chemistry, Ulsan National Institute of Science and Technology (UNIST), Ulsan 689-798, Korea

**ABSTRACT:** The study of electrochemical behavior of bioactive molecules has become one of the most rapidly developing scientific fields. Biotechnology and biomedical engineering fields have a vested interest in constructing more precise and accurate voltammetric/amperometric biosensors. One rapidly growing area of biosensor design involves incorporation of carbon-based nanomaterials in working electrodes, such as one-dimensional carbon nanotubes, two-dimensional graphene, and graphene oxide. In this review article, we give a brief overview describing the voltammetric techniques and how these techniques are applied in biosensing, as well as the details surrounding important biosensing concepts of sensitivity and limits of detection.

Building on these important concepts, we show how the sensitivity and limit of detection can be tuned by including carbon-based nanomaterials in the fabrication of biosensors. The sensing of biomolecules including glucose, dopamine, proteins, enzymes, uric acid, DNA, RNA, and  $H_2O_2$  traditionally employs enzymes in detection; however, these enzymes denature easily, and as such, enzymeless methods are highly desired. Here we draw an important distinction between enzymeless and enzyme-containing carbon-nanomaterial-based biosensors. The review ends with an outlook of future concepts that can be employed in biosensor fabrication, as well as limitations of already proposed materials and how such sensing can be enhanced. As such, this review can act as a roadmap to guide researchers toward concepts that can be employed in the design of next generation biosensors, while also highlighting the current advancements in the field.

**KEYWORDS:** carbon nanotubes, graphene, glucose, dopamine, proteins, uric acid, DNA, RNA,  $H_2O_2$ , biosensors



The use of femto-, pico-, and nanosensitive biosensors is of critical importance not only in obvious medical applications,<sup>1</sup> such as glucose monitoring in diabetics,<sup>2</sup> but also in environmental monitoring, water remediation, molecular imaging, and noxious gas sensing, among other applications.<sup>3–6</sup> In fact, this field is so important that there are multiple dedicated journals focused on either biosensors and/or sensors, with multiple reviews published on a wide range of highly specific sensor-related topics.<sup>4–8</sup> Additionally, the amount of papers published with sensor in the title has increased dramatically from 1131 articles in 1989 to 13461 in 2014 (Figure 1A). In the same way, the amount of papers published with biosensor in the title has also increased exponentially (Figure 1B). What is interesting to note in these graphs is that with the isolation of carbon nanotubes (CNTs) in 1991 and the isolation of graphene in 2004 there has been a rapid rise in the amount of articles published.<sup>9–12</sup> Figure 1C is a graph indicating the rise in the number of publications that contain the title words: sensor, graphene, biosensor, and carbon nanotube. These statistical results are indicative of the importance and application of these carbon nanomaterials in sensors and biosensors.

To date, reviews focused on the electrochemical properties of carbon nanomaterials<sup>9,10</sup> or a single carbon nanomaterial acting as sensors have appeared in the literature.<sup>11,12</sup> However, there are no definitive reviews that focus on the application of the various carbon nanomaterials in the important fields of biosensing and single-molecule biosensing. It is for this and other reasons that this review focuses on the experimental and theoretical use of carbon nanomaterials in biosensors.<sup>13,14</sup> Thus, the main objective of this review is to present a comprehensive overview of the fundamental principles for carbon-based material voltammetric biosensor design, fabrication, and operation mechanisms, as well as to provide insight into their rapidly growing future potential in the fields of biomedical and biological engineering. We also summarize and discuss the most recent developments in voltammetric biosensing, while addressing key challenges and opportunities for next generation biosensing.

The carbon-based electrode was introduced by Adams in 1958.<sup>15</sup> Besides renewability by simple polishing of the working

**Received:** September 9, 2015

**Accepted:** November 18, 2015

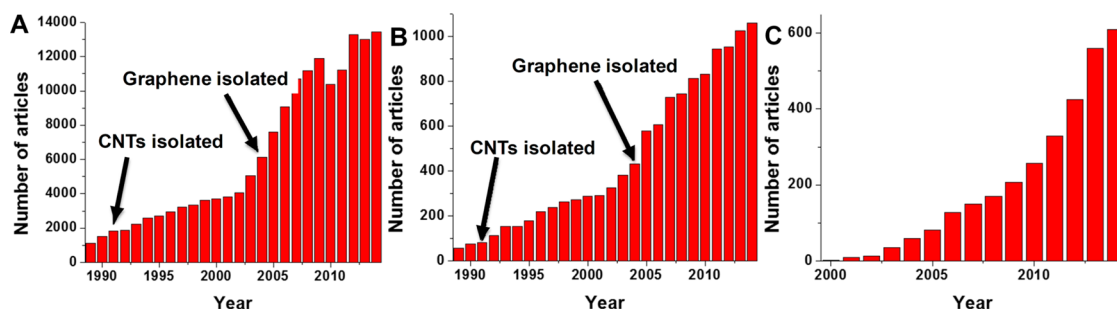


**Figure 1.** Number of articles over the time period of 1989 to 2014 with the keyword sensor in the title (A) and biosensor in the title (B), and number of articles, over the time period of 2000 to 2014, with the keywords sensor or biosensor in combination with graphene or carbon nanotube in the title (C). All statistics were obtained using Thomson Reuters Web of Science.

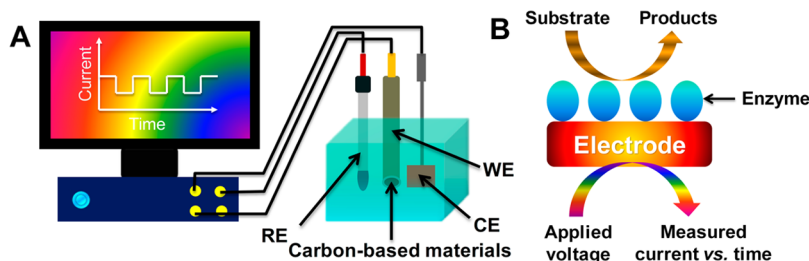


**Figure 2.** (A) Schematic of a typical carbon nanomaterial voltammetric biosensor made up of a reference electrode (RE), carbon-based working electrode (WE), and counter electrode (CE). (B) Basic principle of a voltammetric biosensor.

electrode, the use of carbon or carbon-based materials offers many advantages including easy preparation, uniform distribution of the catalyst, reproducibility, stability, low ohmic resistance, and robustness in aqueous solutions. In the beginning, progress in the development of ordinary carbon-based voltammetric biosensors was limited with respect to detection limits. Basically, these biosensors suffered from a lack of surface architectures, allowing high sensitivity with the desired biochemical/physiological events that characterize the detection of biomolecules responses. As such, there has been a call for more research on the use of graphene and CNTs to reduce the dimensions of voltammetric biosensors elements to sizes which can increase the signal-to-noise ratio for the processes occurring at the interface of the device, as well as methods which utilize multiple enzymatic labels to enhance the signal per event. The use of one-dimensional (1D) and two-dimensional (2D) carbon-based nanomaterials integrated with nanoparticles (NPs), ionic liquids, polymers, enzymes, and DNA offers multiple routes toward constructing voltammetric biosensors which utilize diverse sensing methods.

One-dimensional CNTs (single-walled carbon nanotubes (SWCNTs) and multiwalled carbon nanotubes (MWCNTs)) and 2D graphene (graphene nanoribbon (GNR), graphene oxide (GO), and reduced graphene oxide (rGO)) possess unique mechanical, electrical, and optical properties that present multiple new avenues for utilization in biosensors.<sup>9–12,14–22</sup> The use of graphene/CNTs has been vastly extended by tuning the physicochemical properties through modification of their surface. Although other carbon nanomaterials such as the zero-dimensional fullerenes and carbon quantum dots have been applied as biosensors,<sup>23–25</sup> they are not as widely applied as the 1D and 2D carbon nanomaterials in voltammetric biosensing applications. For this reason, this review will deal specifically with the application of 1D and 2D carbon nanomaterials in voltammetric biosensors.

The 2D graphene (a flat monolayer of  $sp^2$ -bonded carbon atoms tightly packed into a honeycomb lattice, with a thickness of 0.34 nm) has attracted enormous attention due to its mechanical strength, tunable optical properties, surface area (theoretical surface area  $\sim 2630$  m<sup>2</sup>/g), and electrical conductivity.<sup>26–34</sup> Graphene is produced by either top-down (e.g., chemical/mechanical exfoliation of graphite) or bottom-up (e.g., chemical vapor deposition) methods.<sup>33,34</sup> The family of 2D graphene-related materials include structural or chemical derivatives of graphene such as pristine graphene, few-layered graphene (flake-like stacks of less than 10 graphene layers), GNRs, GO (highly oxygenated form of graphene synthesized by harsh oxidation of graphite), and rGO (the product of thermal/chemical GO reduction).<sup>35–42</sup> Depending on the reduction method employed to produce rGO, the functional groups and conductivity of the material can vary dramatically.<sup>35,38,41–43</sup> For this reason, rGO and GO are ideal graphene analogues to be employed in biosensor fabrication as they afford multiple sites for easy surface modification with tunable conductivity.<sup>44–46</sup>

The 1D CNTs can be considered as either a rolled-up GNR sheet (SWNT with a diameter of 0.4–2 nm) or multiple rolled-up GNR sheets (MWCNT with a diameter of 2–100 nm).<sup>47–49</sup> As with graphene, CNTs can be chemically modified, and these modifications have a direct impact on the physicochemical properties of the CNTs such as conductance, mechanical strength, optical properties, *etc.*<sup>50,51</sup> These changes in the CNTs' intrinsic properties can lead to enhanced catalytic or electrical properties in materials which contain these carbon nanomaterials.<sup>52–54</sup>

Since the development of the first O<sub>2</sub> biosensor, biosensors have been employed in a wide range of applications such as analyses of food, beverages, environments, and agriculture, as well as clinical applications.<sup>55–60</sup> In essence, a voltammetric biosensor is an analytical device which converts a biological response into a current signal which is then measured. **Figure**

2A shows the components of a typical voltammetric biosensor, which consists of a working electrode (*e.g.*, platinum, gold, or several forms of carbon, including carbon fiber, epoxy graphite, graphene, glassy carbon, commercial screen-printed electrode, *etc.*), counter electrode, and reference electrode. What makes voltammetric methods ideal for biosensing is that they offer high sensitivity, convenience, good selectivity, simple designs, low costs, and fast analysis.

In this review, the working principles of voltammetric biosensors will be elaborated on in the section “**Voltammetric Biosensors**”. Additionally, the detection limits of electroactive carbon-based materials will be reviewed. “**Overview of Carbon-Based Voltammetric Biosensors**” details the various biosensing techniques that rely on the use of a graphene- or CNT-based material working electrodes. This section is subdivided into subsections dealing with the type of analytes being sensed, that is, hydrogen peroxide, DNA, single molecules, *etc.* Finally, “**Outlook: Future Prospects, Problems, and Challenges**” highlights the outlook, potential future applications, and challenges of carbon-based nanomaterials for detecting biomolecules using the voltammetric method.

## VOLTAMMETRIC BIOSENSORS

**Principles.** Voltammetric biosensors are based on electroanalytical chemistry techniques in which quantitative analyte sensing is made by varying the potential and measuring the resulting current as an analyte reacts electrochemically with the working electrodes surface (see Figure 2B). There are multiple techniques whereby the potential can be varied in a voltammetric sensing technique, such as linear sweep, differential staircase, normal pulse, reverse pulse, and differential pulse. The most commonly applied technique for determination of redox potential and electrochemical reaction rates of analyte solutions is linear sweep cyclic voltammetry (CV).<sup>61</sup> The general shape of a CV is determined by a number of factors such as analyte reduction potential, sweep rate, electrolyte, analyte isomerization, electrode surface, stability of reduced/oxidized analyte, electrochemical reversibility of the analyte, *etc.* The advantages of the CV approach are (i) high sensitivities and low detection limits, (ii) quantitative analysis of processes, and (iii) fast and clear characterization of the processes that take place on the surface of the sensing electrode.<sup>61</sup>

**Sensitivity and Limit of Detection.** In analytical electrochemistry, a calibration curve is used to determine the sensitivity and limit of detection (LOD) of a sensor. While an extremely high sensitivity may seem advantageous, in application, the LOD is of far greater importance toward reproducibility. To calculate the LOD and sensitivity, calibration curves are constructed by plotting measured current (*I*) versus concentration (*C*) of the analyte. Importantly, only the linear portions of these graphs are used to calculate sensitivity and LOD.<sup>12,19,62,63</sup> The sensitivity (*S*) of a sensor is defined as the gradient of the linear portion of the calibration curve, as shown in eq 1.

$$S = \Delta I / \Delta C \quad (1)$$

The LOD is defined as the lowest concentration of analyte that can be reproducibly determined, with a specified level of confidence, in a sample compared to a blank measurement. The LOD can be calculated using eq 2.

$$\text{LOD} = k \times \sigma / S \quad (2)$$

where  $\sigma$  is the standard deviation of the blank measurements (*i.e.*, noise level), *S* is the sensitivity calculated using eq 1, and *k* is the confidence level parameter (*k* = 1, 2, and 3 correspond to a statistical confidence of 68.2, 95.4, and 99.6%, respectively). The confidence level parameter is set as *k* = 3 in the determination of the LOD and is reported as such in this review.<sup>63,64</sup> Alternatively, the confidence level parameter is set as *k* = 10 in the determination of the level of quantification (LOQ).

**Tuning the Sensitivity and Limit of Detection in Carbon-Based Biosensors.** If the current in the working electrode of the sensor can be tuned in a way that less noise is observed (*i.e.*, smaller  $\sigma$ ), then the LOD can be increased. In the same way, the sensitivity of a biosensor can be increased if a larger response is measured when the analyte interacts with the working electrode. Carbon nanomaterials with their large surface areas and high conductivity can be both advantageous and disadvantageous in tuning the LOD and sensitivity in biosensors.

In general, a larger electrode surface area affords an increased total current response for an analyte in solution due to more reactive sites, which is beneficial for sensing small analyte concentrations. However, this increased current response is offset by an increase in the background current which limits the sensitivity and in turn raises the LOD.<sup>9,12,26,65</sup> This effect is noted to a large degree in pure carbon nanomaterial sensors, which require active (nonreduced carbon or oxygenated) sites for sensing. As such, extensive reduction of the carbon surface leads to an increased background current. This problem can be magnified by active carbon sites being reduced electrochemically during the sensing process. For this reason, it is usually necessary to modify the carbon surface, that is, functionalization of the carbon surface and/or attachments of metal NPs, biomolecules, *etc.*, so that reproducible trace detection can be attained.

By these modifications of the carbon electrode surface, one is able to improve the sensitivity and LOD by improving electron transfer between analyte and electrode. For example, when we attach an enzyme directly to the carbon-based sensor, we are able to enhance direct electron transfer between enzyme and electrode without use of a chemical mediator which would be necessary under normal circumstances. It should be noted that an additional benefit of modifying the carbon electrode with biomolecules is that a highly selective signal is produced, provided that their three-dimensional shape is not distorted on attachment.

Another method which can be employed to enhance the sensitivity and LOD in biosensors is to use layer-by-layer self-assembly. Layer-by-layer self-assembly is an uncomplicated and inexpensive method for assembling ultrathin films of organic and inorganic compounds. The benefit of this technique is that it is very easy to control the thickness of the thin film layer. Additionally, research shows that the layer-by-layer method provides not only a direct electron transfer between redox sites and the working electrode but also a satisfactory microenvironment for enzymes.<sup>66,67</sup> For these reasons, layer-by-layer self-assembly techniques have been used for the design and construction of enzyme-containing, as well as enzymeless, biosensors.<sup>68,69</sup>

**Table 1. Recent High-Performance Reports Utilizing CNT-Based Biosensors for the Detection of Various Enzymatic or Nonenzymatic Biomolecules**

modified electrode	sample name	linear range	detection limit	refs
wheat germ agglutinin/SWNTs/SPCE	fetoprotein	1–100 pg mL <sup>-1</sup>	0.1 pg mL <sup>-1</sup>	71
[Fe(CN) <sub>6</sub> (poly(4-vinylpyridine)) <sub>10</sub> ]/MWCNT	L-cystein	20.5–151 nM	6.15 nM	72
oleylamine/NiO/SWCNT	riboflavin	0.009–55.9 μM	1 nM	73
VACNT	C-reactive protein		90 pM	74
conducting polymer/CNT	miRNA	1–10 pM	8 fM	75
AuNP/Ag/molecular beacon	DNA	0.1 fM to 1 pM	0.03 fM	76
CNT–multielectrode array	dopamine	1 nM to 10 mM	1 nM	77
Cu(II)/AgNP/GCE	dopamine	2.81–8.3 μM	0.82 nM	78
Ni/Cu/MWCNT	glucose	25 nM to 800 μM	25 nM	79
L-lysine/MWCNT	H <sub>2</sub> O <sub>2</sub>	1 μM to 3.6 mM	8 nM	80
SnO <sub>2</sub> QD/rGO	urea	16 fM to 3.9 pM	11.7 fM	81
Au/ssDNA/SWCNT	levofloxacin	1.0–10.0 μM	75 nM	82
p-aminophenol/CNT	vitamin C	0.2–12 μM	80 nM	83
Ag nanofilm/MWCNT	zidovudine HIV drug	0.37 μM to 1.5 mM	0.15 μM	84
DNA-modified electrodes	amitrole	0.025–2.4 ng mL <sup>-1</sup>	0.017 ng mL <sup>-1</sup>	85
MWCNT/thionine–chitosan	chlorpyrifos	0.1–1.0 × 10 <sup>5</sup> ng mL <sup>-1</sup>	0.046 ng/mL	86
polylysine/SWCNT	bisphenol A	4.00 nM to 11.5 μM	0.97 nM	87
polyethyleneamine/CNT	cardiac Troponin T	0.1–10 ng mL <sup>-1</sup>	33 pg mL <sup>-1</sup>	88
Pt/Fe/carbon dot	carcinoembryonic antigen	0.003–600 ng mL <sup>-1</sup>	0.8 pg mL <sup>-1</sup>	89
poly(L-Arg)/MWCNTs/GCE	casein	0.1–10 μg mL <sup>-1</sup>	50 nM	90
VACNT/GO	atorvastatin calcium	90 nm to 3.81 μM	9.4 nM	91
poly(pyrrolepropionic acid)/MWCNT	prolactin	10 <sup>-2</sup> –10 <sup>4</sup> ng mL <sup>-1</sup>	3 pg mL <sup>-1</sup>	92
SWCNT	thrombin	10 nM to 100 mM	10 nM	93
AgNP/MWCNT	zolmitriptan	10–800 nM	1.49 nM	94

**Table 2. Recent High-Performance Reports Utilizing Graphene-Based Biosensors for the Detection of Various Enzymatic or Nonenzymatic Biomolecules**

modified electrode	sample name	linear range	detection limit	refs
CuO NP–graphene	glucose	0.5–2000 μM	0.09 μM	95
3D graphene	dopamine	0.1–200 μM	19.4 nM	96
graphene–Orange II	thrombin	1.0–400 pM	0.35 pm	97
graphene–Orange II	lysozyme	5.0–700 pM	1.0 pm	97
graphene–Au	cysteine	0.1–24 μM	20.5 nM	98
Au-polydopamine–thionine–GO	fetoprotein	0.1–150 ng mL <sup>-1</sup>	30 pg mL <sup>-1</sup>	99
graphene	ovalbumin	1 pg mL <sup>-1</sup> to 0.5 μg mL <sup>-1</sup>	0.83 pg mL <sup>-1</sup>	100
pErGO	uric acid	0.1–10 μM	50 nM	101
cobalt oxide/rGO	hydrogen peroxide	5 μM to 1 mM	0.2 μM	102
Au/GO	DNA	1.0 fM to 0.1 μM	0.35 fM	103
Gr/CuPc/PANI	vitamin C	0.5–12 μM	63 nM	104
carbon/Co <sup>2+</sup> -Y	vitamin B <sub>2</sub>	1.7–34 μM	0.71 μM	105
carbon/ZrO <sub>2</sub> /ionic liquids	vitamin B <sub>6</sub>	0.8–550 μM	0.1 μM	106
graphene–hydroxyapatite	luteolin	0.02–10 μM	10 nM	107
TrGO	baicalein	10 nM to 10 μM	6.0 nM	108
rGO–tetraethylene pentamine	carcinoembryonic antigen	0.05–20 ng mL <sup>-1</sup>	13 pg mL <sup>-1</sup>	109
rGO–tetraethylene pentamine	squamous cell carcinoma antigen	0.03–20 ng mL <sup>-1</sup>	10 pg mL <sup>-1</sup>	109

## OVERVIEW OF CARBON-BASED VOLTAMMETRIC BIOSENSORS

One of the primary advantages of using carbon-based electrodes is that they usually are easily renewable when fouled by analyte solutions by simple polishing. Besides renewability, the use of carbon or carbon-based materials offers many advantages including easy preparation, uniform distribution of the catalyst into the paste, reproducibility, stability, and low ohmic resistance. It should also be mentioned here that screen-printed carbon electrodes (SPCE) offer a number advantages over rod tube electrodes (*i.e.*, glassy carbon electrode (GCE)), as they are suitable for working with microscale amounts and

for decentralized assaying. This allows the development of mass-produced portable, accurate, and reproducible sensors.<sup>70</sup>

CNTs have been widely used as an ideal material to fabricate linear sweep voltammetric biosensors, due to their free-standing structure, low background noise, high tensile strength, low cost, wide potential window, high stability, and impressive electrical conductivity. Interestingly, the electrical conductivity of CNTs facilitates rapid electron transfer, but this is not sufficient to explain the major effect that occurs when CNTs are incorporated in biosensors.

The enhanced effect of CNT inclusion in modified voltammetric biosensors (*e.g.*, enzyme-based biosensors,



immunosensors, and nucleic acid biosensors) is believed to be due to the strong  $\pi$ - $\pi$  interactions between CNT and the immobilized host. This immobilization has the added benefit of inhibiting CNT aggregation in solution, which is a common problem encountered when working with CNTs. Additionally, noncovalent modification does not disturb the electronic structure of CNTs, and as such, the CNT maintains its electrical conductivity. These two factors mentioned above contribute to the low detection limits that are found when utilizing CNT-based biosensors. Lastly, CNT hybrid materials (*i.e.*, CNTs combined with conducting polymers, redox mediators, or metal NPs) have been receiving increased attention in biosensors. This is due to the various synergistic effects observed when these hybrid materials, such as the enzymeless biosensors which afford greater durability and are less expensive, are used.

Another very common carbon material recently utilized in biosensors is graphene in its various forms (*i.e.*, rGO, GO, CVD graphene, *etc.*). As for CNTs, pristine graphene can be noncovalently functionalized through strong  $\pi$ - $\pi$  interactions between its surface and the immobilized host. Additionally, rGO offers additional covalent functionalization options due to multiple oxygenated functional groups. Although rGO is less conductive than pristine graphene, it maintains a large degree of conductivity, compared to the insulating GO, as large domains on its basal plane are reduced, thereby forming a  $\pi$ -electron-conjugated system similar to graphene. For these reasons, graphene and chemical derivatives of graphene are emerging as a preferred choice for the fabrication of various biosensors. Furthermore, various polymers, noble metals, metal oxides, spinels, and metal complexes have been used as effective modifiers in conjunction with graphene-based materials for sensing biomolecules. Tables 1 and 2 list recent results for CNT- and graphene-based enzymatic and nonenzymatic biosensors.

In the following sections, the CNT- and graphene-based applications for electrochemical biosensors are reviewed.

**Glucose Sensing.** Diabetes is a chronic condition which leads to elevated blood glucose levels, which if left untreated can lead to major health problems and/or death. For this reason, reliable and accurate glucose detection in blood is of critical importance. Additionally, glucose sensing is important in food and textile industries, as well as environmental monitoring.<sup>110,111</sup> Usually, glucose sensing relies on the use of glucose oxidase (GOx), which catalyzes glucose in the presence of O<sub>2</sub> to afford gluconic acid and H<sub>2</sub>O<sub>2</sub>.<sup>112,113</sup> The concentration of glucose is then determined by monitoring the number of electrons flowing through the enzyme, or the concentration of the as formed H<sub>2</sub>O<sub>2</sub> is determined quantitatively as an indicator of the amount of glucose present in the solution.

As enzymes such as GOx lose activity with changes in temperature or pH, there is a lot of research interest in the development of a cheap, sensitive, and interference-free sensors for nonenzymatic glucose detection.<sup>114–116</sup> In this vein, Mohamedi and colleagues showed that gold nanostructured layers deposited by pulsed laser onto CNTs could be used as a nonenzymatic electrochemical glucose biosensor, LOD 0.1 mM with a sensitivity of 25  $\mu\text{A cm}^{-2} \text{mM}^{-1}$ .<sup>115</sup> They showed it by adjusting the deposition vacuum level and the number of pulses that the electroactive surface area (max 6.55 cm<sup>2</sup> for 10000 laser pulses) and roughness factor could be effectively controlled. Additionally, they found that the as-formed gold nanostructures

contributed toward a lower onset potential for glucose oxidation.

It is evident from this study, among many others, that the CNTs afforded the sensors with unique electrochemical behavior by changing the morphology of the deposited NPs. This method of depositing metal particles as isolated NPs or nanostructures with different morphologies onto CNTs offers one of best strategies to develop efficient voltammetric biosensors. Similarly, graphene-based voltammetric biosensors have also been applied in glucose sensing as graphene materials provide a large surface area and unique electrochemical behavior.<sup>117</sup>

**Glucose Oxidase–Carbon-Nanotube-Based Sensors.** Ramesh and colleagues have shown that the sensitivity and LOD of a glassy carbon electrode (GCE) toward glucose can be improved by modifying the GCE with SWNTs dispersed in a polymer matrix (polyethylenimine, polyethylene glycol, or polypyrrole) and then a layer of GOx.<sup>118</sup> These polymer layers are beneficial to the enzyme as they provide not only binding places but also stability. Importantly, the authors showed that the high purity and large surface area of the SWNTs was of critical importance to the response of the electrode. The use of high-purity SWNTs resulted in a high conductivity, enzyme stability, and fast electron transfer rate. The response time of the electrodes was shown to be less than 5 s with a LOD of 0.2633  $\mu\text{M}$ . You and co-workers have shown that N-doped carbon nanofibers (NCNF) prepared from electrospun polyacrylonitrile fibers have a large electrocatalytic activity toward the oxygen reduction reaction (ORR).<sup>119</sup> This activity is believed to be due to the presence of abundant defective sites and high pyrrolic-N content in the NCNF. These NCNF films coated with GOx and Nafion showed high sensitivity (LOD of 0.6 mM), stability, and selectivity toward glucose. Additionally, this GOx/NCNF/GCE electrode exhibited successful detection of glucose in the presence of commonly existing interfering species such as ascorbic acid (AA), uric acid (UA), and dopamine (1 mM). This work shows that the doping of SWNTs and other carbon nanomaterials with N can be beneficial in increasing the selectivity and sensitivity of glucose biosensors.

Layer-by-layer self-assembly methods have been applied in the fabrication of GOx-containing glucose biosensors, as these layers provide enzyme stability. Importantly, when these self-assembly layers contain either MWNTs or SWNTs, the current response and electrical conductivity between the electrode and the GOx is improved.<sup>66,120</sup> As such, this allows for an increased sensitivity and stability of the GOx. For example, Wang *et al.* showed that the glucose oxidation current of a gold electrode modified by layer-by-layer self-assembly of (poly-[(vinylpyridine)Os(bipyridyl)<sub>2</sub>Cl<sup>2+/3+</sup>]) and GOx SWNTs increases 17 times.<sup>120</sup>

In another study, Wu and colleagues showed that layered multilayers of poly(allylamine), *N*-hydroxysuccinimide-oxidized MWCNTs, cysteamine, gold NPs, and GOx on a platinum electrode could be employed as an amperometric biosensor.<sup>69</sup> The authors showed that the biosensor exhibited a large linear range for glucose detection (0.1–10 mM) and a LOD of 6.7  $\mu\text{M}$ . Additionally, the sensor displayed long-term stability (92% current response retention after 1 month) and was not influenced by the addition of AA, UA, and acetaminophen.

Porterfield *et al.* have shown that GOx and SWNTs can be assembled in a layer-by-layer method by first dispersing the SWNTs in single-stranded DNA (Figure 3A).<sup>121</sup> In this way,

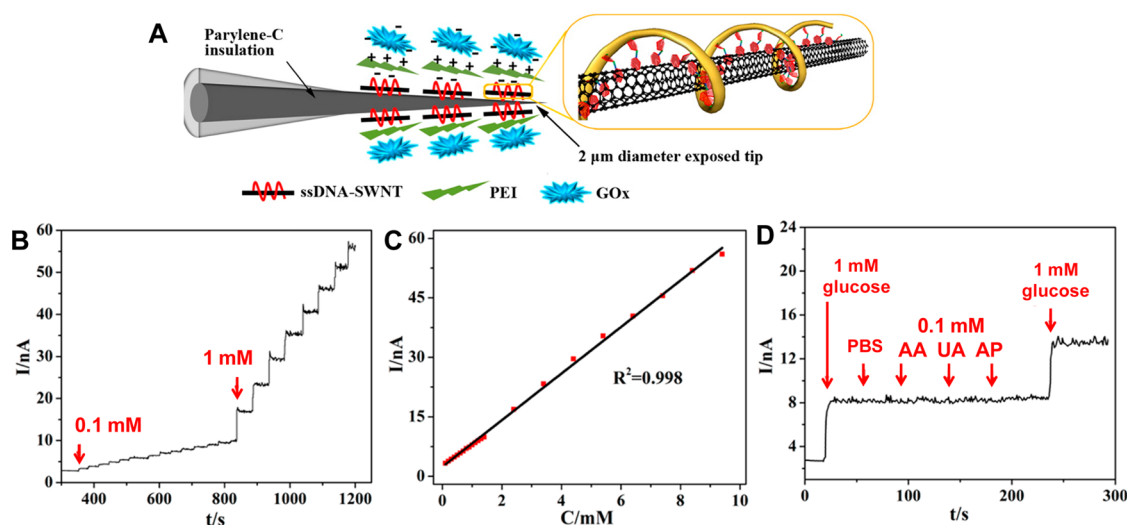


**Figure 3.** (A) Schematic diagram of layer-by-layer electrostatic self-assembly of single-stranded DNA (ssDNA)–SWNT, polyethylenimine (PEI), and GOx on a Pt/Ir electrode (inset: structural closeup of ssDNA–SWNT). (B) Amperometric response of the GOx/polyethylenimine/single-stranded DNA–SWNT/Pt biosensor at +500 mV (*vs* Ag/AgCl) upon successive addition of glucose solution to 20 mL of pH 7.0 PBS stirred at 350 rpm. (C) Calibration curve of amperometric response toward glucose concentration variation. (D) Amperometric responses to PBS, ascorbic acid (0.1 mM AA), uric acid (0.1 mM UA), acetaminophen (0.1 mM AP), and 1 mM glucose. Adapted from ref 121. Copyright 2014 American Chemical Society.

self-assembly can proceed by electrostatic interactions between the negatively charged DNA-coated SWNTs, which was then coated with a thin layer of cationic poly(ethylenimine) and finally negatively charged GOx. This material showed an impressive linear range up to  $\sim 9.4$  mM, with minimal deviation at low concentrations (Figure 3B–D). This biosensors stability and enhanced sensitivity is believed to be due to the electrostatic interactions between the positive and negative layers, as well as the large amount of GOx included in the sensor. Additionally, it can be seen in Figure 3B–D that this biosensor response was not affected by spiking with either phosphate-buffered saline solution (PBS), AA, UA, and acetaminophen.

Recently, Kwon *et al.* immobilized GOx on CNTs (GOx/CNT) to sense glucose, with the authors showing that a larger CNT content contributes to an improved amperometric response.<sup>122</sup> This modified sensor shows increased sensitivity ( $53.5 \mu\text{A mM}^{-1} \text{cm}^{-2}$ ), glucose activity (86% activity maintained after 2 weeks), and large electron transfer rate constant ( $1.14 \text{ s}^{-1}$ ). Interestingly, the Wei group has confirmed an earlier study that CNTs simultaneously modified with GOx and its cofactor, flavine adenine dinucleotide (FAD) show electron transfer kinetics similar to those observed in isolated FAD.<sup>123</sup> This implies that the FAD is directly wired to the CNT, and as such, electron transfer is unimpeded between the cofactor and support structure, allowing for increased sensitivity. Importantly, as the FAD is itself embedded in the GOx, this in turn allows rapid electron transfer.<sup>123</sup>

**Enzymeless Carbon-Nanotube-Based Sensors.** Enzymeless glucose biosensors which rely on NPs for the detection of glucose can similarly be enhanced through the introduction of CNTs.<sup>124–129</sup> For example, Lin and co-workers<sup>79</sup> have shown that the sequential electrodeposition of Ni and CuNPs on a MWCNT-modified GCE (Ni/Cu/MWCNT/GCE) can increase the amperometric response of the biosensor by 2.5–20 times compared to either Ni/GCE, Cu/GCE, Ni/MWCNT/GCE, or Cu/MWCNT/GCE. This sensor exhibits two linear response ranges both in the low (25 nM to 0.8 mM) and high

(2–8 mM) concentration regions, with an impressive LOD of 25 nM. Importantly, when this sensor was applied to glucose detection in human blood serum, it exhibited a recovery rate of  $\geq 95\%$ . This result indicates that the sensor is able to avoid interference from other molecules and could be applied in practical applications.

Choi *et al.* synthesized a CNT–Ni hybrid using atomic layer and chemical vapor deposition of Ni on oxygen- or bromine-functionalized CNT surfaces.<sup>130</sup> The as-fabricated sensor exhibited a wide linear response window ( $5 \mu\text{M}$  to 2 mM), short response time (3 s), small LOD (2  $\mu\text{M}$ ), high sensitivity ( $1384.1 \mu\text{A mM}^{-1} \text{cm}^{-2}$ ), good selectivity, and reproducibility in alkaline media. Alizadeha *et al.*<sup>131</sup> reported the fabrication of a highly sensitive enzyme-free amperometric glucose sensor by codeposition of copper oxide NPs/multiwalled CNTs onto the surface of a GCE. At the optimized potential, the LOD, linear range, and sensitivity of the sensor were calculated as 0.07 ( $\pm 0.03$ )  $\mu\text{mol L}^{-1}$ , 0.5–2000.0  $\mu\text{mol L}^{-1}$ , and  $3968.42 (\pm 0.84) \mu\text{A L mmol}^{-1} \text{cm}^{-2}$ , respectively. The optimized sensor was used to detect glucose in blood samples, with results that are comparable to that of a commercial enzymatic sensor.

It has been reported that a MWCNT and GO hybrid material deposited on a GCE can be used as a scaffold to electrodeposit  $\text{Ni}(\text{OH})_2$  NPs which act as a glucose biosensor.<sup>132</sup> Before the deposition of the  $\text{Ni}(\text{OH})_2$  NPs, the GO is electrochemically reduced (ErGO). This electro-reduction leads to an increase in conductivity in the sensor, while the MWNTs act as conducting bridges to enhance electron transfer between independent ErGO sheets and the GCE. While this sensor exhibits a LOD of 2.7  $\mu\text{M}$ , it is important to note that it exhibits a selective response to glucose in the analysis of a human urine sample.

**Glucose Oxidase–Graphene-Based Sensors.** GOx covalently attached to either ErGO or GO deposited on a GCE has been demonstrated as a biosensor for the detection of glucose in PBS.<sup>133,134</sup> The advantage of using graphene-based materials such as GO is that GO has been shown to be biocompatible while providing carboxylic oxygen functionalities for the GOx

amino groups to covalently attach.<sup>134,135</sup> On the other hand, the use of rGO allows for an enhanced conductivity while still providing attachment sites for the GOx amino groups due to the partially reduced nature of GO.<sup>136,137</sup>

To improve the GOx biosensing ability, Teymourian *et al.* have shown that GOx can be immobilized on a rGO/Fe<sub>3</sub>O<sub>4</sub> magnetic NP-modified GCE.<sup>138</sup> The authors showed that this biosensor has a LOD of 0.05 mM, a linear sensing range of 0.5–12 mM, and a response time of ~6 s. Importantly, the authors demonstrated that the rGO/Fe<sub>3</sub>O<sub>4</sub>-modified GCE readily immobilizes biomolecules, such as human immunoglobulin E, making this a readily applicable biosensing material. The use of graphene/NP composite materials in glucose biosensors has been further demonstrated by Bai and Shiu, who showed that a rGO/AuNP-modified GCE can be further modified to detect glucose when a layer of chitosan/GOx is coated onto the rGO/Au surface.<sup>139</sup> The fabricated sensor exhibits an impressive LOD of 76 μM, with a retention of sensitivity for 0.1 mM of glucose after 36 days of >70% of the original sensitivity.

The carboxylic acid groups on the edges of GO and the amino groups of GOx can covalently link through peptide bonding. Utilizing this phenomenon, Hasan *et al.* showed that a borosilicate glass capillary coated with GO/GOx can be inserted into the intracellular environment of a single human cell to detect glucose. This sensor exhibited a linear electrochemical potential difference over a glucose concentration range of 10–1000 mM.<sup>140</sup> Chia *et al.* reported that an electrochemical glucose biosensor can be fabricated by immobilizing GOx on exfoliated pristine graphene through noncovalent π–π interactions. As for CNTs,<sup>123</sup> this interaction results in enhanced electron transfer kinetics between the FAD redox sites of GOx at the modified electrode surface.<sup>141</sup> As such, the modified nonfunctionalized pristine graphene-containing biosensor resulted in enhanced stability, reproducibility, and selectivity for glucose detection in comparison to unmodified electrodes. These examples show that covalent bonding is not essential for protein adhesion to electrode surfaces.

Chitosan (CS), a polysaccharide with plentiful amino groups, has a pK<sub>a</sub> value of approximately 6.3 and displays pH-dependent solubility. As such, CS provides a matrix for immobilization of enzymes and nanomaterials, which make CS a promising material to modify electrochemical sensors. Keeping this in mind, Fang *et al.* immobilized GOx onto a biocompatible CS–rGO–AuNP hybrid-modified Pt electrode.<sup>142</sup> The sensor showed electrochemical detection of glucose over a wide linear range of 15 μM to 2.13 mM, with a sensitivity of 102.4 μA mM<sup>-1</sup> cm<sup>-2</sup> and LOD of 1.7 μM. Similarly, Ye *et al.* reported that immobilized GOx on a CS/rGO/Au hybrid displays fast electron transfer at a working voltage of –0.45 V (*vs* Ag/AgCl).<sup>143</sup> The sensor gives a linear response to glucose in the 0.05 to 1.2 mM concentration range, with a sensitivity of 13.58 μA mM<sup>-1</sup> cm<sup>-2</sup> and a 0.52 μM LOD.

**Enzymeless Graphene-Based Sensors.** An enzymeless glucose biosensor based on Ni–Co nanostructures electrodeposited by dynamic potential scanning on a rGO-modified GCE has been prepared.<sup>144</sup> The sensor exhibited a LOD of 3.79 μM and a linear glucose detection range of 10 μM to 2.65 mM. With respect to selectivity, this sensor exhibited no noticeable amperometric change on the addition of simple cations and anions such as Fe<sup>3+</sup>, Fe<sup>2+</sup>, SO<sub>4</sub><sup>2-</sup>, BrO<sub>3</sub><sup>-</sup>, IO<sub>3</sub><sup>-</sup>, NO<sub>2</sub><sup>-</sup>, NO<sub>3</sub><sup>-</sup>, and Cl<sup>-</sup>. In contrast, the addition of biomolecules

such as fructose, D-galactose, and AA resulted in a slight amperometric response (<10%), while the addition of UA showed no interference. This amperometric response, while small, is an issue that needs to be addressed for successful application of these types of nanostructures in biosensors. In a similar manner, Szunerits *et al.* showed that electrodeposition of Ni(OH)<sub>2</sub> on a rGO-modified GCE can be used as a glucose biosensor.<sup>145</sup> The authors showed that this electrode exhibits negligible amperometric response on the addition of UA, AA, and dopamine, as well as a LOD of 15 μM. This result is similar to that obtained using the enzymeless Ni(OH)<sub>2</sub>/MWCNT biosensor,<sup>146</sup> which would indicate that Ni(OH)<sub>2</sub> is a material that warrants further investigation in the development of enzymeless glucose biosensors. The authors of this study also noted that the electrofabrication method leads to high reproducibility and stability of the biosensor compared to drop-casting methods. Utilizing a galvanic replacement fabrication method, Chen and co-workers were able to prepare a hollow Pt–Ni-rGO hybrid-functionalized GCE for glucose detection, which displayed enhanced selectivity (no response to AA, UA, 3,4-dihydroxyphenylacetic acid), sensitivity (LOD of ~2 μM), and stability (93% response after 1 month).<sup>146</sup> This material was also applied in the determination of glucose in human blood serum, with an accuracy that is comparable to that of commercially available sensors.

In multiple biosensors, the active sites are adhered to the working electrode through the use of a conductive polymeric binder, which is not active for glucose sensing. However, with the use of graphene-based materials, this can be avoided, as has been demonstrated by Alizadeh *et al.*, who showed that a rGO/CuO NP-modified GCE electrode can be used as a glucose biosensor without adding Nafion as a binder.<sup>95</sup> This electrode showed good selectivity for glucose over other sugars as well as long-term stability (95% response after 30 days).

Tian *et al.* reported the microwave-assisted synthesis of CuO NPs on sulfur-doped graphene (SG) as an electrode material for nonenzymatic glucose detection with a LOD of 80 nM.<sup>147</sup> The improved GOx sensing performance of the CuO NPs deposited on SG compared to rGO is attributed to conductivity of SG, enhanced electron transfer between the Cu–S interaction, and increased surface area. Other biosensors based on graphene, functionalized with metal oxides like Mn<sub>3</sub>O<sub>4</sub> and Co<sub>3</sub>O<sub>4</sub>, have been employed in the sensitive and selective detection of glucose.<sup>148,149</sup>

Zhang *et al.* have shown that the bimetal oxide CuNiO decorated on graphene sheets can be utilized in the highly stable and sensitive enzymeless sensing of glucose with a LOD of 16 μM.<sup>150</sup> In another example of bimetal oxide-based catalysts, Dhara *et al.* used PdCuO deposited on rGO as a nonenzymatic glucose sensor with a LOD of 30 nM.<sup>151</sup> Although, metal NPs are research targets for enzymeless glucose sensing due to their high specific surface area, excellent conductivity, and catalytic activity, it should be noted that these particles are highly prone toward agglomeration, which results in a decrease in catalytic activity. Taking this fact into consideration, many groups have dispersed NPs over graphene to reduce the NP aggregation. This has allowed nonenzymatic glucose sensors to possess rapid response, good stability, selectivity, and low LODs.<sup>152–154</sup>

In most reported cases of enzymeless glucose biosensing mentioned above, a NaOH solution (pH 13) is required to catalyze the oxidation of the metal center which then catalyzes the reduction of the glucose to gluconolactone.<sup>95,144</sup> As such,

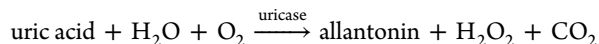


when human samples, such as blood or urine, are tested using these biosensors, the biological samples have been diluted in a NaOH solution.

**Dopamine, Uric Acid, and Ascorbic Acid Sensing.** The quantification of dopamine and its metabolic derivatives is important because of the role played by these substances in mammalian central nervous systems. For example, low concentrations and inactivity of dopamine functioning in the central nervous system may lead to Parkinson's disease, while on the other hand, an elevated dopamine level has been linked to schizophrenia.<sup>155</sup>

Various sensing methods, mainly based on the chemical modification of working electrode materials, have been developed for detection of dopamine. In this regard, CNTs and graphene nanosheets have been widely used to modify the working electrode surfaces for the analysis of dopamine. The use of these carbon materials is highly desired, as they provide enhanced electrical conductivity, large specific surface area, and chemical stability.

UA (2,6,8-trihydroxypurine) is the end product of purine (an essential component of DNA and RNA) metabolism in humans. An abnormally high UA level has been associated with multiple diseases such as gout, hyperuricemia, leukemia, pneumonia, Lesch-Nyhan syndrome, *etc.*<sup>156</sup> For this reason, monitoring the levels of UA is of great importance. Generally, UA biosensors are based on the oxidation of UA by uricase in the presence of O<sub>2</sub> to produce H<sub>2</sub>O<sub>2</sub>, allantoin, and CO<sub>2</sub>.<sup>157</sup> This chemical reaction can be expressed as



According to Noroozifar, the two most promising UA detection techniques, that is, oxidation of UA using phosphotungstate or uricase, have the disadvantage of long reaction times, large LODs, and high operational cost.<sup>158</sup> Therefore, it is clinically important to develop sensitive and effective sensing techniques for analysis of UA. UA is a voltammetrically active chemical, and as such, voltammetric biosensors based on uricase enzyme-modified electrodes are an extremely attractive means of detecting UA.<sup>159</sup> Additionally, the use of enzymeless electrodes, such as NP-modified electrodes, for the detection of UA is highly desired, as these methods hold many advantages, such as simplicity, ease of miniaturization, high selectivity, and low cost.

Considerable attention has been devoted in recent years to the voltammetric determination of UA by CNT and graphene-modified electrodes.<sup>158–163</sup> In comparison to CNT-modified electrodes, graphene, GO, and rGO have been much more successfully explored as biosensors. This is believed to be due to graphene's 2D  $\pi$ -conjugated structure, which makes its electronic structure very sensitive to the local chemical environment.

**Carbon Nanotubes.** Ardakani *et al.* have shown that a CNT/graphite paste electrode modified with [1,1'-binaphthalene]-4,4'-diol can be employed in the sensitive and simultaneous detection of dopamine, folic acid (FA), and UA.<sup>164</sup> The addition of the [1,1'-binaphthalene]-4,4'-diol into the paste electrode increases the sensitivity of the electrode and allows for LODs of 0.49, 4.28, and 7.69 mM for dopamine, UA, and FA, respectively. The electrode exhibited negligible amperometric response toward 100 mM (Na<sup>+</sup>, Cl<sup>-</sup>, K<sup>+</sup>), 80 mM (Mg<sup>2+</sup>, Ca<sup>2+</sup>), and 6 mM (L-lysine, glucose, glutamic acid, glycine, L-cystine, L-cysteine, acetaminophen, nicotinamide adenine dinucleotide (NADH)) spiking into a 0.1 mM

dopamine solution. The precursor and metabolites of dopamine (*i.e.*, levodopa, epinephrine, and norepinephrine) interfered with the detection of dopamine, showing the general applicability of this sensor toward dopamine and its metabolites. In another study, this same group showed that in a similar way the CNT/graphite paste can be modified with the Schiff base, 2,2'-[1,4-phenylenediyl bis-(nitrilomethylidene)]bis(4-hydroxyphenol) to afford similar simultaneous and sensitive results for dopamine, FA, and UA.<sup>165</sup> Interestingly, this electrode could also be used to simultaneously determine dopamine and acetaminophen, which differs from the previous result and shows the applicability of modification with the Schiff base.

The selective detection of dopamine is challenging in biological samples, as its oxidation potential range is very close to those of the commonly interfering analytes AA and UA.<sup>166,167</sup> Utilizing a GCE modified with ferrocene (Fc)-filled double-walled CNTs (Fc@DWNTs), Li *et al.* have shown that dopamine sensing can be achieved.<sup>168</sup> In this study, the authors noted, however, that the sensitivity and the LOD (0.3  $\mu$ M) was not as high as that reported by other groups. However, by building on their previous study, this group has shown that a Fc-filled SWCNT (Fc@SWNTs)-modified GCE was far more responsive and sensitive (LOD, 0.1  $\mu$ M).<sup>169</sup> This is believed to be due to the mechanism of electro-oxidation and reduction, which is bidirectional (dopamine oxidation and reduction) for the Fc@SWNTs, while it is unidirectional (only dopamine oxidation) for the Fc@DWNTs. This difference in electroactivity is believed to be due to the dopamine not entering the DWNTs, while in contrast, it can enter the SWNTs, which is only one carbon layer thick and contains more defects.

The Vasantha group have reported on the sonochemical synthesis of a nickel tetrasulfonated phthalocyanine (NiTsPc)-functionalized multiwalled CNT hybrid, where the NiTsPc acts as a dispersing agent for the MWCNTs.<sup>170</sup> The authors showed that a GCE coated with this MWCNT–NiTsPc hybrid can be used for monitoring dopamine in the presence of UA and AA. This sensor displayed a linear response range from 20 nM to 1.384 mM with a LOD of 1 nM.

By electrodepositing NiO NPs on a CNT/dihexadecylphosphate film-modified GCE, Filho and colleagues have shown that it is possible to simultaneously determine dopamine and epinephrine.<sup>171</sup> The authors found this simultaneous detection to be possible due to the difference between the two analyte reduction peaks of  $\sim$ 360 mV, which is in contrast to what is normally found in the detection of dopamine and its metabolites.<sup>164</sup> The LOD for dopamine and epinephrine were determined to be 50 and 82 nM, respectively. It should also be noted that this biosensor was successfully applied in the detection of dopamine and epinephrine in cerebrospinal fluid, human blood serum, and lung fluid.

The Anandan *et al.* group reported on the simultaneous detection of dopamine and UA by modification of a GCE with a silicate (N-[3(trimethoxysilyl)propyl]ethylenediamine; EDAS) network which interlinks gold NPs (3–8 nm) and MWCNTs.<sup>172</sup> This sensor exhibited a wide linear response for AA and dopamine over the concentration range of  $1 \times 10^{-7}$  to  $9 \times 10^{-6}$  M and  $1 \times 10^{-7}$  to  $8 \times 10^{-6}$  M with LODs of 0.07 and 0.08  $\mu$ M, respectively. Tsierkezos *et al.* reported the simultaneous detection of dopamine, UA, and AA by modifying a GCE with boron-doped MWCNTs (B-MWCNTs). This sensor exhibited dopamine, UA, and AA detection at working



potentials of  $\sim 0.267$ ,  $\sim 0.412$ , and  $\sim 0.127$  V with LODs of 0.11, 0.65, and 1.21  $\mu\text{M}$ , respectively.<sup>173</sup>

A multielectrode array (MEA) dopamine sensing chip has been created by electroplating CNTs onto an indium–tin oxide MEA.<sup>77</sup> This sensor was used to sense dopamine (LOD, 1 nM) release from mouse striatal brain slices (coronal and sagittal slices), and these results corresponded with the expected results found in other studies using carbon fiber electrodes (Figure 4).<sup>174,175</sup> This MEA was further applied to determine real-time

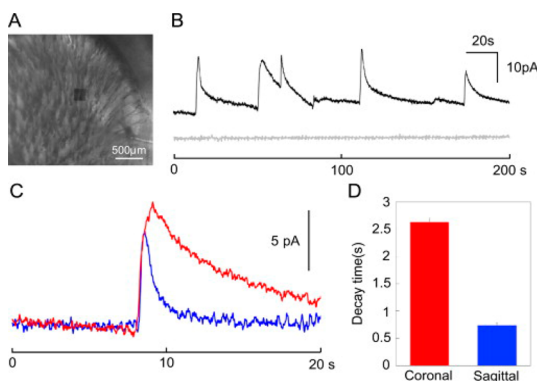


**Figure 4.** Real-time measurements of dopamine release from mouse striatal brain slices. (A) Mouse striatal slice cut in the coronal plane and mounted on a  $4 \times 10^4 \mu\text{m}^2$  CNT plated indium–tin oxide MEA. (B) Amperometric responses to dopamine discharge from a coronal striatal slice at +0.3 V (black) or 0 V (gray). (C) Superimposed waveforms of dopamine responses from coronal (red) and a sagittal section (blue). (D) Mean half-decay time ( $t_{1/2}$ ) for coronal and sagittal sections ( $n = 6$ ). Adapted with permission from ref 77. Copyright 2013 Elsevier B.V.

sensing in hippocampal neuronal cultures and hippocampal slices by monitoring the action potentials and field postsynaptic potentials. The results from these experiments show that this MEA can be applied in real-time sensing, and that the probe is noninvasive as neuronal cells cultured on these MEAs survived for more than 1 month.

Ionic liquids have been shown to be biocompatible toward biomolecules, as well as capable of enhancing their bioactivity.<sup>176,177</sup> In this vein, Noroozifar and colleagues showed that by utilizing the ionic liquid 3-hydroxypropanamium acetate together with a nanosized zeolite and MWCNT paste the simultaneous detection of UA and dopamine could be achieved.<sup>178</sup> Utilizing differential pulse voltammetry (DPV), the authors showed that the linear ranges of detection were 0.812 to 301  $\mu\text{M}$  (LOD, 0.116  $\mu\text{M}$ ) and 0.931 to 336  $\mu\text{M}$  (LOD, 0.133  $\mu\text{M}$ ) for dopamine and UA, respectively. These biosensors were used to analyze human urine and blood serum samples, with recovery rates of  $\sim 100\%$  across all samples, indicating the potential use of this material in commercial applications.

Besides the enzymeless detection of dopamine detailed above, the use of enzymes in conjunction with CNTs has been employed in the determination of dopamine. In this manner, Pereira *et al.* immobilized horseradish peroxidase from zucchini (*Cucurbita pepo* L.) directly onto MWCNTs using covalent bonding.<sup>78</sup> These functionalized MWCNTs were then mixed with graphite and paraffin oil to create a dopamine biosensor. The biosensor was successfully applied in the detection of dopamine in pharmaceutical formulations with an accuracy equivalent to high-performance liquid chromatography

(HPLC). Additionally, it was shown that this biosensor performance is not compromised in the presence of AA and UA.

Noroozifar *et al.* fabricated an enzymeless holmium fluoride ( $\text{HoF}_3$ ) NP/MWCNT-functionalized GCE for the sensitive determination of UA in the presence of interfering analytes AA and dopamine.<sup>158</sup> Comparison of the electrocatalytic activity of the GCE/MWCNT/ $\text{HoF}_3$  NPs and GCE/MWCNT sensors showed that  $\text{HoF}_3$  NPs are the dominating participant in the electrocatalytic activity of UA in the presence of AA and dopamine. The fabricated sensor exhibited a linear response range from 0.2 to 500  $\mu\text{M}$  with a LOD of 0.16  $\mu\text{M}$ . To confirm the practical application of the sensor, the electrode was successfully employed in the detection of UA in human serum and urine samples with recovery rates of 95.5 and 102.2%, respectively.

Liu *et al.* reported the nonenzymatic sensing of UA using a CNT ionic liquid paste electrode that was modified *in situ* with electropolymerized poly( $\beta$ -cyclodextrin) ( $\beta$ -CD).<sup>179</sup> The as-fabricated working electrode shows a linear response range from 0.6 to 400  $\mu\text{M}$  with a LOD of 0.3  $\mu\text{M}$  in the presence of ascorbic acid, with the selective response of this sensor being due to host–guest recognition between  $\beta$ -CD and UA. Recently, the Mascarenhas group reported the selective detection of UA in the presence of ascorbic acid, dopamine, and L-tyrosine by utilizing FeNPs coated on CNTs.<sup>180</sup> Under optimized experimental conditions, the differential pulse voltammetry curve displayed two linear concentration ranges for UA of  $7.0 \times 10^{-8}$  to  $1.0 \times 10^{-6}$  M and  $2.0 \times 10^{-6}$  to  $1.0 \times 10^{-5}$  M with a LOD of  $(4.80 \pm 0.35) \times 10^{-8}$  M. To demonstrate the practical applicability, the electrode was successfully applied to the determination of UA in (spiked) human urine samples with good recovery rates.

Numnuam *et al.* fabricated an amperometric UA biosensor by immobilizing uricase on an electrospun nanocomposite of a chitosan–CNT nanofiber covering an electrodeposited layer of AgNPs on a Au electrode.<sup>160</sup> The basis of the UA detection method was to monitor the change in the reduction current for the dissolved  $\text{O}_2$ , which forms during oxidation of uric acid by the immobilized uricase. This biosensor's ability to detect UA (LOD, 1  $\mu\text{M}$ ) was not affected by the introduction of AA, glucose, and lactic acid. This biosensor was also successfully applied in the determination of UA in human serum samples, with a sensitivity equivalent to that obtained using enzymatic colorimetric detection.

**Graphene/Carbon Nanotube Composites.** One of the problems associated with the application of CNTs in sensing is the fouling that takes place. With the accumulation of oxidation products on the surface of the CNTs (fouling), the sensitivity and LOD of the biosensor can be altered negatively. For this reason, CNTs are often incorporated with other nanomaterials to prevent fouling.<sup>181–183</sup> This section deals with the use of CNT/graphene materials in dopamine, UA, and AA biosensors,<sup>184</sup> which have the added benefit of antifouling on the CNTs through incorporation of the graphene.

Chen and colleagues have shown that dopamine and acetaminophen can be simultaneously determined using a MWCNT/GO composite-modified GCE.<sup>185</sup> The composite material is formed simply through  $\pi$ – $\pi$  interactions between the GO and the MWCNT by sonication of the two components together. The LODs for the biosensor were 22 and 47 nM for dopamine and acetaminophen, respectively. Importantly, the authors showed that the composite material

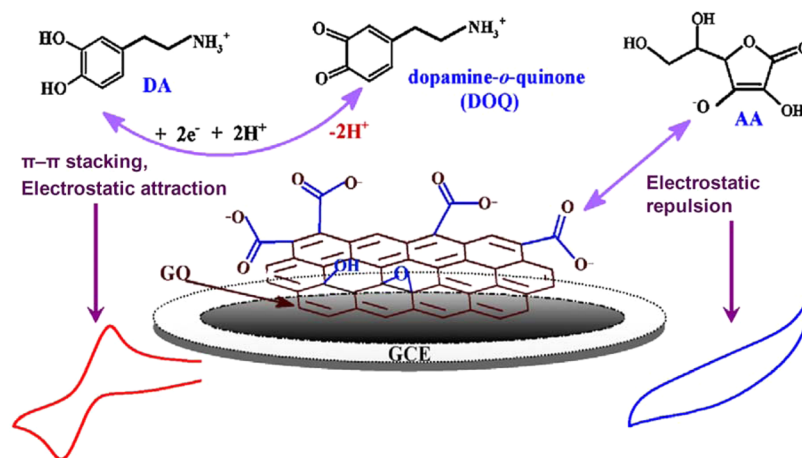


Figure 5. Difference in the electrochemistry of dopamine (adsorbed) and ascorbic acid (repelled) on a GO/GCE. Adapted with permission from ref 193. Copyright 2013 Elsevier B.V.

out-performed both the GO-modified GCE and the MWCNT-modified GCE, while interference studies demonstrated that UA, AA, and NADH have negligible effect on the simultaneous sensing ability of the biosensor. Additionally, the biosensor proved to be stable over 1 week (91.3% signal retention) as well as successive measurements ( $\sim 3\%$  standard deviation). In a related study, it has been shown that a MWCNT-bridged mesocellular graphene foam, nanocomposite-modified GCE can be used to simultaneously determine AA, dopamine, UA, and tryptophan.<sup>186</sup> The authors of this study showed that this biosensor exhibited a far greater electrochemical response in terms of selectivity and catalytic activity compared to GCEs modified with mesocellular graphene foam, MWNTs, or MWNT/GS.

To further enhance the sensing ability of a GCE modified with a GO/MWCNT composite, Yang *et al.* have shown that including cetyltrimethylammonium bromide (CTAB) in the composite allows for the selective and sensitive simultaneous detection of dopamine (LOD,  $1.0 \mu\text{M}$ ), AA (LOD,  $1.5 \mu\text{M}$ ), UA (LOD,  $1.0 \mu\text{M}$ ), and nitrite (LOD,  $1.5 \mu\text{M}$ ).<sup>187</sup> Perhaps, this enhanced electrochemical activity can be attributed to the highly porous 3D nanohybrid structure that the CTAB-GO/MWNT composite forms, which offers more active sites for dopamine oxidation, compared to the smooth packed surface of CTAB-GO/GCE.

Using a PtNP-coated graphene-CNT (Pt-G-CNT) hybrid, Ramakrishnan *et al.* demonstrated a high electrocatalytic activity toward the oxidation of AA, dopamine, and UA in  $0.1 \text{ M}$  phosphate buffer solution (pH 7.0).<sup>188</sup> Under optimal conditions, the authors reported simultaneous detection of AA, dopamine, and UA, in the linear concentration ranges of 200–900, 0.2–30, and 0.1–50 mM, respectively, with LODs of 0.186 (AA), 9.199 (dopamine), and 9.386  $\text{mA mM}^{-1} \text{cm}^{-2}$  (UA). The fabricated sensor was also used in the simultaneous detection of the three biomolecules in a vitamin C tablet solution, human serum, and urine. In another study, the Yuan group reported the simultaneous determination of dopamine, AA, and UA using a MWCNT/rGO hybrid functionalized with PAMAM and AuNPs (rGO-PAMAM-MWCNT-AuNPs).<sup>189</sup> This hybrid material exhibited large electrocatalytic activities, which translated into linear response ranges for the determination of AA, DA, and UA in mixed analytes systems of 20 to 1.8 mM (LOD 6.7 mM), 10 to 0.32 mM (LOD 3.3 mM), and 1 to 0.114 mM (LOD 0.33 mM), respectively.

**Graphene.** The use of graphene-based electrodes in the detection of dopamine has been widely reported.<sup>190–194</sup> Depending on the type of graphene material employed, the electroactivity is enhanced in differing ways. For example, it is believed that in graphene/rGO-based materials the electroactivity toward dopamine is enhanced by the large surface area and superior conductivity.

Two separate groups have shown that a GCE<sup>190</sup> or a carbon fiber electrode<sup>191</sup> can be modified through the electrochemical reduction of GO (ErGO) onto their surface. These electrodes were then used in the simultaneous detection of AU, UA, and dopamine. In both of these studies, the ErGO-modified electrode showed a separation of three analyte peaks, while a broad merged peak with a lower response was observed for the unmodified surface. The LODs for the ErGO/carbon fiber electrode were determined to be 4.5 (AA), 0.77 (dopamine), and 2.23  $\mu\text{M}$  (UA), while for the ErGO/GCE, they were 0.3 (AA), 0.5 (dopamine), and 0.5  $\mu\text{M}$  (UA). In a related study, Nancy *et al.* showed that solar reduced GO could be used to modify a GCE without the addition of a binder.<sup>192</sup> As with the previously mentioned studies, this electrode could be used in the simultaneous oxidation and detection of AU, UA, and dopamine; however, the authors only reported the LOD for dopamine (2.8  $\mu\text{M}$ ). It is important to note that although this biosensor is believed to be stable under electrochemical detection conditions, no long-term stability studies were conducted.

In a similar way, Gao and co-workers have shown that a GO-modified GCE can be used in the highly sensitive and selective detection of dopamine in the presence of AA.<sup>193</sup> The dopamine LOD for the electrode was determined to be 0.27  $\mu\text{M}$ , while the addition of AA does not affect the signal. It is believed that electrostatic repulsion between the GO and AA makes oxidation of the AA at the electrode surface impossible. In contrast, the  $\pi$ - $\pi$  stacking and electrostatic attraction between the dopamine and GO allows for facile oxidation to take place. The different electrochemical responses of dopamine and ascorbic acid on the working electrode are shown in Figure 5.

To overcome the selectivity problems occurring with the introduction of analytes which interfere with the dopamine signal, Bagherzadeh and Heydari showed that by modifying a carbon paste electrode with graphene nanosheets dopamine could be preconcentrated on the electrodes surface.<sup>194</sup> This preconcentration method allows for the sensitive (LOD, 8.5

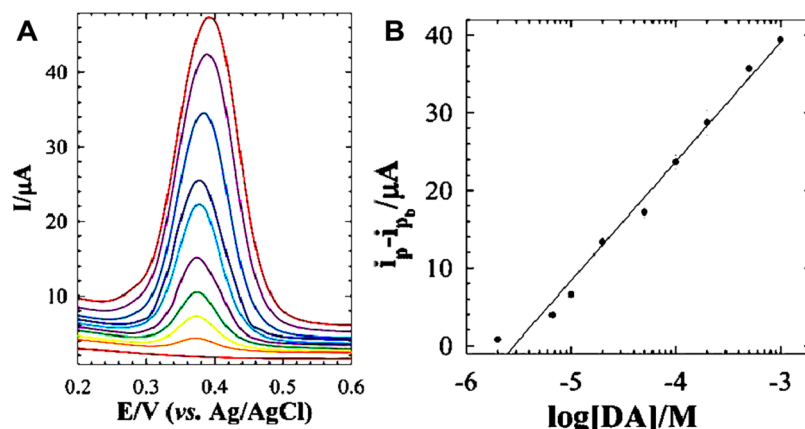


Figure 6. (A) DPV curves recorded on the carbon-paste-electrode/graphene nanosheet in dopamine-free PBS, after 25 min preconcentration in PBS containing different concentrations of dopamine. (B) Calibration curve obtained from changes in the DPV anodic peak current vs dopamine concentration. Adapted with permission from ref 194. Copyright 2013 Royal Society of Chemistry.

$\mu M$ ) and selective determination of dopamine in the presence of interfering analytes. This method employs a dopamine preconcentration step followed by stripping the electrodes in a dopamine-free solution, as such any possibility of interference from other interfering analytes is removed (Figure 6). Similar to the GO case, it is believed that the residual carboxylic acid groups in the graphene nanosheets attract the dopamine electrostatically, which increases the overall  $\pi$ - $\pi$  stacking between dopamine and graphene.

Qi *et al.* have prepared pristine graphene (PG) using organic salt-assisted exfoliation; this PG was then applied in the simultaneous electrochemical determination of AA, DA, and UA with LODs of 6.45, 2.00, and 4.82  $\mu M$ .<sup>195</sup> The reason the authors used PG over chemically converted graphene (CCG) is that some oxygen-containing functional groups on the CCG surface are negatively charged and provide an electrostatic repulsion to the also negatively charged AA. As such, CCG-based sensors are much less sensitive than PGs toward the detection of AA.

As has been noted so far, one way to enhance the sensitivity of a biosensor is to increase the surface area. In this way, 3D graphene synthesized by chemical vapor deposition, freeze-casting, and electrochemical polymerization techniques (polypyrrole-coated 3D graphene) has been explored for dopamine sensing.<sup>96,196</sup> These materials exhibited remarkable sensitivity and LODs, due to the high conductivity and large specific surface area of the graphene.

Chemical vapor deposition 3D graphene foam electrodes have been manufactured and applied in dopamine detection (LOD, 25 nM) in the presence of UA.<sup>196</sup> To improve the LOD, selectivity, and sensitivity of 3D foams, Liu *et al.* coated a graphene foam electrode with polypyrrole which binds favorably with dopamine.<sup>96</sup> The 3D polypyrrole-coated foam electrode displayed predicted selectivity, sensitivity, wide linear response range (0.1–200  $\mu M$ ), and slightly improved LOD (19.4 nM). It should be noted, however, that this coated material was shown to be selective for dopamine detection in the presence of both UA and AA.

Graphene-based electrodes have additionally been modified with various polymers, noble metals, metal oxides, spinels, and metal complexes to produce either doped graphene or other graphene composite materials. Some of these materials can be applied in biosensors for the simultaneous sensing of dopamine, AA, and/or UA.<sup>197–203</sup>

A screen-printed carbon electrode modified with N-doped graphene material, synthesized through thermal expansion/reduction of GO and melamine, has been used in the simultaneous sensing of dopamine, AA, and UA (Figure 7).<sup>197</sup> While the authors believe the shift in the peak oxidation

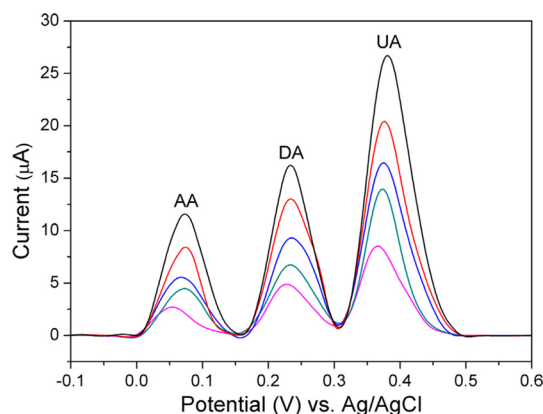


Figure 7. Linear sweep voltammetry plots using a screen-printed carbon electrode modified with N-doped graphene 0.1 M PBS containing varying concentrations of AA, dopamine (DA), and UA at a sweep rate of 20 mV/s. From bottom to top, the concentrations are 0.6, 0.7, 0.8, 1, 1.2 mM for AA, 0.12, 0.14, 0.16, 0.19, and 0.22 mM for DA, and 0.1, 0.15, 0.17, 0.2, and 0.25 mM for UA, respectively. Adapted with permission from ref 197. Copyright 2013 Elsevier B.V.

potentials, which allows simultaneous detection, arises from enhanced oxidation of the analytes at the pyrrolic-N groups, they do point out that the observed effect is due to the total N-doping of the material. The LOD (0.93  $\mu M$ ) of this material is similar to that of undoped graphene; however, its simultaneous sensing abilities should allow its further application.

Utilizing the enhanced nitrogen activity toward analytes, various groups have modified graphene using nitrogen-containing polymers to achieve simultaneous sensing. By modifying a GCE with a polyaniline-coated GO material, Viswanathan and co-workers showed that UA (LOD, 0.2  $\mu M$ ), AA (LOD, 20  $\mu M$ ), and dopamine (LOD, 0.5  $\mu M$ ) can be simultaneously determined in solution.<sup>198</sup> The enhanced oxidation peak potential observed is attributed to electrostatic and  $\pi$ - $\pi$  interactions between the analytes and the polyaniline/



GO composite material. In another preparation method, Liu *et al.* prepared an over-oxidized polyimidazole/GO-modified GCE, by electrochemically cycling the GCE in a mixture of GO and polyimidazole.<sup>199</sup> This electrode was then utilized in the simultaneous determination of UA, AA, guanine, adenine, and dopamine, while no interference was noted for these five analytes upon introduction of the following interfering analytes: NaCl, KCl, KNO<sub>3</sub>, NaSO<sub>4</sub>, ZnCl<sub>2</sub>, CaCl<sub>2</sub>, citric acid, glucose, bovine serum albumin, immunoglobulin, and hemoglobin.

Utilizing self-assembly methods, GCE has been modified to introduce nitrogen and graphene materials. Weng *et al.* showed that by dipping a GCE electrode into a GO solution followed by a chitosan solution, a N-containing layered electrode could be obtained.<sup>200</sup> This electrode could then be applied in the simultaneous detection of UA (LOD, 0.1  $\mu\text{M}$ ) and dopamine (LOD, 0.05  $\mu\text{M}$ ). Zhang and co-workers have shown that by using a self-assembly method a hollow N-doped carbon sphere spacer can be introduced between graphene layers.<sup>201</sup> The biosensor was then used in the detection of UA, AA, and dopamine with very impressive LODs of 18, 650, and 12 nM, respectively. These electrodes were subsequently employed in the detection of dopamine, UA, and AA in human urine samples with an impressive recovery rate of  $\sim 100\%$  for all analytes.

The solar-reduced GO-modified GCE biosensor manufactured by Nancy and colleagues<sup>192</sup> could be further modified by cycling a Ni acetate/solar rGO/GCE in 0.1 M NaOH. Unlike the solar-rGO-modified GCE, this Ni-OH/solar-rGO-modified GCE could be employed in the simultaneous and sensitive detection of AA, UA, and dopamine (LOD, 0.12  $\mu\text{M}$ ).<sup>202</sup> This electrode was also applied in the successful determination of the three analytes in human blood serum and urine samples.

Zeng and colleagues showed that vinyl-functionalized SiO<sub>2</sub>-coated GO could be molecularly imprinted with dopamine.<sup>203</sup> This imprinted polymer was then deposited onto a GCE and could be used in the highly selective detection of dopamine through an extraction and rebinding of dopamine mechanism. Importantly, this sensor's performance was not affected by the introduction of norepinephrine and epinephrine into the analyte solution. This molecular imprinting method should allow for the manufacture of very selective biosensors in the future.

Zhang *et al.* explored the important effect of oxygen functionalities in ErGO-modified GCEs on the electrochemical oxidation of UA.<sup>162</sup> They found that the partial ErGO-modified GCE displayed the highest sensitivity toward the electro-oxidation of UA. This electrode also showed a good linear correlation between the oxidation peak current and the concentration of UA ranging from 100 nM to 10  $\mu\text{M}$  with a LOD of 50 nM. These modification studies have shown that tuning the activity and sensitivity of rGO-based electrode films toward the electro-oxidation of UA can be achieved through chemical doping or formation of nanocomposites.<sup>159–161</sup> In the same way, it has been shown the ErGO-modified electrodes can be used for the simultaneous detection of UA, AA, and dopamine.<sup>163</sup> The fouling effect was noticed on this biosensor when the pH was neutral or basic; however, in acidic solution, this effect was not observed. This is believed to be due to the formation of polydopamine on the surface of the electrode, indicating that electro-oxidation proceeds slowly, which agrees with a diffusion-rate-controlled process.

As has been noted above, N-doped graphene can be used to detect UA.<sup>163</sup> It should be noted, however, that the N-doping

methods currently employed are not controllable, and as such, the sensitivity/selectivity of these electrodes can be improved.<sup>204–206</sup> Through the utilization of a rGO/AgNP-modified GCE, it is possible to simultaneously and sensitively determine the UA, AA, dopamine, and tryptophan in commercial and human urine samples.<sup>161</sup> Interestingly, this electrode showed negligible fouling, which is believed to be due to the enhanced catalytic activity induced in the AgNPs through the introduction of rGO.

Chen *et al.* prepared GO supported porous bimetallic alloyed palladium silver (PdAg) nanoflowers using an *in situ* reduction process.<sup>207</sup> The authors then used this material to fabricate a sensor which can selectively detect AA, dopamine, and UA with low detection limits of 0.057, 0.048, and 0.081  $\mu\text{M}$ . In contrast for the simultaneous detection of AA, DA, and UA, the LODs were 0.185, 0.017, and 0.654  $\mu\text{M}$ , respectively. In another study, Liu *et al.*<sup>208</sup> showed that electrodeposited Au-Pt bimetallic nanoclusters decorated on GO can be applied in the detection of DA and UA with linear detection ranges of  $6.82 \times 10^{-8}$  to  $4.98 \times 10^{-2}$  M and  $1.25 \times 10^{-7}$  to  $8.28 \times 10^{-2}$  M and LODs of  $2.07 \times 10^{-8}$  and  $4.07 \times 10^{-8}$  M, respectively.

Yang designed a sensor based on CTAB-functionalized rGO/ZnS for the simultaneous electrochemical detection of dopamine, UA, and AA.<sup>209</sup> In addition to its electrocatalytic activities toward the oxidation of AA (LOD 30  $\mu\text{M}$ ), dopamine (LOD 0.5  $\mu\text{M}$ ), and UA (LOD 0.4  $\mu\text{M}$ ), the biosensor is capable of resolving overlapping peaks, decreasing overpotential, and enhancing current response.

Pruneanu *et al.* have developed electrochemical sensors for dopamine based on gold electrodes, modified with graphene-AuAg (Au/Gr-AuAg) or graphene-Au (Au/Gr-Au) composites.<sup>210</sup> The Au/Gr-AuAg electrode showed improved peak current density, linear range, and LOD in comparison to the Au/Gr-Au electrode, which corroborates other studies which incorporate bimetallic alloys in graphene-based biosensors. The LOD of Au/Gr-AuAg for dopamine in the absence of AA and UA was calculated to be  $2.05 \times 10^{-7}$  M, which is superior to the detection limit in their presence ( $2.16 \times 10^{-6}$  M).

Many other studies have been reported regarding the detection of dopamine, UA, and AA, simultaneously as well as discretely. For example, Li *et al.*<sup>211</sup> reported a silver nanowire-reduced graphene oxide-based biosensor, and Zou *et al.* reported hemin-functionalized graphene oxide sheets for detection of dopamine, UA, and AA.<sup>212</sup> Additionally, core-shell and rod-shaped magnetite structures decorated on graphene exhibit enhanced selectivity for dopamine detection in the presence of UA and AA.<sup>213,214</sup>

**Protein and Protein Monomer Sensing.** For the case of small-molecule (nonenzymatic) analysis, it is important to measure the activities of functional protein molecules such as bioenzymes released from cells, under different microenvironmental conditions, to understand the fundamentals of cell biology for therapeutic, diagnostic, and tissue engineering applications.<sup>215</sup> Two examples of the fundamental importance of enzyme detection would be that of  $\alpha$ -fetoprotein and lysozyme.

$\alpha$ -Fetoprotein (AFP), a protein with a molecular weight of 70 kDa, is produced by the liver and umbilical vesicle of the fetus during pregnancy. However, elevated AFP expression is widely known as a biomarker for hepatocellular carcinoma (liver cancer).<sup>216,217</sup> As such, the early detection of AFP is highly desired. At present, several methods are employed in AFP sensing such as fluorescence, electrogenerated chemilu-

minescence, and voltammetric immunoassay. Among these methods, voltammetric immunoassay has received much attention in recent years due to its unique properties, such as a low detection limit, small analyte volume, simple instrumentation, minimal manipulation, simplicity, and high sensitivity.

Lysozymes are proteins found in multiple organisms and have physiological and pharmaceutical functions such as anti-inflammatory, antiviral, immune modulatory, antihistaminic and antitumor activities.<sup>218,219</sup> As such, the level of lysozymes in the body can have dramatic health effects, for example, a reduced level of lysozymes in newborns is associated with bronchopulmonary dysplasia (chronic lung disease).<sup>220</sup> From these examples, one is able to see the necessity to develop biosensors that can selectively detect proteins at very low and high concentrations.

**Protein-Relevant Monomer Sensing Using Carbon Nanotubes.** L-Cysteine, a sulfur-containing  $\alpha$ -amino acid, serves an important structural role in many proteins because of its chemical activity in the formation of complexes with various ionic species and biomolecules.<sup>221,222</sup> L-Cysteine is used in some proprietary antibiotics for the treatment of skin damage<sup>223</sup> as well as an antioxidant in the food industry.<sup>224</sup> Therefore, the selective and sensitive determination of L-cysteine in food processing, biochemistry, pharmaceuticals, and clinical analysis is highly required.<sup>225</sup> Goulart *et al.* reported that a MWCNT/Au nanorod composite-modified GCE could be used in the electrocatalytic oxidation/detection of L-cysteine.<sup>226</sup> It was shown that the advantage of using this electrode is that it oxidizes L-cysteine at very low potential (0.0 V vs Ag/AgCl) at which the other normally interfering thiol compounds like homocysteine, glutathione, and N-acetylcysteine do not undergo oxidation. The biosensor exhibited a stability, quick response time (1 s), large  $k_{\text{cat}}$  value (120 nA  $\mu\text{M}^{-1}$ ), large linear response range (5.0–200 mM), and low LOD (8.25 nM). In an extension to this work, Kubota *et al.* modified a GCE using a MWCNT/poly(4-vinylpyridine)-Fe(CN)<sub>5</sub> metallopolymer material.<sup>72</sup> This electrode, with a remarkable 100% maximum response in merely 0.1 s, was then used to detect L-cysteine with a LOD of 20.5 nM<sup>-1</sup>. It should be noted that the authors did not report the confidence level for which this LOD was reported, as such the higher of the two LOD values reported is presented here.

Riboflavin (vitamin B<sub>2</sub>), while not an enzyme, is an enzymatic cofactor that is critical in many enzymatic processes in the body. For this reason, its detection is important to understand biological functions as well as the effects of inadequate intake on the human body. In this vein, Santhanalakshmi *et al.* prepared and optimized an oleylamine-capped nickel oxide NP/MWCNT composite which formed through electrostatic adsorption between the capped NPs and acid-functionalized MWCNTs (Figure 8).<sup>73,227</sup> A modified GCE with this composite was then used for the electrochemical detection of riboflavin. The electrode exhibited a LOD of 1 nM, and the sensitivity was not significantly interfered by the water-soluble vitamins B<sub>1</sub>, B<sub>3</sub>, B<sub>6</sub>, C, and folic acid. These results enhance the practical application of this composite for riboflavin detection. Additionally, the biosensor shows only 1.24% decrease in initial response after the storage at 4 °C for a month.

Madrakian *et al.* have shown by electrodepositing AuNPs onto a MWCNT-modified GCE that this electrode can be used in the simultaneous determination of the amino acid tyrosine,

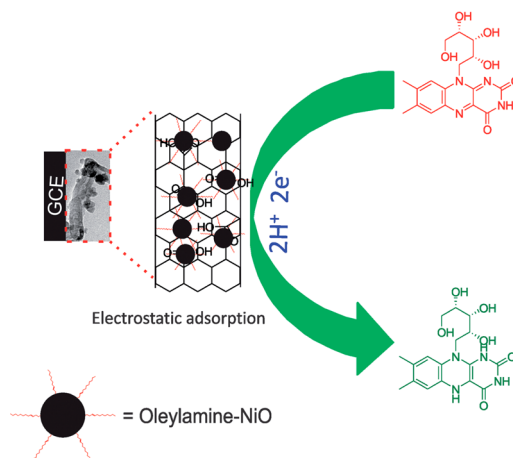


**Figure 8.** Schematic illustration of electrostatic adsorption of oleylamine-capped nickel oxide NP onto the acid-functionalized MWCNTs surface. Adapted with permission from ref 73. Copyright 2014 Royal Society of Chemistry.

acetaminophen, and AA in pharmaceutical preparations and humans serum samples.<sup>227</sup> To verify the feasibility of the simultaneous determination of tyrosine, acetaminophen, and AA by the biosensor, experiments were carried out where one analyte concentration was changed while keeping the others constant (Figure 9). As can be seen in Figure 9, the LODs for the tyrosine, acetaminophen, and AA analytes were calculated to be 0.21, 0.03, and 0.76  $\mu\text{M}$ , respectively.

Gupta *et al.*<sup>74</sup> grew vertically aligned carbon nanofibers using plasma-enhanced chemical vapor deposition to fabricate nanoelectrode arrays in a 3 × 3 configuration. These fabricated nanofibers were used for biosensing C-reactive protein (CRP) using CV and EIS. CRP is an acute phase protein which is synthesized in liver and secreted in the bloodstream, causing infection or inflammation, and thus is a biomarker for cardiac disease. The CV responses show a 25% reduction in redox current upon the immobilization of anti-CRP on the electrode, where a 30% increase in charge transfer resistance is seen from EIS. These nanofibers show high specificity toward CRP in the presence of possibly interfering nonspecific myoglobin antigen with the detection limit of 90 pM, which is low enough for clinical application.

**Protein Sensing Using Carbon Nanotubes.** Pregnancy-associated plasma protein-A (PAPP-A) is an enzyme tested for during prenatal screening to determine if down syndrome is present in the fetus.<sup>228</sup> Ding *et al.* developed a novel electrochemical immunosensor for competitive detection of PAPP-A in serum.<sup>229</sup> A GCE was modified with a SWCNT/chitosan composite and then coated with PAPP-A. This electrode was then incubated with a known volume of biotin-anti-PAPP-A antibody and unknown concentrations of PAPP-A. After being washed, this electrode was incubated with streptavidin-alkaline phosphatase, which bound with the remaining biotin-anti-PAPP-A, and then this reaction was tested electrochemically (Figure 10). The LOD of this biosensor was calculated to be 39 ng/mL, and it exhibited stability, reproducibility, and negligible voltammetric response from interfering molecules in the serum.

To detect the human carcinoembryonic antigen, Feng *et al.* modified a GCE using a multilayer-by-layer drop-coating/electrodeposition assembly method of rGO, MWCNTs, and Prussian blue NPs. Onto this assembly were anchored AuNPs,

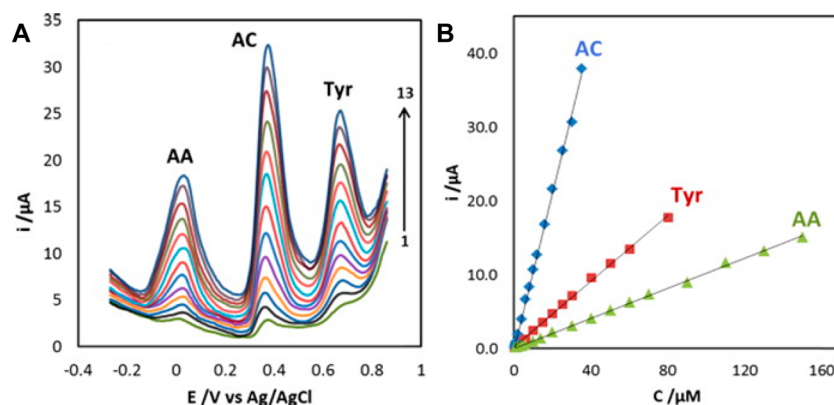


Figure 9. (A) DPVs at AuNP/MWCNT/GCE at pH 6.0 and different concentrations of tyrosine (Tyr), acetaminophen (AC), and AA. From 1 to 13, the concentrations are 0.5 to 80  $\mu\text{M}$  for Tyr, 0.5 to 30  $\mu\text{M}$  for AC, and 1 to 150  $\mu\text{M}$  for AA. (B) Plots of the oxidation peak currents as a function of Tyr (red), AC (blue), and AA (green) concentrations. Adapted with permission from ref 227. Copyright 2014 Elsevier B.V.

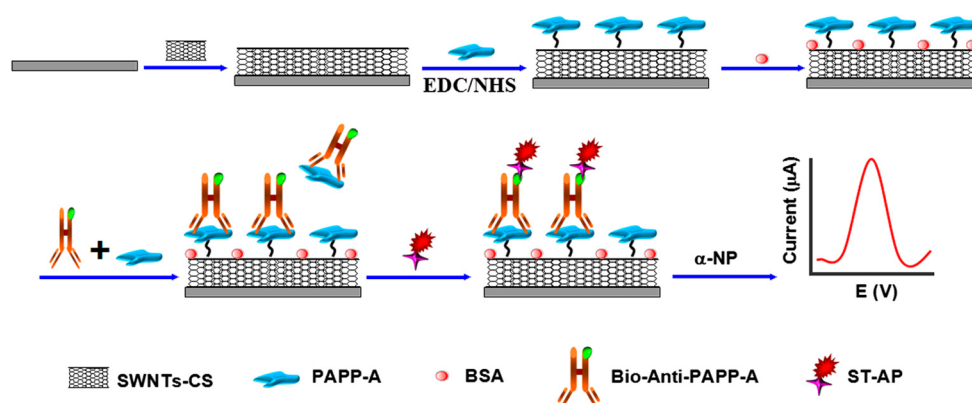


Figure 10. Schematic showing the preparation of the electrochemical immunosensor for the detection of PAPP-A. Adapted with permission from ref 229. Copyright 2013 Elsevier B.V.

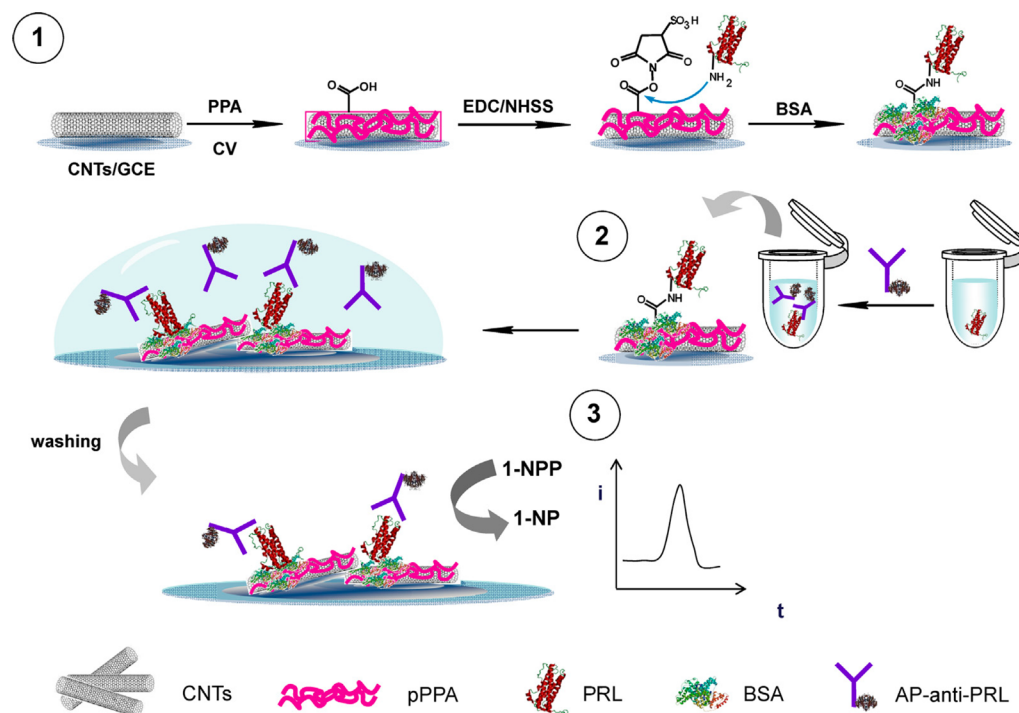
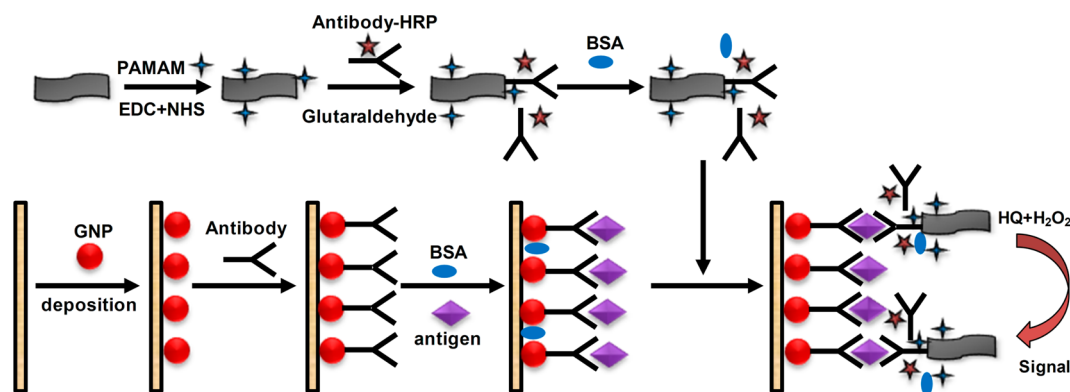


Figure 11. Stepwise illustration of the fabrication and sensing of the prolactin antibody (AP-anti-PRL)/ poly(pyrrrolepropionic acid) (PPA)/ CNT/GCE immunosensor. Adapted with permission from ref 92. Copyright 2014 Elsevier B.V.





**Figure 12.** Schematic showing the preparation of the polyamidoamine dendrimer (PAMAM)/rGO(graphene)/enzyme-labeled AFP antibody (anti-HRP) and its use as a label in the detection of AFP using a AuNP(GNP)/AFP antibody-modified electrode. Modified with permission from ref 235. Copyright 2014 Elsevier B.V.

which could immobilize the carcinoembryonic antigen antibody.<sup>230</sup> It was found that the electrode performs optimally with five layers of rGO–MWCNT–Prussian blue and exhibited a highly selective LOD of  $60 \text{ pg mL}^{-1}$ . This electrode was then applied in serum samples and exhibited recovery rates of 96–110%. Additionally, the authors reported that the biosensor exhibited negligible variation in response after 3 weeks, indicating the sensors stability. In another study, it has been shown that by immobilizing a thrombin binding aptamer onto a SWCNT-modified GCE, thrombin can be detected without using a label.<sup>93</sup> This electrode showed an impressive linear range of 10 nM to 100 mM and a LOD of 10 nM. It should be noted that this LOD and linear range were determined by adding the electrocatalytic mediator  $\text{Ru}(2,2'\text{-bipyridine})_3^{2+}$ , which results in a higher sensitivity due to an enhanced oxidation of the guanine nucleotides. By coating a Ag electrode with polyethylenimine onto CNTs followed by anticardiac Troponin T, Filho and colleagues demonstrated that the cardiac marker cardiac Troponin T can be detected.<sup>88</sup> This sensor was applied in the detection of the cardiac marker in human serum samples, which can be used in the diagnosis of acute myocardial infarction.

The Yu group showed that a GCE modified with MWCNTs, Nafion, and thionine-coated AuNPs can be used to sense cardiovascular biomarker netrin 1.<sup>231</sup> Under an optimized condition, this immunoelectrode could sense netrin 1 at a voltage of  $-300 \text{ mV}$ , with a LOD of  $30 \text{ fg mL}^{-1}$ , and a linear response range of 0.09 to  $1800 \text{ pg mL}^{-1}$ . Dutra *et al.* reported a sensitive nanostructured immunoelectrode for electrochemical detection of the dengue virus NS1 protein fabricated by depositing a layer of CNT followed by poly(allylamine) on a GCE.<sup>232</sup> The electrochemical properties of immunoassay were indirect and produced at a controlled potential by the reaction between  $\text{H}_2\text{O}_2$  and a peroxidase enzyme conjugated to anti-NS1 antibodies. This sensor exhibited a linear range of 0.1– $2.5 \text{ } \mu\text{g mL}^{-1}$  and a LOD of  $0.035 \text{ } \mu\text{g mL}^{-1}$ .

To detect the phosphoprotein casein in dairy products, Wang *et al.* sequentially immobilized AuNPs and the casein antibody onto a MWCNT-modified GCE with a film of electrodeposited poly-L-arginine.<sup>90</sup> The immunosensor displayed a LOD of  $5 \times 10^{-8} \text{ g mL}^{-1}$  and could be applied in the selective and sensitive determination of casein in cheese samples with recovery rates between 92 and 100%. Since casein is one of the major allergens found in dairy products, this study shows relevant practical application. By immobilizing the hormone prolactin

antibody onto an electrodeposited poly(pyrrole propionic acid) film on a CNT-modified GCE, Sedeno and co-workers were able to detect the hormone prolactin (Figure 11).<sup>92</sup> The immunosensor exhibited a LOD of  $3 \text{ pg/mL}$  and could be used in the successful determination of prolactin in human serum and urine samples with recovery rates between 97 and 103%. It is believed that the use of a conducting polymer in conjunction with the CNTs allows for enhanced electron transfer and thereby an increase in analytical performance.

**Protein-Relevant Monomer Sensing Using Graphene.** The detection of L-cysteine reported for CNT-modified electrodes has also been reported for graphene-based biosensors. It is well-known that the electrochemical property of a modified electrode is strongly related with the homogeneous distribution of NPs and the density.<sup>233</sup> In this way, Xu *et al.* modified a GCE with a graphene–AuNP hybrid, where these AuNPs were very close to uniformity in size (9 nm) and distribution.<sup>98</sup> These electrodes were then applied in the sensitive detection of L-cysteine (LOD, 20.5 nM) and showed negligible voltammetric response on the addition of arginine, tyrosine, glutamic acid, glucose, urea, and  $\text{K}^+$ ,  $\text{Na}^+$ , and  $\text{Ca}^{2+}$ . These electrodes were also applied in the detection of L-cysteine in human urine with a 100% recovery rate. It is believed that the voltammetric response of this electrode to L-cysteine is attributed to both the excellent conductivity of graphene as well as the catalytic properties of the AuNPs. Using an electrochemical deposition method, Majd and colleagues showed that uniform MnO NPs can be evenly deposited on a rGO-modified GCE.<sup>234</sup> This electrode was used to detect L-cysteine, with the electrode displaying a linear response over the 1– $120 \text{ } \mu\text{M}$  concentration range and a LOD of 75 nM.

**Protein Sensing Using Graphene.** AFP sensing is normally achieved using labeling, as has been demonstrated by Shen *et al.*, who developed a polyamidoamine dendrimer/rGO/enzyme-labeled AFP antibody in the detection of AFP on a AuNP AFP-antibody-modified GCE electrode (Figure 12).<sup>235</sup> In these type of labeling methods, the electrode is immersed in a solution containing AFP and thereafter into the labeled AFP antibody. The electrochemical response of this labeled AFP antibody is then determined. To avoid these multistep procedures, it is desirable to develop label-free methods for AFP detection. In this vain, Peng and co-workers showed that a GCE electrode modified with a AuNP/polydopamine/thionine/GO material and then incubated in anti-AFP could be used in the label-free detection of AFP.<sup>99</sup> This biosensor

showed a remarkable LOD of 0.03 nM and could be applied successfully in AFP monitoring in serum samples with an AFP recovery rate between 92 and 106%.

Erdem and colleagues have shown that a graphene-based electrochemical impedance spectroscopy aptosensor can be used in the detection of lysozyme.<sup>236</sup> The aptosensor was fabricated by coating a pencil graphite electrode with a mixture of chitosan/GO on this modified surface, and the antilysozyme DNA aptamer was immobilized by incubation. This electrode could then be used in the direct detection of lysozyme with a LOD of 28.53 nM. It should be noted that this sensor was sensitive to interference from other enzymes such as bovine serum albumin or thrombin.

These biosensing methods using immunosensor graphene-modified electrodes seem to have no limits, with Eissa *et al.* showing that the egg allergen ovalbumin can be detected using a graphene-based label-free voltammetric biosensor.<sup>97,100,109</sup> These types of electrodes with their small LODs are applicable in a wide variety of applications. It should be noted that most probably, a large reason behind these small LODs can be attributed to the conductivity of graphene-based materials. Wu *et al.* have reported the simultaneous detection of the cervical cancer markers carcinoembryonic antigen and squamous cell carcinoma antigen utilizing a GCE modified with a rGO-tetraethylene pentamine onto which the carcinoembryonic and squamous cell carcinoma antibodies were immobilized.<sup>109</sup> This sensing method additionally relied on the labeling of the antigens with AuNPs to increase the sensitivity, and as such, the LODs were 0.013 and 0.010 ng/mL for the squamous cell carcinoma antigen and carcinoembryonic antigen, respectively. These biosensors were then successfully applied in the detection of the antigens in serum samples with recovery rates between 96.0 and 104%. By functionalizing a GCE with a rGO/electroactive Orange II dye composite material onto which a thrombin or lysozyme binding aptamer was immobilized, Guo *et al.* have shown that thrombin can be detected (Figure 13).<sup>97</sup> The use of Orange II is important as it not only prevents the agglomeration of the as-formed graphene nanocomposite in solution but also endows graphene nanosheets with electroactive properties. These biosensors could then be successfully applied in the sensitive and selective determination of thrombin (LOD, 0.35 pM) and lysozyme (LOD, 1.0 pM).

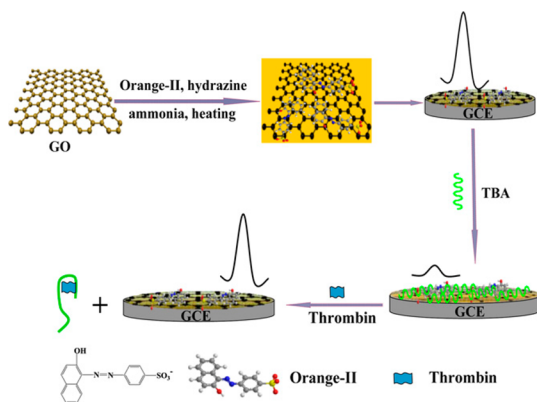


**Figure 13.** Biosensor fabrication and thrombin sensing utilizing the GCE/rGO/electroactive Orange II dye/thrombin binding aptamer biosensor as proposed by Guo *et al.* Adapted with permission from ref 97. Copyright 2013 Elsevier B.V.

Wang *et al.* reported a selective label-free electrochemical biosensor based on graphene–AuNPs for the detection of thrombin with a LOD of 0.01 nM and a linear response range of 0.3–50 nM.<sup>237</sup> Xue *et al.* reported a one-pot synthesis of thio- $\beta$ -cyclodextrin-functionalized graphene–gold NP composites (SH- $\beta$ -CD-Gr/AuNPs) which were deposited onto a GCE to sense thrombin. The as-fabricated sensor shows a wide linear range for thrombin from  $1.6 \times 10^{-17}$  to  $8.0 \times 10^{-15}$  M and a LOD of  $5.2 \times 10^{-18}$  M.<sup>238</sup> Due to the ferrocene probe employed and the host–guest interaction of ferrocene with CD, an amplified response and improved sensitivity was observed.

**Hydrogen Peroxide Sensing.** Hydrogen peroxide ( $\text{H}_2\text{O}_2$ ) detection is important in food processing and pharmaceutical formulations for oral hygiene, such as mouthwashes and dental whitening gels. There are several methods for the detection of  $\text{H}_2\text{O}_2$ , such as titrimetry, spectrophotometry, fluorimetry, and chemiluminescence. However, these methods require time-consuming sample preparation and expensive reagents. On the other hand, the voltammetric detection technique is a robust, simple, rapid, and reproducible method for reliable sensing of  $\text{H}_2\text{O}_2$  in pharmaceutical, food, and dental formulations. The voltammetric and chronoamperometry detection of  $\text{H}_2\text{O}_2$  can be achieved through direct oxidation at carbon and platinum electrodes.<sup>239–243</sup> Unfortunately, due to the large potentials (300–600 mV vs reference electrode) applied to these working electrode, there is significant interference. To overcome these interferences, different approaches based on the chemical and electrochemical modifications of working electrodes surfaces with carbon nanomaterials have been proposed. Importantly,  $\text{H}_2\text{O}_2$  detection is used as an indirect method in the detection of multiple analytes.

In voltammetric detections, oxidation/reduction of  $\text{H}_2\text{O}_2$  at electrodes is limited by poor electrode kinetics and high overpotentials, which cause the degradation of the sensing response. In this regard, CNTs have been widely used in  $\text{H}_2\text{O}_2$  detection, as they have the ability to decrease the overpotential and increase electrode sensitivity. It should be noted, however, that the dispersion of CNT in the structural material plays an important role in the performance of composites toward biosensing. Thus, the CNTs should be functionalized to enhance their dispersibility in the composite.

On the other hand, the 2D structure of graphene provides both edge and basal planes which interact easily with the NPs and nanocatalysts. In this way, the addition of metal NPs onto the graphene surface could (a) increase its active surface area to facilitate the adsorption of an analyte and (b) accelerate electron transfer between the electrode and detection molecules.

**Carbon Nanotubes.** Clausen *et al.* applied a MWCNT/hemin composite for voltammetric detection of  $\text{H}_2\text{O}_2$  in mouthwash and dental whitening gel.<sup>244</sup> The proposed sensor was applied in the determination of  $\text{H}_2\text{O}_2$  in samples using the CV method (–1.0 to +0.3 V vs Ag/AgCl). Interestingly, the increase in the proportion of hemin in the composite decreases the cathode peak potential for  $\text{H}_2\text{O}_2$  reduction, which is probably due to masking of the conductivity of the MWCNTs by high hemin content. The voltammetric linear range with respect to  $\text{H}_2\text{O}_2$  concentration was determined to be 0.6  $\mu\text{M}$  to 7.2 mM, with a LOD of 0.2  $\mu\text{M}$ . The advantage of this method is that it does not require extensive preliminary sample treatment. As such, it has direct application in  $\text{H}_2\text{O}_2$  detection in oral hygiene formulations with accuracy equivalent to volumetric titrimetry.

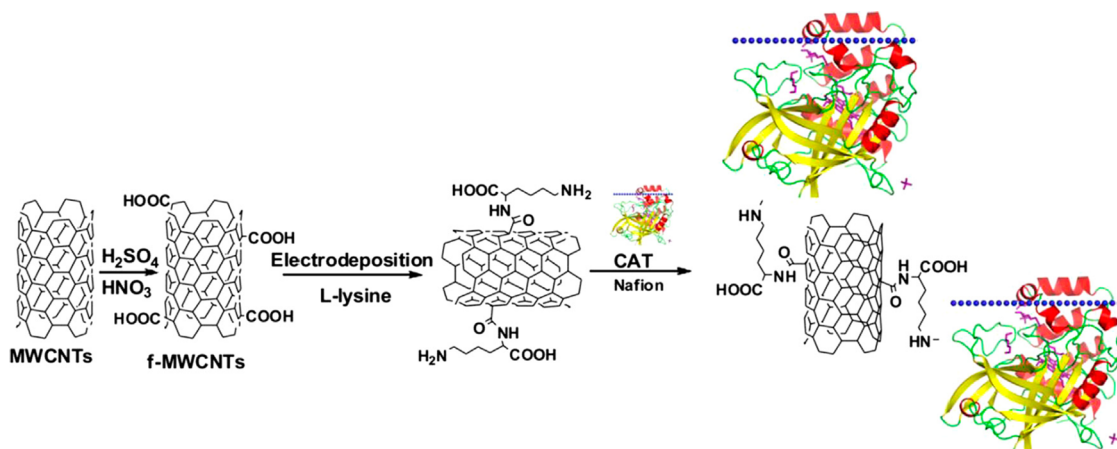


Figure 14. Stepwise representation of manufacture of the CAT/L-lysine/MWCNT-modified GCE. Adapted with permission from ref 80. Copyright 2014 Elsevier B.V.

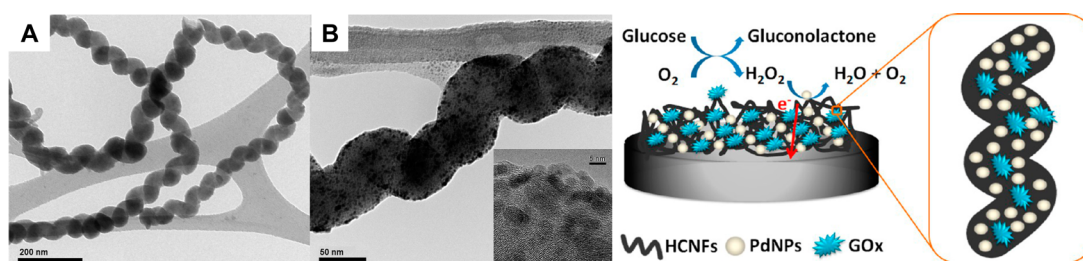


Figure 15. TEM images showing (A) unmodified helical carbon nanofiber (HCNFs) and (B) PdNP-decorated HCNFs and (right) representation of glucose and  $\text{H}_2\text{O}_2$  sensing using the Nafion/Pd-HCNF/GCE sensor. Adapted from ref 248. Copyright 2013 American Chemical Society.

In a similar way, Zhang and co-workers have reported a hemin/GO/CNT-modified GCE for the dual sensing of  $\text{H}_2\text{O}_2$  and simultaneous detection of the biomolecules AA, dopamine, UA, and tryptophan.<sup>245</sup> The hemin is purposefully chosen as it can be successfully employed in the catalytic reduction of  $\text{H}_2\text{O}_2$  due to its intrinsic peroxidase-like activity. The combination of GO and CNT produces a porous 3D hybrid which can facilitate the discrimination of species which can get oxidized and reduced at same potential, such as AA, dopamine, UA, and tryptophan. Additionally, the electrochemical discrimination of the hemin/GO/CNT electrode toward AA, dopamine, UA, and tryptophan is influenced by the difference in  $\pi$ - $\pi$  interaction of the respective molecules with the composite. The electrode showed 88.2–92.4% retention of the initial electrochemical signal after 7 days storage at 4 °C in a PBS buffer.

Another dual selective and sensitive biosensor for nicotinamide adenine dinucleotide (NADH) and  $\text{H}_2\text{O}_2$  has been successfully fabricated by Chen *et al.*<sup>246</sup> The authors modified a GCE with amino-functionalized MWCNTs, which were then used as a substrate immobilized with neutral red, poly(neutral red), and flavin adenine dinucleotide. For NADH and  $\text{H}_2\text{O}_2$ , the hybrid composite allows reduction overpotentials at +0.05 and  $-0.1$  V (*vs* Ag/AgCl), respectively. In contrast, on an unmodified GCE, there are no oxidation or reduction peaks observed over the  $-0.8$  to  $+0.4$  V range. The LODs for the biosensor were calculated to be 1.3 and 0.1 nM for NADH and  $\text{H}_2\text{O}_2$ , respectively. The biosensor was applied in the determination of NADH and  $\text{H}_2\text{O}_2$  in bovine calf serum samples with recovery rates of between 96 and 102%. Since both NADH and  $\text{H}_2\text{O}_2$  play a vital role in biological processes,

this dual biosensor could act as a springboard to develop biosensors using both oxidase and dehydrogenase.

Lou *et al.* reported a L-lysine/MWCNT-based composite-modified GCE could be used as a dual biosensor for  $\text{H}_2\text{O}_2$  and  $\text{IO}_3^-$ .<sup>80</sup> The biosensor was fabricated by coating a GCE with acid-functionalized MWCNTs onto which L-lysine was electrodeposited; this surface was then used to immobilize the heme protein catalase (CAT) (Figure 14). The advantage of using CAT as the bioactive unit is that it retains its enzymatic activity even after deposition on the L-lysine/MWCNT composite. Additionally, the MWCNTs facilitate the direct electron transfer with the electrode surface and the CAT. The study of these CAT/L-lysine/MWCNT/GCEs in different deoxygenated pH solutions shows that the modified electrode can be used for electroanalytical or other applications over a wide range of different pH values.

Glennon *et al.* reported that electrochemically deposited cadmium oxide (CdO) NPs, 50 nm diameter, on a GCE modified with MWCNT can be used in the detection of  $\text{H}_2\text{O}_2$ .<sup>247</sup> The biosensor exhibited a large electrocatalytic activity for  $\text{H}_2\text{O}_2$  at 1.2 V *vs* Ag/AgCl over a broad pH range. The authors note that CdO is favorable over other metal oxide NPs with respect to sensitivity, LOD (0.1  $\mu\text{M}$ ), selectivity of  $\text{H}_2\text{O}_2$ , and reproducibility. Interestingly, at pH 7, the sensor did not suffer interference from the injection of dopamine acid, UA, and AA, as well as exhibiting long-term stability. Wagberg and colleagues showed that a GCE modified with palladium NPs deposited on helical carbon nanofiber (HCNF) (Figure 15) coated with Nafion could be used for sensing  $\text{H}_2\text{O}_2$ , while the same electrode immobilized with GOx could be used in glucose sensing.<sup>248</sup> The advantage of this Nafion/Pd-HCNF/



GCE sensor over other electrodes for biosensing is that the NPs are well-distributed and small, offering superior electrocatalytic performance, while the HCNFs provide excellent conductivity and high surface area. The amperometric studies showed LODs of 3.0  $\mu\text{M}$  and 0.03 mM for  $\text{H}_2\text{O}_2$  and glucose sensing at an applied potential of 0.5 V.

Limtrakul *et al.* reported the size-tailored synthesis of polyvinylpyrrolidone (PVP) and 4-dimethylaminopyridine (DMAP)-capped AuNPs and their facile deposition onto anodic aluminum oxide-templated carbon nanotubes (AuNP/CNT) *via* electrostatic self-assembly.<sup>249</sup> The enhanced CV signal obtained from the AuNP/CNT material is ascribed to reduced charge transfer resistance from the small amount of capping agent on the Au surfaces and the dense/homogeneous distribution of AuNPs on the CNTs. This sensor gave a wide linearity range for  $\text{H}_2\text{O}_2$  detection from 5  $\mu\text{M}$  to 45.80 mM with the LOD of 0.23  $\mu\text{M}$ . More recently, the Manan group synthesized a AgNP–CNT–rGO composite, using a hydrothermal method, which showed excellent electrocatalytic activity for the reduction of  $\text{H}_2\text{O}_2$  with a rapid amperometric response time less than 3 s.<sup>250</sup> This composite exhibited a linear detection range of 0.1–100 mM, with a LOD of 0.9  $\mu\text{M}$ .

**Graphene.** Hwang and co-workers have reported a simple and cost-efficient green procedure for the reduction of GO and the synthesis of rGO/mono- and bimetallic hybrids using an *Azadirachta indica* extract as a reducing agent.<sup>251</sup> These materials were then used to fabricate nonenzymatic electrodes by coating the prepared hybrid materials on the surface of a GCE. The Ag–Au/rGO-based biosensor showed excellent selectivity, a wide linear response range (0.1–5 mM), stability, and LOD of  $\sim 1$   $\mu\text{M}$  for  $\text{H}_2\text{O}_2$ . The enhanced performance of this biosensor is believed to be due to (1) increased electrical conductivity, (2) enhanced catalytically active surface area, and (3) multiple active defective sites, including expanded interlayer spacing that can effectively trap the analyte.

As has been mentioned above, Gao *et al.* have shown that  $\text{H}_2\text{O}_2$  and glucose can be sensed utilizing a GCE functionalized with a  $\text{Ni}(\text{OH})_2/\text{ErGO}$ –MWCNT composite.<sup>132</sup> The LOD for  $\text{H}_2\text{O}_2$  was not as impressive as that obtained for the Ag–Au/rGO-modified electrode. However, it should be noted that this electrode does not suffer interference response from  $\text{K}^+$ ,  $\text{NO}_3^-$ ,  $\text{Na}^+$ ,  $\text{Cl}^-$ , UA, and AA, and it was applied in the detection of  $\text{H}_2\text{O}_2$  (104% recovery) in milk samples. Li *et al.* reported the electrochemical deposition of cobalt oxide NPs on the surface of a ErGO-modified GCE could be used as a reproducible and stable  $\text{H}_2\text{O}_2$  sensor.<sup>102</sup> This electrode showed a linear response range of 5  $\mu\text{M}$  to 1 mM and a LOD of 0.2  $\mu\text{M}$ , with a detection accuracy that is equivalent to the commonly used  $\text{KMnO}_4$  titration method.

It has been noted that catalysts synthesized by depositing metal or metal oxides onto graphene usually suffer from dissolution and agglomeration during voltammetric tests. These factors lead to degradation of the catalyst activity and hence the performance of the biosensors. To overcome these disadvantages, metals wrapped in graphene sheets have been investigated as catalysts. In this regard, Liu *et al.* reported the synthesis of enzymeless graphene-wrapped  $\text{Cu}_2\text{O}$  nanocube-modified GCEs that could be used in the detection of  $\text{H}_2\text{O}_2$  and glucose.<sup>252</sup> The  $\text{Cu}_2\text{O}$ /graphene electrode showed a good response toward  $\text{H}_2\text{O}_2$  (LOD, 20.8  $\mu\text{M}$ ) and glucose (LOD, 3.3  $\mu\text{M}$ ), with linear response ranges of 0.3 to 7.8 mM and 0.3 to 3.3 mM, respectively. The authors reported that the graphene coating on the  $\text{Cu}_2\text{O}$  nanocubes effectively improves the

electrochemical cycling stability of the fabricated sensor as well as the electron transfer rate. According to the authors, the graphene played a major role in detection performance in that it can (1) largely reduce the size of the nanocubes, (2) prevent the nanocubes from aggregating, and (3) enhance the electrochemical stability.

Nalini and colleagues fabricated an enzyme-based  $\text{H}_2\text{O}_2$  biosensor by the simultaneous electrodeposition of GO, AgNPs, and the enzyme (horseradish peroxidase or cholesterol oxidase) onto a graphite electrode.<sup>253</sup> These electrodes showed  $\text{H}_2\text{O}_2$  LODs of 0.514 and 5  $\mu\text{M}$  for the GO/AgNP–cholesterol oxidase/GCE and GO/AgNP–horseradish peroxidase/GCE, respectively. Both of these electrodes showed optimized response at pH 7 and negligible amperometric response to the addition of interfering agents AA, UA, and dopamine. The authors showed that the pH and temperature effect are directly related to the enzymatic activity of the horseradish peroxidase and cholesterol oxidase. Interestingly, these enzymes exhibit a large catalytic activity which is believed to be due to the AgNP/GO microenvironment. In another study, it has been reported that nickel oxide can be electrodeposited onto an ErGO-coated GCE electrode.<sup>254</sup> This electrode can then be further modified using the myoglobin protein and Nafion to give a  $\text{H}_2\text{O}_2$  and trichloroacetic acid sensor that functioned in PBS at a pH of 3. After 3 weeks of storage, this electrode exhibited 94% of its initial response and an initial LOD of 0.71  $\mu\text{M}$  for  $\text{H}_2\text{O}_2$ .

Fan *et al.* have shown that enzyme loss and catalytic deactivation of horseradish peroxidase in a  $\text{H}_2\text{O}_2$  sensor can be overcome by encapsulating the peroxidase in graphene capsules.<sup>255</sup> This hybrid material was then deposited in a layer-by-layer method with poly(sodium 4-styrenesulfonate) onto a ITO surface to form a  $\text{H}_2\text{O}_2$  biosensor with a wide linear response range of 0.01–12  $\text{mmol L}^{-1}$  and a LOD of 3.3  $\text{mmol L}^{-1}$ .

To provide another alternative to avoid catalytic degradation due to enzyme loss, Yang *et al.* reported a nonenzymatic  $\text{H}_2\text{O}_2$  sensor by modifying graphene with cobalt hexacyanoferrate NPs (CoHCFNPs).<sup>256</sup> Additionally, there are several other reports which focus on nonenzymatic  $\text{H}_2\text{O}_2$  detection, wherein graphene modified with complexes or nanocomposites of metals like Ag, Au, Pt, and Cu have been utilized.<sup>257–260</sup>

**DNA and MicroRNA Sensing.** In recent years, there has been an increasing interest in the study of DNA sensing due to their fundamental significance in life sciences (e.g., gene identification, molecular diagnostics, pathogen detection, and forensic investigation). Among the various DNA analyses techniques, developing highly sensitive voltammetric biosensors for the detection of specific oligonucleotide sequences (especially at low concentrations equivalent to physiological levels) has recently attracted considerable interest.

Graphene has the ability to interact strongly and uniquely with the various nucleobases; in this way, it has been reported by Kim and co-workers that graphene can be used in ultrafast DNA sequencing.<sup>13,261,262</sup> These techniques allow for single-molecule sensing by utilizing the quantum conductance effect. By applying gate voltage, the quantum conductance gives the finger prints of the HOMO energy levels of adsorbed nucleobases, which can then be utilized for 2D molecular electronics spectroscopy. This is important as it allows for the sensing of single DNA methylations, which is important in cancer detection.<sup>14,263</sup> Usually, DNA biosensors are electrodes modified with a DNA probe molecule, which can then interact

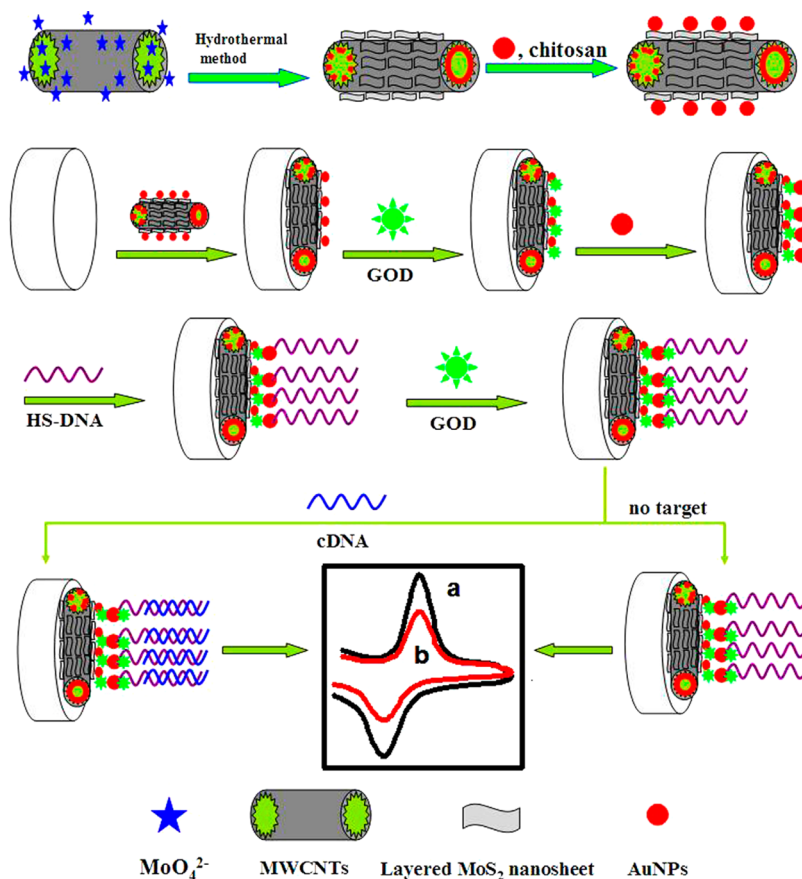


Figure 16. Schematic procedure for DNA biosensor fabrication. Glucose oxidase (GOD) is immobilized onto the MoS<sub>2</sub>-MWCNT/AuNP-modified surface. Onto this GOD-modified surface, the ssDNA (HS-DNA) probe molecule was attached. This electrode could then be using in the detection of femtomolar concentrations of target DNA (cDNA). Adapted with permission from ref 269. Copyright 2014 Elsevier B.V.

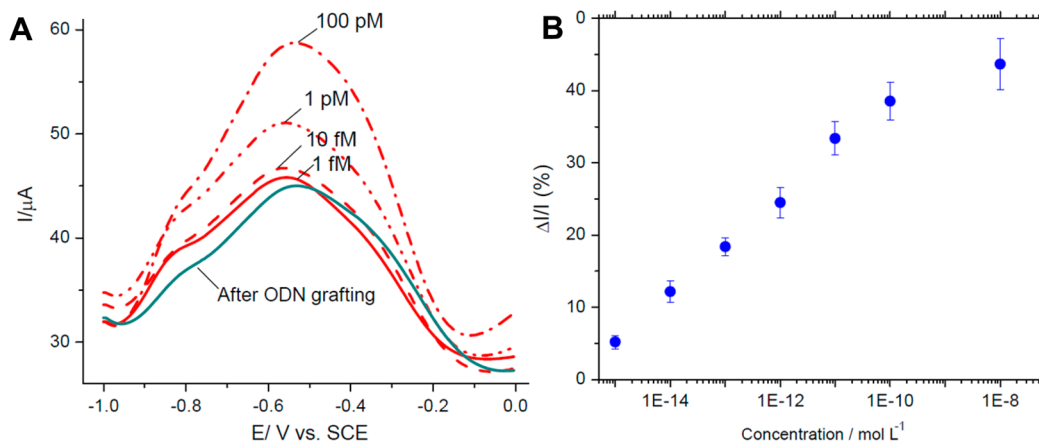


Figure 17. (A) Single-wave voltammograms recorded on the ODN-141-P-modified electrode with and without hybridization with complementary miRNA-141: 1 fM, 10 fM, 1 pM, and 100 pM. (B) Relative change in current upon hybridization with concentrations of miRNA-141 spanning the 1 fM to 10 nM range. Adapted from ref 75. Copyright 2013 Elsevier B.V.

and produce a voltammetric signal with introduction of the DNA analyte.

Both CNTs and graphene are ideal candidates for use in DNA and RNA sensing as they are able to form  $\pi$ - $\pi$  bonds between their conjugated  $\pi$  systems and the nucleobases. Additionally, due to their inherent electrical conductivity, these materials amplify the DNA/RNA sensing signal. This is important because the DNA/RNA sensing signal is usually

weak and requires various methods of amplification such as addition of electron shuttling enzymes or NPs.<sup>76,264–267</sup>

**Carbon Nanotubes.** To differentiate between single-stranded DNA (ssDNA) and double-stranded DNA (dsDNA), Kashanian *et al.* reported that a chitosan-CNT-modified GCE electrode can be used in conjunction with the copper probe molecule [Cu(2,9-dimethyl-1,10-phenanthroline)(1,10-phenanthroline-5,6-dion)Cl]Cl.<sup>244</sup> The ssDNA or dsDNA was immobilized onto the modified

electrode surface, and then [Cu(2,9-dimethyl-1,10-phenanthroline)(1,10-phenanthroline-5,6-dion)Cl]Cl was introduced with a concentration of 20  $\mu\text{M}$ .<sup>268</sup> Considerably larger and well-defined redox peaks are observed for dsDNA than ssDNA, which indicates that the copper complex binds preferentially to the dsDNA-immobilized electrode surface. This indirect method can, as such, be used to electrochemically discriminate between dsDNA and ssDNA.

In another study, Huang and colleagues reported DNA signal amplification through modification of a GCE using multiple amplification methods, such as AuNPs, GOx, and a molybdenum disulfide/MWCNT (MoS<sub>2</sub>/MWCNT) composite (Figure 16).<sup>269</sup> The MoS<sub>2</sub>/MWCNT composite material is chosen due to its extraordinary electrical conductivity, while GOx was chosen as it does not require a mediator in direct electron transfer DNA detection; these two components as such result in faster response and larger sensitivity. This biosensor exhibited a LOD of 0.79 fM for the target DNA and could be applied in target DNA sensing in serum samples. The selectivity of the sensor is impressive with single- and triple-base mismatches detected as well as long-term stability (*i.e.*  $\sim 3.9\%$  decrease after 15 days).

Miodek *et al.* employed a two-step electrochemical patterning method to fabricate a biosensor that consists of MWCNTs, polypyrrole (PPy), redox polyamidoamine dendrimers, and the redox marker ferrocene for electrochemical DNA detection.<sup>270</sup> This hybrid material shows good performance in the electrochemical detection of DNA hybridization with a LOD of 0.3 fM. Additionally, the authors showed that they could identify the *rpoB* gene of *Mycobacterium tuberculosis* in PCR samples.

Pham *et al.* modified a GCE with an electroactive polymer 5-hydroxy-1,4-naphthoquinone-*co*-(3-(5-hydroxy-1,4-dioxo-1,4-dihydronaphthalen-2(3)-yl)propanoic acid/CNT composite for the label-free (reagentless) detection of the microRNA prostate cancer biomarker (miRNA-141) with a LOD of 8 fM.<sup>75</sup> The probe DNA (ODN-141-P) was immobilized on the modified electrode and showed a selective voltammetric response to the miRNA-141 target molecule (Figure 17). Additionally, no interference was detected for the noncomplementary miRNA sequences molecules miR-103 and miR-29b-1. The authors chose the nanostructured polymer film as it possesses very large electroactivity in neutral aqueous medium. This activity is due to the quinine group embedded in the polymer backbone. In the same way, Tang and co-workers utilized a GCE modified with MWCNT onto which the DNA probe for miRNA-24 was immobilized for the label free electrochemical detection of cell proliferation miRNA-24.<sup>271</sup> The DPV method used in this study for the detection of miRNAs is based on the enhancement in the oxidation peaks of guanine and adenine in the miRNA probe and target. It is believed that this signal enhancement is due to the probe miRNA no longer coiling around the MWCNTs (which quenches the electrochemical signal) but binding with the miRNA-24 which allows enhanced electrochemistry. The LOD of the composite material was determined to be 1 pM, which is 3 orders lower than that of existing screen-printed electrodes modified with electro-deposited inosine-substituted capture sensors for miRNA-122 detection.

The Tang group has prepared a MWCNT–polyamidoamine dendrimer, methylene blue as a redox indicator, and hybrid material by a simple electrochemical method for sensing of microRNA (miRNA).<sup>272</sup> The as-manufactured biosensor

exhibited an LOD of  $\sim 0.5$  fM and a linear range up to 100 nM. The hybrid was also successfully applied in the detection of miRNA-24 in a total RNA sample extracted from HeLa cells.

**Graphene.** Zhang and colleagues reported that functionalizing graphene with amino groups led to far more successful immobilization of probe DNA than is found using unmodified graphene.<sup>273</sup> The authors showed that this modified DNA biosensor exhibited a greater detectable change using an electrochemical quartz crystal microbalance,  $\Delta F = 121.57$  Hz versus  $\Delta F = 18.63$  Hz, for unmodified graphene. This biosensor could then be applied in the ultrasensitive detection of target DNA with a LOD of 0.8 nM under optimized conditions. In the same way, Du *et al.* showed that an ErGO-modified GCE with an immobilized peptide nucleic acid (PNA) probe could be used for DNA detection *via* PNA–DNA hybridization.<sup>274</sup> To electrochemically visualize the hybridization event, the electrochemical indicator methylene blue (MB) is added, which intercalates in the grooves of the dsDNA. Interestingly, the peak currents for MB reduction increase linearly with the logarithm of the complementary target DNA concentrations, and as such, the linear DNA range extends from 100 nM to 1 pM with a LOD of 0.545 pM. The DNA sensor showed high sensitivity and specificity for the detection of the target DNA, with one nuclear base mismatch recognition, due to the utilization of the probe PNA and the ability of ErGO to increase the electron transfer reaction rate. In the same way, it has been shown that the DNA sequence related to transgenic maize (MON810) can be sensed on an ErGO-functionalized carbon ionic liquid electrode on which the probe DNA was immobilized.<sup>275</sup> This illustrates the applicability of these types of electrodes. As transgenic maize can only be sold in certain markets worldwide, such sensing abilities could be readily applied.

As with CNTs, significant efforts have been directed at increasing the sensitivity of graphene-based biosensors through amplification.<sup>103,276–278</sup> These amplification methods include functionalization with enzymes, NPs, orientation of the probe DNA, and inclusion of the highly conductive graphene materials.

To increase the sensitivity of their biosensor, Wang *et al.* electrochemically deposited AuNPs onto a rGO-functionalized GCE, whereafter the probe DNA was immobilized on the AuNPs through a thiol bond.<sup>103</sup> The use of these AuNPs led to an increase in selectivity (single base mismatch discrimination) and sensitivity (LOD, 0.35 fM). Interestingly, over a 1 week period, the authors noted negligible change in voltammetric response reproducibility, indicating the stability of the biosensor. Cao and colleagues modified a GCE with a GO/MoS<sub>2</sub>/AuNP composite onto which the probe DNA was immobilized.<sup>277</sup> This probe DNA was then allowed to bind with the complementary DNA target strand in a solution which contained AuNPs coated with horseradish peroxidase as an electrochemical indicator to amplify the sensing signal. Due to this amplification enhancement, this electrode exhibited a linear sensing region of 50 fM to 5.0 nM with a LOD of 2.2 fM. In a similar way, Huang *et al.* showed that a GCE can be modified with a WS<sub>2</sub>/GO material onto which AuNPs and subsequently probe DNA was immobilized.<sup>278</sup> Both of these biosensors, which include group six sulfide materials, exhibit selectivity for single- and three-base DNA mismatches. Interestingly, the inclusion of group 6 sulfide materials required the use of chitosan to effectively immobilize the probe DNA, even in the



presence of AuNPs, which was not needed when these materials were absent.<sup>103,277,278</sup>

There have been many reports on AuNP-modified graphene nanostructures for electrochemical detection of DNA.<sup>279–282</sup> Interestingly, the AuNPs can be replaced with cheaper AgNPs to amplify the signal, as has been shown by Huang and co-workers.<sup>283</sup> In this study, the authors used the electroactive dye methylene blue to increase the sensitivity of the AgNP/polydopamine–graphene/probe DNA-functionalized GCE. Importantly, the authors added 6-mercaptopentanol after immobilization of the probe DNA to orientate the probe DNA in a way that allows for good biosensing. The multiple amplification methods used in this study, such as conductive polymer, probe orientation, AgNPs, allowed for a LOD of 3.2 fM and a linear sensing range of 0.1 pM to 0.1 nM.

Zheng *et al.* reported that 5-methylcytosine and cytosine can be simultaneously determined in basic solution with the use of an ErGO-modified GCE.<sup>284</sup> This biosensor showed LODs for 5-methylcytosine and cytosine of 0.7 and 0.9  $\mu\text{M}$ , respectively. Interestingly, this electrode could be used in the determination of cytosine and 5-methylcytosine in oligonucleotides. This result is important as methylation of nucleotides is associated with cancers. The ultrasensitive biosensing ability of graphene toward the different nucleobases has been demonstrated by Akhavan and colleagues.<sup>285</sup> In their study, the authors showed that a solution containing a mixture of the four nucleobases, ssDNA, or dsDNA can be quantitatively analyzed to determine the amount of nucleobases in the target solution using a graphite electrode modified by electrodeposition of graphene nanowalls. The LOD for the biosensor was determined to be 9.4 zM with a linear sensing range of 0.1 fM to 10 mM. The stability of this electrode in a nucleobase solution is impressive with no decrease in current response over 100 scans; however, in oligonucleotide solutions, the current reduction was 35% over 10 scans. This reduction in current is accompanied by 25% standard deviation between electrode batches. For these reasons, multiple groups have attempted to stabilize graphene-based biosensors for nucleobase detection.

By coating a GCE with rGO and then electrochemically depositing poly[2,6-pyridinedicarboxylic acid], Li *et al.* showed that their fabricated (GCE/rGO/poly(2,6-pyridinedicarboxylic acid)) biosensor could be used in the simultaneous determination of guanine and adenine.<sup>286</sup> This electrode displayed stability during the simultaneous detection of guanine (LOD, 0.01  $\mu\text{M}$ ) and adenine (LOD, 0.02  $\mu\text{M}$ ). However, with the introduction of the other nucleobases, in the form of calf thymus DNA, the electrode was shown to be unstable. In two separate reports, the group of Yang has shown that poly(xanthurenic acid) can be electrochemically deposited on a GO-modified GCE, which can then be used in the simultaneous determination of guanine and adenine.<sup>287,288</sup> The authors showed in these papers that depending on the electrodeposition method employed the LOD can be altered. When a pulse potentiostatic method was employed, the LOD for adenine and guanine were 0.6 and 0.4  $\mu\text{M}$ , respectively. However, when a cyclic voltammetry deposition method was employed, the LOD for adenine and guanine were 0.15 and 0.032  $\mu\text{M}$ , respectively. The authors believe the sensitivity and stability of these biosensors are due to the interface of the poly(xanthurenic acid)/GO, which is rich in negative charges and has a large surface area that contributes to enhancement in the adsorption of the positively charged guanine and adenine through strong  $\pi$ – $\pi^*$  interactions or electrostatic adsorption.

Zheng *et al.*<sup>289</sup> fabricated a multilayer-by-layer assembly of polyaniline/pristine graphene composite, DNA probe, and bovine serum albumin for the electrochemical detection of DNA. The biosensor is capable of sensing the complementary DNA from 0.01 pM to 1  $\mu\text{M}$  depending on the ratio of polyaniline to graphene. Being a strong organic conductor with charges, polyaniline helps otherwise weakly adhesive graphene to stick to the GCE, thereby enhancing stability and performance of the biosensor. Jafari *et al.*<sup>290</sup> also employed a multilayered polyaniline, GO, probe DNA, and cerium oxide NP-modified electrode to detect ssDNA. In this study, fast Fourier transform square-wave voltammetry of the ssDNA immobilized on the surface was detected electrochemically using the added  $[\text{Ru}(\text{bpy})_3]^{2+/3+}$  redox pair. The biosensor was able to detect the target *Aeromonas hydrophila* DNA oligonucleotide sequence over a linear range of  $1 \times 10^{-15}$  to  $1 \times 10^{-8}$  mol L<sup>-1</sup> and was applied to a real sample for detection of DNA extracted from *A. hydrophila* with a LOD of 0.01 mg mL<sup>-1</sup>.

Recently, GO-modified pencil graphite electrodes (PGEs) were prepared by immobilizing GO on the electrode through a passive adsorption technique. This electrode could then be used in the electrochemical determination of miRNA-34a RNA when a miRNA-34a complementary DNA probe was introduced into the analyte solution.<sup>291</sup> The bioprobe and fabricated sensor shows selective response toward the target miRNA with a LOD of 28.1 pmol.

Hu *et al.*<sup>292</sup> reported a simple electrochemical RNA biosensor based on biocompatible graphene quantum dots (GDQ) which were deposited onto a DNA-modified electrode and then further functionalized with horseradish peroxidase (HRP). The HRP catalyzes H<sub>2</sub>O<sub>2</sub>-mediated oxidation of 3,3',5,5'-tetramethylbenzidine (TMB), which results in a strong electrochemical reduction signal; this translates into a LOD of 0.14 fM. Azimzadeh *et al.*<sup>293</sup> fabricated a biosensor based on a GCE electrode functionalized with thiolated probe-functionalized gold nanorods attached to GO sheets. This sensor was then applied in the detection of miRNA-155 with a LOD of 0.6 fM and a linear detection range of 2.0 fM to 8.0 pM.

**Other Analyte Sensing. Carbon Nanotubes.** CNTs have been successfully used in the field of voltammetric biosensors to greatly enhance the response signal and sensitivity for a variety of other analytes. This is especially noteworthy in the pharmaceutical, and medical industries in the sensing of molecules, such as the anti-HIV drug zidovudine,<sup>84</sup> the anxiolytic buspirone hydrochloride,<sup>294</sup> the neuroleptic promethazine,<sup>295</sup> the anticancer drug 5-fluorouracil,<sup>296</sup> paracetamol,<sup>297</sup> levodopa,<sup>298</sup> and the selective serotonin receptor agonist zolmitriptan among many others.<sup>94</sup> Additionally, these biosensors have been used in the detection of multiple biologically relevant molecules such as the ascorbate anion,<sup>299</sup> mesalazine,<sup>300</sup> fluvoxamine,<sup>301</sup> carbohydrates,<sup>302</sup> the hazardous pollutants amitrole,<sup>85</sup> and bisphenol A,<sup>87,303</sup> xanthine,<sup>304</sup> 17 $\alpha$ -ethinylestradiol,<sup>305</sup> as well as the neurotransmitters serotonin<sup>306,307</sup> and epinephrine.<sup>308</sup>

Zidovudine is an anti-retroviral drug used in the treatment of HIV; however, zidovudine is very toxic, and as such, its detection and determination in human serum is of critical importance. In this vein, a zidovudine sensor has been fabricated by Rafati *et al.*, who electrodeposited a Ag nanofilm onto a MWCNT-modified GCE.<sup>84</sup> This biosensor was applied in the detection of zidovudine in human plasma with an average recovery rate of 98.6%. In another study, Uslu *et al.* showed that

a AgNPs/MWCNT/GCE prepared by casting MWCNTs and AgNPs on a GCE could be used in the voltammetric determination of the selective serotonin receptor agonist zolmitriptan.<sup>94</sup> The biosensor displayed a LOD for zolmitriptan of 1.47 nM and was not effected by interfering agents in human urine samples as well as additives in a commercially available drugs.

The use of psychosomatic drugs is becoming more significant worldwide as the stigma associated with mental illness (*i.e.*, anxiety disorder, depression, schizophrenia, *etc.*) is fading due to education and awareness. Buspirone hydrochloride is an anxiolytic widely used for the treatment of anxiety disorder with the added benefit that it does not create a physical dependence.<sup>308,309</sup> Cheemalapati *et al.* have shown that a simple MWCNT-modified GCE can be used for the sensitive detection of buspirone hydrochloride.<sup>294</sup> Depending on the potentiometric method employed for detection, the LOD was determined to be 0.22 or 0.18  $\mu\text{M}$  for the CV or DPV method, respectively. In the determination of buspirone hydrochloride in commercially available tablets, the biosensors exhibited a recovery rate of 96–100%. Similarly, Rivas and colleagues have shown that promethazine can be quantified using a bamboolike MWCNT-modified GCE.<sup>295</sup> To increase the dispersion of the MWCNTs, the authors employed calf thymus dsDNA which resulted in the MWCNTs being well-separated and affording grooves between the double helix where promethazine can bind to undergo oxidation. In contrast, when calf thymus ssDNA is used, there are no grooves for the promethazine to bond to, resulting in a decrease in the oxidation peak and thus sensitivity. The LODs for the GCE/MWCNT dsDNA and the GCE/MWCNT ssDNA were calculated to be 0.023 and 0.39  $\mu\text{M}$ , respectively. This increase in sensitivity is believed to be due to the preconcentration effect that occurs when the dsDNA interacts with the promethazine.

Furthermore, the Lorenzo group reported the fabrication of insulin sensors based on GCEs modified with Nafion multiwalled CNTs coated with nickel hydroxide NPs.<sup>310</sup> Under optimum conditions, this electrode exhibited impressive sensitivity ( $5.0 \text{ A mol cm}^{-2} \mu\text{M}^{-1}$ ), low LOD (85 nM), negligible surface fouling, and wide dynamic range (up to 10.00  $\mu\text{M}$ ), which is ascribed to the large specific surface area and high electrical conductivity of this hybrid material. Additionally, this electrode is capable of sensing insulin in the presence of interfering substances such as AA, UA and acetaminophen.

Madrakian *et al.* have fabricated a MWCNT-modified GCE for the reproducible and stable simultaneous determination of the immunosuppressant mycophenolatemofetil and its active metabolite mycophenolic acid.<sup>311</sup> The LODs for mycophenolatemofetil and mycophenolic acid were determined to be 0.9 and 0.4  $\mu\text{M}$ , respectively. These biosensors were applied to determine the analytes in urine and serum samples and were found to have a sensitivity equivalent to the HPLC determination method. To determine the concentration of the cholesterol-lowering drug atorvastatin calcium in serum and urine samples, Filho and co-workers fabricated what they termed a vertically aligned CNT/GO electrode grown on a Ti substrate.<sup>82,91</sup> The analysis method employed relies on differential pulse adsorptive stripping voltammetry. To improve this performance the CNT tips were exfoliated to increase the edge plane density and surface area by exposing the structure of the graphene. The LOD of the biosensor was determined to be 9.4 nM, and the biosensor did not experience voltammetric response from the excipients commonly found in pharmaceut-

ical makeups such as microcrystalline cellulose, croscarmellose sodium, lactose monohydrate, magnesium stearate, and calcium carbonate. In a similar way, Cesarino and colleagues have shown that the antibiotic Levofloxacin can be detected using a Au electrode modified with a vertically aligned CNT/ssDNA composite material.<sup>82</sup> The biosensor exhibited a LOD of 75.2 nM and was used in the detection of Levofloxacin in human urine samples with recovery rates of 97–101%. This biosensor gives results equivalent to those obtained using HPLC; however, it has the added benefit of onsite screening which is not applicable to HPLC.

Vitamin C is widely applied in the pharmaceutical, chemical, cosmetic, and food industry as an antioxidant supplement; for this reason, its determination is of importance in multiple fresh fruits *etc.* Gheibi *et al.* have shown that a paste electrode fabricated by mixing graphite, MWCNTs, *p*-aminophenol, and paraffin can be used in the stable, sensitive, and reproducible voltammetric determination of AA in fresh fruit and vegetable juices.<sup>83</sup> This modification with *p*-aminophenol allows the oxidation peak for AA to be moved 320 mV less positive compared to the unmodified graphite/MWCNT paste electrode. The biosensor exhibits a LOD of 0.8 nM and AA analysis values that are equivalent to those obtained using the official 2,6-dichlorophenolindophenol titration method. Vitamin C is important as an antioxidant; however, in the ascorbate form, it is also physiologically important as a regulator in multiple neurotransmission pathways.<sup>312</sup> For this reason, Mao *et al.* have fabricated a vertically aligned CNT-sheathed carbon nanofiber microelectrode for the *in vivo* determination of ascorbate in rat brains.<sup>299</sup> Importantly, the electrodes' ascorbate determination performance was not inhibited by the *in vivo* interfering substances glutamate, dopamine, UA, 5-hydroxytryptamine, and ascorbic oxidase. Although the LOD was not reported for this biosensor, the authors did show that the basal level of striatum ascorbate measured ( $0.25 \pm 0.06 \text{ mM}$ ) was within the expected range.

To simultaneously determine the concentration of four carbohydrates, Chen *et al.* reported the use of a CNT–nickel NP paste electrode that relies on a CV and capillary electrophoresis method.<sup>302</sup> The LODs for the sugars (sucrose, glucose, fructose) and the sugar alcohol (mannitol) were 0.21, 0.23, 0.32, and 0.14  $\mu\text{M}$ , respectively. These electrodes were successfully applied in the determination of these four sugars in an herbal drug, demonstrating its real-life application. To selectively determine the sucrose concentration in sugar beets, Ensafi and colleagues employed a MWCNT-modified GCE coated with sucrose-imprinted electropolymerized *o*-phenylenediamine layer.<sup>313</sup> The imprinting was obtained by polymerizing the *o*-phenylenediamine in the presence of sucrose onto the MWCNT/GCE electrochemically, whereafter the sucrose template was removed using an acetonitrile/acetic acid solution. This biosensor was then incubated in the analyte solutions to immobilize the sucrose. After this immobilization, the sucrose was electrochemically oxidized to determine its concentration with a LOD of 3  $\mu\text{M}$ .

Amitrole is an herbicide widely used in agricultural practices; however, the EPA and European Union have banned its use in food crops due its known carcinogenic effect. For this reason, Ensafi *et al.* fabricated a modified pencil graphite electrode biosensor for the voltammetric determination of amitrole in water and soil samples.<sup>85</sup> The pencil graphite electrode was modified first by dip-coating in a suspension of MWCNTs and chitosan and then immobilizing dsDNA on this layer.

Importantly, as noted in the promethazine study of Rivas,<sup>295</sup> only the dsDNA was able to intercalate the amitrole in the DNA grooves. The LOD for this biosensor was calculated to be 0.017 ng mL<sup>-1</sup>, and the detection capacity was not affected by multiple cations, organic herbicides, and anions in concentrations 300–1000 times larger than the analyte concentration. Other toxic compounds, such as bisphenol A, have been detected using CNT-modified electrodes. For example, Han and colleagues have shown that a GCE coated with a SWCNT/polylysine/tyrosinase composite material can be used in the successful determination of bisphenol A with a LOD of 0.97 nM.<sup>87</sup> This sensor was used to determine the concentration of bisphenol A in plastic spoon samples with a detection capability equivalent to that of HPLC. Wang *et al.* have fabricated an amperometric immunosensor for the detection of the organophosphate insecticide chlorpyrifos by drop-coating a GCE with a MWCNT/thionine/chitosan nanocomposite film onto which the antichlorpyrifos monoclonal antibody was immobilized.<sup>86</sup> This sensor could be applied in the determination of chlorpyrifos in the presence of the interfering agents carbofuran, phoxim, carbaryl, and 3-hydroxycarbofuran. The sensor displayed a LOD of 46 pg mL<sup>-1</sup> and could be successfully employed in the detection of chlorpyrifos in vegetable samples. The sensor exhibits reproducible results upon washing the immobilized chlorpyrifos from the antichlorpyrifos monoclonal antibody by immersion into a 0.1 M glycine–HCl solution. However, this reproducibility wanes after 10 cycles, indicating the antibodies gradual removal. In another study, de Wael and co-workers showed that by immobilizing an analyte specific aptamer on a MWCNT-modified GCE, hydroxylated polychlorinated biphenyls in human serum could be determined with a LOD of 7.1  $\mu$ M.<sup>314</sup> In contrast, the biosensor exhibited a LOD of 0.01  $\mu$ M in a pH 7.4 solution. With the use of an aptamer specifically binding to hydroxylated polychlorinated biphenyls, no interference is observed when molecules with similar structure, such as butyl paraben, matairesinol, and bisphenol A, are added.

For the sensing of the ascorbate ion, the determination of the neurotransmitters serotonin and epinephrine is highly important.<sup>312</sup> Lou *et al.* have shown that the organic dye basic red 9 can be electropolymerized on a f-MWCNT-coated GCE film.<sup>306</sup> This manufactured biosensor can then be used in the stable determination of serotonin (LOD, 7.0  $\mu$ M) and epinephrine (LOD, 9.0  $\mu$ M) using a DPV method. By injecting serotonin or adrenaline into bovine calf serum, the manufactured biosensor exhibited recovery rates of 103 and 106%, respectively. Utilizing a Pt electrode modified with a MWCNT/polypyrrole layer onto which AgNPs were electrodeposited from a colloidal AgNP solution, Machado *et al.* determined serotonin levels in serum samples using a DPV method.<sup>307</sup> This sensitive biosensor exhibited high reproducibility and reproducibility with a LOD of 0.15  $\mu$ M. For practical applications, the analysis of serotonin in the plasmatc serum sample showed recovery rates between 97.9 and 103.1% for samples spiked with 1.0, 1.5, and 2.0  $\mu$ M of serotonin.

In a novel use of a biosensor, Sun *et al.* have shown that a GCE modified with a functionalized MWNT/CD8+ T-cell antibody mixture could be employed to count CD8+ T-cells which play an important part in acute cellular rejection in liver transplants.<sup>315</sup> The biosensors' voltammetric response relies on the electrochemistry of the K<sub>3</sub>[Fe(CN)<sub>6</sub>] probe when there is an interaction between the CD8+ T-cells and antibodies at the electrode interface; this creates a barrier for electron transfer

which results in a lower current signal for the probe. This biosensor was shown to have a linear response range of 50–6000 cells mL<sup>-1</sup> and a LOD of 40 cells mL<sup>-1</sup>.

**Graphene.** As for CNT-based biosensors, graphene-based biosensors have been employed in the detection of multiple analytes which have significance in the pharmaceutical, food and medical fields among many others. For example, Jain *et al.* modified a GCE by drop-coating a mixture of graphene and polyaniline–Bi<sub>2</sub>O<sub>3</sub> to form a hybrid film.<sup>316</sup> The as-fabricated biosensor was then applied in the sensitive and selective voltammetric detection of anti-inflammatory drug etodolac. The biosensor exhibited a LOD of  $\sim$ 10.03 ng mL<sup>-1</sup> and was successfully applied in the determination of etodolac in pharmaceutical formulations with mean recovery rates of 98.76%. In another study, it has been shown that the antipyretic and analgesic drug acetaminophen can be detected using a GCE modified with NiO NPs and ErGO.<sup>317</sup> The electrodes were fabricated either through the simultaneous electro-deposition of ErGO/NiO NPs or by sequential electro-deposition of ErGO followed by NiO NPs. The biosensor formed using the one-step process displayed a LOD of 20 nM and was successfully applied in the determination of acetaminophen in commercial pharmaceutical tablets and urine samples. The sensitive determination of the acetaminophen using this biosensor is believed to be due to the favorable redox kinetics at the ErGO/NiO NPs, which affords a large accessible reactive area and catalytic activity.

To detect the bacteriocidal antibiotic drug kanamycin, Wei and co-workers have shown that an immunosensor can be fabricated by modifying a GCE with graphene which was further functionalized with glutaraldehyde and Ag@Fe<sub>3</sub>O<sub>4</sub> NPs onto which the kanamycin antibody was attached.<sup>318</sup> These biosensors (LOD, 15 pg mL<sup>-1</sup>) were successfully applied in the detection of kanamycin in pork meat. The sensors detection ability is believed to be due to graphene's large specific surface area, which allows more kanamycin to be immobilized and excellent electrical conductivity which promotes electron transfer. Phenformin is a mostly banned antidiabetic agent due to the fact that it can cause lactic acidosis; however, it still occurs in some herbal remedies *etc.* In this vein, Zeng *et al.* modified a GCE by drop-coating a graphene/CdS composite film, onto which DNA was immobilized.<sup>319</sup> This biosensor (LOD, 0.34  $\mu$ M) was then applied in the determination of phenformin in urine and pharmaceutical formulations with recovery rates of 92–94%. The biosensor determination relies on the indirect measurement of the electro-oxidation of guanine and adenine, which decreases as phenformin interacts with the DNA.

Graphene sensors have been applied in the detection of toxic compounds, as demonstrated by Wang and colleagues, who modified a GCE with a CoO/rGO composite for the simultaneous detection of the pesticide carbofuran and insecticide carbaryl.<sup>320</sup> This electrode showed the linear response over a wide concentration range of 0.2–70  $\mu$ M for carbofuran and 0.5–200  $\mu$ M for carbaryl, with LODs of 4.2 and 7.5  $\mu$ g/L, respectively. This electrode was also employed in the detection of carbofuran and carbaryl in fruit and vegetables with recovery rates of 96–104%, which is equivalent to results obtained using HPLC. Eissa *et al.* have developed a label-free voltammetric biosensor for the sensitive detection of the cyanobacterium produced toxin microcystin-LR.<sup>321</sup> The authors immobilized the MC-LR-targeting aptamer onto graphene-modified SPCE electrodes. The specificity of this



aptamer allows for highly selective and sensitive analyte detection. The LOD of the developed biosensor was 1.9 pM, and it was successfully applied in the determination of microcystin-LR in fish samples. One big advantage of using this sensor is that it does not require the fabrication of a labeled MC-LR-targeting aptamer which reduces costs and complexity of the biosensor.

Tuantranont *et al.* have reported that a screen-printed electrode coated with a graphene/Cu(II)-phthalocyanine-tetrasulfonic acid tetrasodium salt/polyaniline hybrid material can be used in the selective determination of AA.<sup>104</sup> This biosensor was not affected by the addition of dopamine and UA interfering agents and exhibited a LOD of 63 nM. In this hybrid, CuPc working as catalyst for the oxidation of ascorbic acid, while graphene increases the electrochemical surface area, enhances the immobilization (by  $\pi$ - $\pi$  interaction) of CuPc and the electron transfer between CuPc and working electrode. Xia and co-workers have reported the sensitive detection of the vitamin folic acid using a GCE modified with rGO onto which polypyrrole and Keggin-type phosphomolybdic acid were electrodeposited.<sup>322</sup> Two of the three oxidation peaks of the phosphomolybdic acid are utilized in the biosensing, as the introduction of folic acid results in a linear decrease in the oxidation peak potential with an increase in concentration. This biosensor exhibited a LOD of 30 pM and could be applied in folic acid detection in human serum with recovery rates between 95 and 101%.

Besides the detection of vitamins, the sensing of sugars and other natural products is highly desired for medical as well as food processing application. Antiochia *et al.* have reported that a commercially available screen-printed graphene electrode can be modified by casting an osmium-polymer/fructose dehydrogenase solution onto its surface.<sup>323</sup> This electrode could then be used in the sensing of fructose (LOD, 0.8  $\mu$ M) in the presences of the interfering agents AA, glucose, and sucrose. This electrode displays remarkable stability with retention of 95% of its initial amperometric response after 2 months. When applied in the detection of fructose in various fruit and beverage samples, this sensor exhibited a performance equal to that of a commercially available enzymatic spectrophotometric assay kit.

By electrodepositing a nitrogen-doped graphene/CNTs (NGR-NCNTs) hybrid onto a GCE, Jiang *et al.* reported the simultaneous and sensitive voltammetric determination of caffeine and vanillin.<sup>324</sup> Under optimized conditions, this biosensor displayed LODs of 0.02 and 0.0033  $\mu$ M for caffeine and vanillin, respectively. This biosensor was applied to real samples using two methods: (a) the direct determination method of the analytes in a chocolate chip cookie and (b) the standard addition method for detection in chocolate and milk tea. In another study, Yang and co-workers have shown that caffeine and theophylline can be simultaneously detected using a AuNP-chitosan-ionic liquid (1-butyl-3-methylimidazolium tetrafluoroborate) composite coated onto a rGO-modified GCE.<sup>325</sup> From SEM and TEM analysis, it can be seen that the AuNPs are evenly distributed in the films. The LODs for caffeine and theophylline were calculated to be 1.32 and 4.42 nM, respectively. This electrode displayed good stability after 60 days (93% response retention) and could be used in the determination of analytes in beverages, pharmaceutical formulations, as well as serum and urine samples.

Gallic acid, ferulic acid, and caffeic acid are naturally occurring products that may have potential use in various medical applications. To determine the concentration of gallic

acid in green and black tea, Luo and colleagues modified a GCE with a polyethylenimine-rGO composite.<sup>326</sup> This biosensor exhibited a LOD of 0.07 mg L<sup>-1</sup>, and this was not affected by the addition of interfering agents such as K<sup>+</sup>, F<sup>-</sup>, Mg<sup>2+</sup>, Ca<sup>2+</sup>, glycine, glutamic acid, lysine, AA, dopamine, UA, catechinic acid, anthocyanin, and caffeic acid. In a similar way, Filik *et al.* modified a GCE with a Nafion-GO composite by drop-casting, and this biosensor was then used in the detection of caffeic acid in white wine samples.<sup>327</sup> In the analysis of these samples, the biosensor exhibited a detection capacity equal to that of HPLC with no interference from coumaric acid, sinapic acid, ferulic acid, or AA. Liu *et al.* have shown ferulic acid in human urine/serum samples and plant (*Angelica sinensis*) samples can be determined using an ErGO-modified GCE.<sup>328</sup> This biosensor exhibited a LOD of 20.6 nM over a wide linear response range of 84.9 nM to 38.9  $\mu$ M and recovery rates of between 97 and 104% for the biological samples tested.

Pang *et al.* reported the detection of luteolin in peanut shells using a rGO-modified GCE onto which hydroxyapatite was coated.<sup>107</sup> This biosensor exhibits a large linear response range for luteolin of 0.2 nM to 0.1  $\mu$ M and a LOD of 0.1 nM. The electroactivity of this biosensor is attributed to its large surface area, ease of luteolin adsorption, as well as electrocatalytic effect at the rGO/hydroxyapatite interface. Similarly, Zhang and colleagues have modified a GCE by coating it with thermally rGO, and then this biosensor could be used in the sensing of the baicalein flavonoid.<sup>108</sup> This biosensor exhibited a linear response range from 10 nM to 10  $\mu$ M with a LOD of 6.0 nM. These various studies mentioned show the benefit of using graphene in biosensing organic conjugated compounds which easily interact with the graphene surface through  $\pi$ - $\pi$  interactions.

Li *et al.*<sup>329</sup> reported a biosensor based on Fe<sub>3</sub>O<sub>4</sub> nanobead immobilized graphene for the electrochemical detection of 17 $\beta$ -estradiol (17 $\beta$ -E2) in water, with a LOD of 0.819 nM. Yola *et al.*<sup>330</sup> have manufactured a tyrosine biosensor with Au nanocubes attached to a 2-aminoethanethiol-functionalized GO-modified GCE. The bioprobe shows the detection range for tyrosine to be  $1.0 \times 10^{-9}$  to  $2.0 \times 10^{-8}$  M and LOD of  $1.5 \times 10^{-10}$  M. Chen *et al.*<sup>331</sup> have used a Au-modified PDDA/graphene electrode for biosensing of the angiogenic polypeptide, which is a member of the pancreatic ribonuclease family and is overly generated in blood serum of various cancer patients.

## OUTLOOK: FUTURE PROSPECTS, PROBLEMS, AND CHALLENGES

This review has focused on recent research progress in the development of carbon-based voltammetric biosensors, with specific focus on biosensors that incorporate the 1D and 2D carbon nanomaterials, such as CNTs and graphene. The main reason for the use of carbon nanomaterials is that they allow the electron transfer rates to be increased in most cases, which in turn results in increased analyte sensitivity. However, this sensitivity can be enhanced even further by chemical modification of the surface, as well as the surface architecture of these carbon materials. These surface modifications should allow further innovative surface functionalizations by integrating the carbon materials with NPs, ionic liquids, polymers, enzymes, DNA, *etc.*, which will increase the applicability of these biosensors. Additionally, through changing the surface architecture, it is possible to increase not only the electrical

conductivity but also the surface area, both of these factors should increase the sensitivity of the biosensors.

An additional benefit of using carbon nanomaterials is that it should be easier to reduce the size of the biosensors with new fabrication techniques. One needs only to look at the research presented by Gogotsi and co-workers, who have shown that intracellular environments and organelles can be probed without disrupting the cell when using AuNP-functionalized iron-oxide-filled/CNT.<sup>332</sup> However, this is only the beginning of these types of nanofabrication applications, with theoretical work by Rajan *et al.* showing that single-molecule differentiation is possible when using a graphene nanoribbon.<sup>14</sup> This prospect is exciting as single base mismatches could be an indicator of cancerous growth. In fact, single-base mismatches have been detected, albeit on a larger scale than desired.<sup>103,269,276</sup>

One important point to remember when reading the biosensor literature is that many reports claim selectivity and sensitivity for various electrodes toward molecules; however, many of these electrodes are manufactured in the same manner as other electrodes or are the same electrode. This leads the authors of this review to wonder if many biosensors are as selective as reported to be; for example, the ErGO/GCE and rGO/GCE have been reported to simultaneously sense AA, UA, and dopamine or simultaneously sense 5-methylcytosine and cytosine or ferulic acid.<sup>108,190,284,328</sup> Since these sensings are at nearly the same potential, the expected overlapping would result in poor selectivity and reproducibility. The ability to determine each species selectively in the presence of all these species is an important issue in electroanalytical research. In a similar way, the CNT/GCE has been reported to simultaneously sense immunosuppressant mycophenolatemofetil and its active metabolite mycophenolic acid, or buspirone, or dopamine or atorvastatin calcium.<sup>77,91,294,311</sup> For this reason, we would suggest a thorough review of the published literature to make sure the proposed sensor, which is reported as showing selectivity during interference studies, is rather just being probed incorrectly. In order to overcome these difficulties, further efforts are required in the development of novel materials to modify the working electrodes.

Fouling of electrodes is a significant problem in biosensing. However, with an enhanced electron transfer rate afforded by the inclusion of carbon materials, this problem is significantly reduced. Further studies need to be conducted in this area to see if this holds true with prolonged exposure and sensing of analytes. Additionally, stability of the sensor is of great importance especially in the case of sensors which rely on the use of antigens, aptamers, or enzymes. For this reason, a favorable environment which mimics the cell wall or interior is highly desired, yet this environment must not reduce the electron mobility and rate of sensing as that would lead to either a decrease in sensitivity or an increase in fouling. By inclusion of highly conductive carbon nanomaterials into this biologically favorable environment, it is possible that this issue can be overcome. Another way of increasing sensitivity in biosensing is to use labels that increase the sensitivity of the biosensor by tagging the analyte, thereby allowing an electrochemical reaction to occur or by enhancing the already existing electrochemical reaction used in the sensing.<sup>333–335</sup>

We believe that the knowledge of bio- and electrochemistry, solid-state and surface physics, bioengineering, and data processing offers the possibility of a next generation of highly specific, sensitive, selective, and reliable voltammetric bio-

sensors. As shown in Figure 1, it seems likely that the increasing trend in biosensor research will continue in the years ahead. This is likely as applications that are relevant to mental and physical health are becoming more important as the medical field expands and advances in areas which seemed impossible just a few years ago. As such, the applicability of portable biosensors in mobile clinics has the ability to profoundly influence the health service provided. Additionally, these applications are not restricted to the medical field but have varied applications in the food, water purification, and agricultural industries among many others.

## AUTHOR INFORMATION

### Corresponding Author

\*Address correspondence to [jitendra@unist.ac.kr](mailto:jitendra@unist.ac.kr), [kimks@unist.ac.kr](mailto:kimks@unist.ac.kr).

### Notes

The authors declare no competing financial interest.

## ACKNOWLEDGMENTS

This work was supported by National Research Foundation of Korea (National Honor Scientist Program: 2010-0020414).

## VOCABULARY

**functionalized graphene**, covalent and noncovalent functionalized graphene or graphene oxide; **cyclic voltammetry**, analysis of an analyte made by varying the potential and measuring the resulting current as the analyte reacts electrochemically with the working electrodes; **amperometric sensors**, a sensor which employs cyclic voltammetry; **electrochemical biosensors**, a sensor that measures electrochemical species consumed and/or generated during a biological interaction process of a biologically active substance

## REFERENCES

- (1) Lam, B.; Das, J.; Holmes, R. D.; Live, L.; Sage, A.; Sargent, E. H.; Kelley, S. O. Solution-Based Circuits Enable Rapid and Multiplexed Pathogen Detection. *Nat. Commun.* **2013**, *4*, 2001.
- (2) Atkinson, M. A.; Eisenbarth, G. S.; Michels, A. W. Type 1 Diabetes—Progress and Prospects. *Lancet* **2014**, *383*, 69–82.
- (3) Orozco, J.; García-Gradilla, V.; D'Agostino, M.; Gao, W.; Cortés, A.; Wang, J. Artificial Enzyme-Powered Microfish for Water-Quality Testing. *ACS Nano* **2013**, *7*, 818–824.
- (4) Paleček, E.; Tkáč, J.; Bartošík, M.; Bertók, T.; Ostatná, V.; Paleček, J. Electrochemistry of Nonconjugated Proteins and Glycoproteins. Toward Sensors for Biomedicine and Glycomics. *Chem. Rev.* **2015**, *115*, 2045–2108.
- (5) Suginta, W.; Khunkaewla, P.; Schulte, A. Electrochemical Biosensor Applications of Polysaccharides Chitin and Chitosan. *Chem. Rev.* **2013**, *113*, 5458–5479.
- (6) Liu, Y.; Dong, X.; Chen, P. Biological and Chemical Sensors Based on Graphene Materials. *Chem. Soc. Rev.* **2012**, *41*, 2283–2307.
- (7) Ronkainen, N. J.; Halsall, H. B.; Heineman, W. R. Electrochemical Biosensors. *Chem. Soc. Rev.* **2010**, *39*, 1747–1763.
- (8) Song, S.; Qin, Y.; He, Y.; Huang, Q.; Fan, C.; Chen, H.-Y. Functional Nanoprobes for Ultrasensitive Detection of Biomolecules. *Chem. Soc. Rev.* **2010**, *39*, 4234–4243.
- (9) Ambrosi, A.; Chua, C. K.; Bonanni, A.; Pumera, M. Electrochemistry of Graphene and Related Materials. *Chem. Rev.* **2014**, *114*, 7150–7188.
- (10) Stankovich, S.; Dikin, D. A.; Dommett, G. H. B.; Kohlhaas, K. M.; Zimney, E. J.; Stach, E. A.; Piner, R. D.; Nguyen, S. T.; Ruoff, R. S. Graphene-Based Composite Materials. *Nature* **2006**, *442*, 282–285.
- (11) Balasubramanian, K.; Burghard, M. Biosensors Based on Carbon Nanotubes. *Anal. Bioanal. Chem.* **2006**, *385*, 452–468.

- (12) Fang, Y.; Wang, E. Electrochemical Biosensors on Platforms of Graphene. *Chem. Commun.* **2013**, *49*, 9526–9539.
- (13) Min, S. K.; Kim, W. Y.; Cho, Y.; Kim, K. S. Fast DNA Sequencing with a Graphene-Based Nanochannel Device. *Nat. Nanotechnol.* **2011**, *6*, 162–165.
- (14) Rajan, A. C.; Rezapour, M. R.; Yun, J.; Cho, Y.; Cho, W. J.; Min, S. K.; Lee, G.; Kim, K. S. Two Dimensional Molecular Electronics Spectroscopy for Molecular Fingerprinting, DNA Sequencing and Cancerous DNA Recognition. *ACS Nano* **2014**, *8*, 1827–1833.
- (15) Adams, R. N. Carbon Paste Electrodes. *Anal. Chem.* **1958**, *30*, 1576–1576.
- (16) Georgakilas, V.; Otyepka, M.; Bourlinos, A. B.; Chandra, V.; Kim, N.; Kemp, K. C.; Hobza, P.; Zboril, R.; Kim, K. S. Functionalization of Graphene: Covalent and Non-Covalent Approaches, Derivatives and Applications. *Chem. Rev.* **2012**, *112*, 6156–6214.
- (17) Chung, C.; Kim, Y.; Shin, D.; Ryoo, S. R.; Hong, B. H.; Min, D. H. Biomedical Applications of Graphene and Graphene Oxide. *Acc. Chem. Res.* **2013**, *46*, 2211–2224.
- (18) Li, J.; Lu, Y.; Ye, Q.; Cinke, M.; Han, J.; Meyyappan, M. Carbon Nanotube Sensors for Gas and Organic Vapor Detection. *Nano Lett.* **2003**, *3*, 929–933.
- (19) Brownson, A. C.; Kampouris, D. K.; Banks, C. E. Graphene Electrochemistry: Fundamental Concepts Through to Prominent Applications. *Chem. Soc. Rev.* **2012**, *41*, 6944–6976.
- (20) Wang, Y.; Li, Z. H.; Wang, J.; Li, J. H.; Lin, Y. H. Graphene and graphene oxide: Biofunctionalization and Applications in Biotechnology. *Trends Biotechnol.* **2011**, *29*, 205–212.
- (21) Zhao, W. W.; Xu, J. J.; Chen, H. Y. Photoelectrochemical DNA Biosensors. *Chem. Rev.* **2014**, *114*, 7421–7441.
- (22) Chen, D.; Feng, H.; Li, J. Graphene Oxide: Preparation, Functionalization, and Electrochemical Applications. *Chem. Rev.* **2012**, *112*, 6027–6053.
- (23) Liu, Q.; Lu, X.; Li, J.; Yao, X.; Li, J. Direct Electrochemistry of Glucose Oxidase and Electrochemical Biosensing of Glucose on Quantum Dots/Carbon Nanotubes Electrodes. *Biosens. Bioelectron.* **2007**, *22*, 3203–3209.
- (24) Goyal, R. N.; Singh, S. P. Voltammetric Quantification of Adenine and Guanine at C60 Modified Glassy Carbon Electrodes. *J. Nanosci. Nanotechnol.* **2006**, *6*, 3699–3704.
- (25) Tuček, J.; Kemp, K. C.; Kim, K. S.; Zbořil, R. Iron-Oxide-Supported Nanocarbon in lithium-Ion Batteries, Medical, Catalytic, and Environmental Applications. *ACS Nano* **2014**, *8*, 7571–7612.
- (26) Zheng, D.; Vashist, S. K.; Dykas, M. M.; Saha, S.; Al-Rubeaan, K.; Lam, E.; Luong, J. H. T.; Sheu, F. S. Graphene versus Multi-Walled Carbon Nanotubes for Electrochemical Glucose Biosensing. *Materials* **2013**, *6*, 1011–1027.
- (27) Novoselov, K. S.; Geim, A. K.; Morozov, S. V.; Jiang, D.; Zhang, Y.; Dubonos, S. V. Electric Field Effect in Atomically Thin Carbon Films. *Science* **2004**, *306*, 666–669.
- (28) Kim, K. S.; Zhao, Y.; Jang, H.; Lee, S. Y.; Kim, J. M.; Kim, K. S.; Ahn, J. H.; Kim, P.; Choi, J. Y.; Hong, B. H. Large-Scale Pattern Growth of Graphene Films for Stretchable Transparent Electrodes. *Nature* **2009**, *457*, 706–710.
- (29) Bae, S.; Kim, H.; Lee, Y.; Xu, X.; Park, J. S.; Zheng, Y.; Balakrishnan, J.; Lei, T.; Kim, H. R.; Song, Y. I.; Kim, Y. J.; Kim, K. S.; Özyilmaz, B.; Ahn, J. H.; Hong, B. H.; Iijima, S. Roll-to-Roll Production of 30-Inch Graphene Films for Transparent Electrodes. *Nat. Nanotechnol.* **2010**, *5*, 574–578.
- (30) Stoller, M. D.; Park, S.; Zhu, Y.; An, J.; Ruoff, R. S. Graphene-Based Ultracapacitors. *Nano Lett.* **2008**, *8*, 3498–3502.
- (31) Geim, A. K.; Novoselov, K. S. The Rise of Graphene. *Nat. Mater.* **2007**, *6*, 183–191.
- (32) Service, R. F. Carbon Sheets an Atom Thick Give Rise to Graphene Dreams. *Science* **2009**, *324*, 875–877.
- (33) Stankovich, S.; Dikin, D. A.; Piner, R. D.; Kohlhaas, K. A.; Kleinhammes, A.; Jia, Y.; Wu, Y.; Nguyen, S. T.; Ruoff, R. S. Synthesis of Graphene-Based Nanosheets via Chemical Reduction of Exfoliated Graphite Oxide. *Carbon* **2007**, *45*, 1558–1565.
- (34) Li, X.; Cai, W.; An, J.; Kim, S.; Nah, J.; Yang, D.; Piner, R.; Velamakanni, A.; Jung, I.; Tutuc, E.; Banerjee, S. K.; Colombo, L.; Ruoff, R. S. Large-Area Synthesis of High-Quality and Uniform Graphene Films on Copper Foils. *Science* **2009**, *324*, 1312–1314.
- (35) Salas, E. C.; Sun, Z.; Lüttge, A.; Tour, J. M. Reduction of Graphene Oxide via Bacterial Respiration. *ACS Nano* **2010**, *4*, 4852–4856.
- (36) Tiwari, R. N.; Ishihara, M.; Tiwari, J. N.; Yoshimura, M. Synthesis of Graphene Film from Fullerene Rods. *Chem. Commun.* **2012**, *48*, 3003–3005.
- (37) Tiwari, R. N.; Ishihara, M.; Tiwari, J. N.; Yoshimura, M. Flame-Annealing Assisted Synthesis of Graphene Films from Adamantine. *J. Mater. Chem.* **2012**, *22*, 15031–15036.
- (38) Dimiev, A. M.; Tour, J. M. Mechanism of Graphene Oxide Formation. *ACS Nano* **2014**, *8*, 3060–3068.
- (39) Tiwari, J. N.; Nath, K.; Kumar, S.; Tiwari, R. N.; Kemp, K. C.; Le, N. H.; Youn, D. H.; Lee, J. S.; Kim, K. S. Stable Platinum Nanoclusters on Genomic DNA–Graphene Oxide with a High Oxygen Reduction Reaction Activity. *Nat. Commun.* **2013**, *4*, 2221.
- (40) Tiwari, J. N.; Kemp, K. C.; Nath, K.; Tiwari, R. N.; Nam, H. G.; Kim, K. S. Interconnected Pt-Nanodendrite/DNA/Reduced-Graphene-Oxide Hybrid Showing Remarkable Oxygen Reduction Activity and Stability. *ACS Nano* **2013**, *7*, 9223–9231.
- (41) Le, N. H.; Seema, H.; Kemp, K. C.; Ahmed, N.; Tiwari, J. N.; Park, S.; Kim, K. S. Solution-Processable Conductive Micro-Hydrogels of Nanoparticle/Graphene Platelets Produced by Reversible Self-Assembly and Aqueous Exfoliation. *J. Mater. Chem. A* **2013**, *41*, 12900–12908.
- (42) Park, S.; Hu, Y.; Hwang, J. O.; Lee, E. S.; Casabianca, L. B.; Cai, W.; et al. Chemical Structures of Hydrazine-Treated Graphene Oxide and Generation of Aromatic Nitrogen Doping. *Nat. Commun.* **2012**, *3*, 638.
- (43) Song, S. H.; Park, K. H.; Kim, B. H.; Choi, Y. W.; Jun, G. H.; Lee, D. J.; et al. Enhanced Thermal Conductivity of Epoxy-Graphene Composites by Using Non-Oxidized Graphene Flakes with Non-Covalent Functionalization. *Adv. Mater.* **2013**, *25*, 732–737.
- (44) Zhang, J.; Zhang, F.; Yang, H.; Huang, X.; Liu, H.; Zhang, J.; et al. Graphene Oxide as a Matrix for Enzyme Immobilization. *Langmuir* **2010**, *26*, 6083–6085.
- (45) Zuo, X.; He, S.; Li, D.; Peng, C.; Huang, Q.; Song, S.; et al. Graphene Oxide-Facilitated Electron Transfer of Metalloproteins at Electrode Surfaces. *Langmuir* **2010**, *26*, 1936–1939.
- (46) Kang, S. M.; Park, S.; Kim, D.; Park, S. Y.; Ruoff, R. S.; Lee, H. Simultaneous Reduction and Surface Functionalization of Graphene Oxide by Mussel-Inspired Chemistry. *Adv. Funct. Mater.* **2011**, *21*, 108–112.
- (47) Iijima, S. Helical Microtubules of Graphitic Carbon. *Nature* **1991**, *354*, 56–58.
- (48) Lota, G.; Fic, K.; Frackowiak, E. Carbon Nanotubes and Their Composites in Electrochemical Applications. *Energy Environ. Sci.* **2011**, *4*, 1592–1605.
- (49) DeVolder, M. F. L.; Tawfik, S. H.; Baughman, R. H.; Hart, A. J. Carbon Nanotubes: Present and Future Commercial Applications. *Science* **2013**, *339*, 535–539.
- (50) Datsyuk, V.; Kalyva, M.; Papagelis, K.; Parthenios, J.; Tasis, D.; Siokou, A.; et al. Chemical Oxidation of Multiwalled Carbon Nanotubes. *Carbon* **2008**, *46*, 833–840.
- (51) Karousis, N.; Tagmatarchis, N.; Tasis, D. Current Progress on the Chemical Modification of Carbon Nanotubes. *Chem. Rev.* **2010**, *110*, 5366–5397.
- (52) Liu, Y.; Gao, L. A Study of the Electrical Properties of Carbon Nanotube-NiFe<sub>2</sub>O<sub>4</sub> Composites: Effect of the Surface Treatment of the Carbon Nanotubes. *Carbon* **2005**, *43*, 47–52.
- (53) Alonso-Lomillo, M. A.; Rüdiger, O.; Maroto-Valiente, A.; Velez, M.; Rodriguez-Ramos, I.; Muñoz, F. J.; et al. Hydrogenase-Coated Carbon Nanotubes for Efficient H<sub>2</sub> Oxidation. *Nano Lett.* **2007**, *7*, 1603–1608.



- (54) Zhang, J.; Liu, X.; Blume, R.; Zhang, A.; Schlögl, R.; Su, D. S. Surface-Modified Carbon Nanotubes Catalyze Oxidative Dehydrogenation of n-Butane. *Science* **2008**, *322*, 73–77.
- (55) Nurunnabi, M.; Cho, K. J.; Choi, J. S.; Huh, K. M.; Lee, Y. Targeted Near-IR QDs-Loaded Micelles for Cancer Therapy and Imaging. *Biomaterials* **2010**, *31*, 5436–5444.
- (56) Malhotra, B. D.; Singhal, R.; Chaubey, A.; Sharma, S. K.; Kumar, A. A. Recent Trends in Biosensors. *Curr. Appl. Phys.* **2005**, *5*, 92–97.
- (57) Claussen, J. C.; Kumar, A.; Jaroch, D. B.; Khawaja, M. H.; Hibbard, A. B.; Porterfield, D. M.; Fisher, T. S. Nanostructuring Platinum Nanoparticles on Multilayered Graphene Petal Nanosheets for Electrochemical Biosensing. *Adv. Funct. Mater.* **2012**, *22*, 3399–3405.
- (58) Sharma, S.; Madou, M. J. Micro and Nano Patterning of Carbon Electrodes for BioMEMS. *Bioinspired, Biomimetic Nanobiomater.* **2012**, *1*, 252–265.
- (59) Yin, P. T.; Shah, S.; Chhowalla, M.; Lee, K. B. Design, Synthesis, and Characterization of Graphene–Nanoparticle Hybrid Materials for Bioapplications. *Chem. Rev.* **2015**, *115*, 2483–2531.
- (60) Park, D. W.; et al. Graphene-Based Carbon-Layered Electrode Array Technology for Neural Imaging And Optogenetic Applications. *Nat. Commun.* **2014**, *5*, 5258.
- (61) Muratova, I. S.; Kartsova, L. A.; Mikhelson, K. N. Voltammetric vs. Potentiometric Sensing of Dopamine: Advantages and Disadvantages, Novel Cell Designs, Fundamental Limitations and Promising Options. *Sens. Actuators, B* **2015**, *207*, 900–906.
- (62) Carrara, S.; Baj-Rossi, C.; Boero, C.; De Micheli, G. Do Carbon Nanotubes Contribute to Electrochemical Biosensing? *Electrochim. Acta* **2014**, *128*, 102–112.
- (63) Miller, J. N.; Miller, J. C. *Statistics and Chemometrics for Analytical Chemistry*, 6th ed.; Prentice Hall: London, 2010.
- (64) MacDougall, D.; Crummett, W. B. Guidelines for Data Acquisition and Data Quality Evaluation in Environmental Chemistry. *Anal. Chem.* **1980**, *52*, 2242–2249.
- (65) Martín, A.; Escarpa, A. Graphene: The Cutting–Edge Interaction Between Chemistry And Electrochemistry. *TrAC, Trends Anal. Chem.* **2014**, *56*, 13–26.
- (66) Deng, C.; Chen, J.; Nie, Z.; Si, S. A Sensitive and Stable Biosensor Based on the Direct Electrochemistry of Glucose Oxidase Assembled Layer-by-Layer at the Multiwall Carbon Nanotube-Modified Electrode. *Biosens. Bioelectron.* **2010**, *26*, 213–219.
- (67) Shi, G.; Sun, Z.; Liu, M.; Zhang, L.; Liu, Y.; Qu, Y.; Jin, L. Electrochemistry and Electrocatalytic Properties of Hemoglobin in Layer-by-Layer Films of SiO<sub>2</sub> with Vapor–Surface Sol–Gel Deposition. *Anal. Chem.* **2007**, *79*, 3581–3588.
- (68) Iost, R. M.; Crespihlo, F. N. Layer-by-layer self-assembly and electrochemistry: Applications in biosensing and bioelectronics. *Biosens. Bioelectron.* **2012**, *31*, 1–10.
- (69) Wu, B. Y.; Hou, S. H.; Yin, F.; Zhao, Z. X.; Wang, Y. Y.; Wang, X. S.; Chen, Q. Amperometric Glucose Biosensor Based on Multilayer Films via Layer-by-Layer Self-Assembly of Multi-Wall Carbon Nanotubes, Gold Nanoparticles and Glucose Oxidase on the Pt Electrode. *Biosens. Bioelectron.* **2007**, *22*, 2854–2860.
- (70) Biscay, J.; Costa Rama, E.; Gonzalez-Garcia, M. B.; Julio-Reviejo, A.; Pingarron-Carrazon, J. M.; Garcia, A. C. Amperometric Fructose Sensor based on Ferrocyanide Modified Screen-Printed Carbon Electrode. *Talanta* **2012**, *88*, 432–438.
- (71) Yang, H.; Li, Z.; Wei, X.; Huang, R.; Qi, H.; Gao, Q.; et al. Detection and Discrimination of alpha-Fetoprotein with a Label-Free Electrochemical Impedance Spectroscopy Biosensor Array Based on Lectin Functionalized Carbon Nanotubes. *Talanta* **2013**, *111*, 62–68.
- (72) Corrêa, C. C.; Jannuzzi, S. A. V.; Santhiago, M.; Timm, R. A. T.; Formiga, A. L. B.; Kubota, L. T. Modified Electrode Using Multi-Walled Carbon Nanotubes and a Metallopolymer for Amperometric Detection of L-Cysteine. *Electrochim. Acta* **2013**, *113*, 332–339.
- (73) Kumar, D. R.; Manoj, D.; Santhanalakshmi, J. Electrostatic Fabrication of Oleylamine Capped Nickel Oxide Nanoparticles Anchored Multiwall Carbon Nanotube Nanocomposite: A Robust Electrochemical Determination of Riboflavin At Nanomolar Levels. *Anal. Methods* **2014**, *6*, 1011–1020.
- (74) Gupta, R. K.; Periyakaruppan, A.; Meyyappan, M.; Koehne, J. E. Label-Free Detection of C-Reactive Protein Using a Carbon Nanofiber Based Biosensor. *Biosens. Bioelectron.* **2014**, *59*, 112–119.
- (75) Tran, H. V.; Piro, B.; Reisberg, S.; Tran, L. D.; Duc, H. T.; Pham, M. C. Label-Free and Reagentless Electrochemical Detection of micro-RNAs Using a Conducting Polymer Nanostructured by Carbon Nanotubes: Application to Prostate Cancer Biomarker miR-141. *Biosens. Bioelectron.* **2013**, *49*, 164–169.
- (76) Gao, F. L.; Zhu, Z.; Lei, J. P.; Geng, Y.; Ju, H. X. Sub-Femtomolar Electrochemical Detection of DNA Using Surface Circular Strand-Replacement Polymerization and Gold Nanoparticle Catalyzed Silver Deposition for Signal Amplification. *Biosens. Bioelectron.* **2013**, *39*, 199–203.
- (77) Suzuki, I.; Fukuda, M.; Shirakawa, K.; Jiko, H.; Gotoh, M. Carbon Nanotube Multi-Electrode Array Chips for Noninvasive Real-Time Measurement of Dopamine, Action Potentials, and Postsynaptic Potentials. *Biosens. Bioelectron.* **2013**, *49*, 270–275.
- (78) de Souza Ribeiro, F. A.; Tarley, C. R. T.; Borges, K. B.; Pereira, A. C. Development of a Square Wave Voltammetric Method for Dopamine Determination Using a Biosensor Based on Multiwall Carbon Nanotubes Paste and Crude Extract of *Cucurbita pepo* L. *Sens. Actuators, B* **2013**, *185*, 743–754.
- (79) Lin, K. C.; Lin, Y. C.; Chen, S. M. A Highly Sensitive Nonenzymatic Glucose Sensor Based on Multi-Walled Carbon Nanotubes Decorated with Nickel and Copper Nanoparticles. *Electrochim. Acta* **2013**, *96*, 164–172.
- (80) Vilian, A. T. E.; Chen, S. M.; Lou, B. S. A Simple Strategy for the Immobilization of Catalase on Multi-Walled Carbon Nanotube/Poly (L-Lysine) Biocomposite for the Detection of H<sub>2</sub>O<sub>2</sub> and Iodate. *Biosens. Bioelectron.* **2014**, *61*, 639–647.
- (81) Dutta, D.; Chandra, S.; Swain, A. K.; Bahadur, D. SnO<sub>2</sub> Quantum Dots-Reduced Graphene Oxide Composite for Enzyme-Free Ultrasensitive Electrochemical Detection of Urea. *Anal. Chem.* **2014**, *86*, 5914–5921.
- (82) Moraes, F. C.; Silva, T. A.; Cesarino, I.; Lanza, M. R. V.; Machado, S. A. S. Antibiotic Detection in Urine Using Electrochemical Sensors Based on Vertically Aligned Carbon Nanotubes. *Electroanalysis* **2013**, *25*, 2092–2099.
- (83) Gheibi, S.; Karimi-Maleh, H.; Khalilzadeh, M. A.; Bagheri, H. J. A New Voltammetric Sensor for Electrochemical Determination of Vitamin C in Fruit Juices and Fresh Vegetable Juice Using Modified Multi-Wall Carbon Nanotubes Paste Electrode. *J. Food Sci. Technol.* **2015**, *52*, 276–284.
- (84) Rafati, A. A.; Afraz, A. Amperometric Sensing of anti-HIV Drug Zidovudine on Ag Nanofilm-Multiwalled Carbon Nanotubes Modified Glassy Carbon Electrode. *Mater. Sci. Eng., C* **2014**, *39*, 105–112.
- (85) Ensafi, A. A.; Amini, M.; Rezaei, B. Biosensor Based on dsDNA Decorated Chitosan Modified Multiwall Carbon Nanotubes for Voltammetric Biodetection of Herbicide Amitrole. *Colloids Surf., B* **2013**, *109*, 45–51.
- (86) Sun, X.; Cao, Y.; Gong, Z.; Wang, X.; Zhang, Y.; Gao, J. An Amperometric Immunosensor Based on Multi-Walled Carbon Nanotubes-Thionine-Chitosan Nanocomposite Film for Chlorpyrifos Detection. *Sensors* **2012**, *12*, 17247–17261.
- (87) Han, M.; Qu, Y.; Chen, S.; Wang, Y.; Zhang, Z.; Ma, M.; Wang, Z.; Zhan, G.; Li, C. Amperometric Biosensor for Bisphenol a Based on a Glassy Electrode Modified with a Nanocomposite Made from Polylysine, Single Walled Carbon Nanotubes and Tyrosinase. *Microchim. Acta* **2013**, *180*, 989–996.
- (88) Gomes-Filho, S. L. R.; Dias, A. C. M. S.; Silva, M. M. S.; Silva, B. V. M.; Dutra, R. F. A Carbon Nanotube-Based Electrochemical Immunosensor for Cardiac Troponin T. *Microchem. J.* **2013**, *109*, 10–15.
- (89) Deng, W.; Liu, F.; Ge, S.; Yu, J.; Yan, M.; Song, X. A Dual Amplification Strategy for Ultrasensitive Electrochemiluminescence Immunoassay Based on a Pt Nanoparticles Dotted Graphene–Carbon

Nanotubes Composite and Carbon Dots Functionalized Mesoporous Pt/Fe. *Analyst* **2014**, *139*, 1713–1720.

(90) Cao, Q.; Zhao, H.; Yang, Y.; He, Y.; Ding, N.; Wang, J.; et al. Electrochemical Immunosensor for Casein Based on Gold Nanoparticles and Poly(L-Arginine)/ Multi-Walled Carbon Nanotubes Composite Film Functionalized Interface. *Biosens. Bioelectron.* **2011**, *26*, 3469–3474.

(91) Silva, T. A.; Zanin, H.; Vicentini, F. C.; Corat, E. J.; Fatibello-Filho, O. Differential Pulse Adsorptive Stripping Voltammetric Determination of Nanomolar Levels of Atorvastatin Calcium in Pharmaceutical and Biological Samples Using a Vertically Aligned Carbon Nanotube/Graphene Oxide Electrode. *Analyst* **2014**, *139*, 2832–2841.

(92) Serafín, V.; Agüí, L.; Yáñez-Sedeño, P.; Pingarrón, J. M. Determination of Prolactin Hormone in Serum and Urine Using an Electrochemical Immunosensor Based on Poly(Pyrrrolepropionic Acid)/Carbon Nanotubes Hybrid Modified Electrodes. *Sens. Actuators, B* **2014**, *195*, 494–499.

(93) Park, K.; Kwon, S. J.; Kwak, J. A Label-Free Electrochemical Aptasensor for Thrombin Using a Single-Wall Carbon Nanotube (SWCNT) Casted Glassy Carbon Electrode. *Electroanalysis* **2014**, *26*, 513–520.

(94) Karadas, N.; Bozal-Palabiyik, B.; Uslu, B.; Ozkan, S. A. Functionalized Carbon Nanotubes-with Silver Nanoparticles to Fabricate a Sensor for the Determination of Zolmitriptan in its Dosage Forms and Biological Samples. *Sens. Actuators, B* **2013**, *186*, 486–494.

(95) Alizadeh, T.; Mirzaghoolipour, S. A Nafion-Free Non-Enzymatic Amperometric Glucose Sensor Based on Copper Oxide Nanoparticles–Graphene Nanocomposite. *Sens. Actuators, B* **2014**, *198*, 438–447.

(96) Liu, J.; He, Z.; Xue, J.; Tan, T. T. Y. A Metal-Catalyst Free, Flexible and Free-Standing Chitosan/Vacuum-Stripped Graphene/Polypyrrole Three Dimensional Electrode Interface for High Performance Dopamine Sensing. *J. Mater. Chem. B* **2014**, *2*, 2478–2482.

(97) Guo, Y.; Han, Y.; Guo, Y.; Dong, C. Graphene-Orange II Composite Nanosheets with Electroactive Functions as Label-Free Aptasensing Platform for "Signal-On" Detection of Protein. *Biosens. Bioelectron.* **2013**, *45*, 95–101.

(98) Xu, F.; Wang, F.; Yang, D.; Gao, Y.; Li, H. Electrochemical Sensing Platform for L-Cysteine Based on Nearly Uniform Au Nanoparticles Decorated Graphene Nanosheets. *Mater. Sci. Eng., C* **2014**, *38*, 292–298.

(99) Peng, H. P.; Hu, Y.; Liu, A. L.; Chen, W.; Lin, X. H.; Yu, X. B. Label-Free Electrochemical Immunosensor Based on Multi-Functional Gold Nanoparticles–Polydopamine–Thionine–Graphene Oxide Nanocomposites Film for Determination Of Alpha-Fetoprotein. *J. Electroanal. Chem.* **2014**, *712*, 89–95.

(100) Eissa, S.; L'Hocine, L.; Sijaj, M.; Zourob, M. A Graphene Based Label-Free Voltammetric Immunosensor for Sensitive Detection of the Egg Allergen Ovalbumin. *Analyst* **2013**, *138*, 4378–4384.

(101) Bach, S.; Boudaoud, A.; Emery, N.; Baddour-Hadjean, R.; Pereira-Ramos, J. P.  $K_0.5V_2O_5$ : A Novel Li Intercalation Compound as Positive Electrode Material for Rechargeable Lithium Batteries. *Electrochim. Acta* **2014**, *119*, 38–42.

(102) Li, S. J.; Du, J. M.; Zhang, J. P.; Zhang, M. J.; Chen, J. A Glassy Carbon Electrode Modified with a Film Composed of Cobalt Oxide Nanoparticles and Graphene for Electrochemical Sensing of  $H_2O_2$ . *Microchim. Acta* **2014**, *181*, 631–638.

(103) Wang, J.; Shi, A.; Fang, X.; Han, X.; Zhang, Y. Ultrasensitive Electrochemical Supersandwich DNA Biosensor Using a Glassy Carbon Electrode Modified with Gold Particle-Decorated Sheets of Graphene Oxide. *Microchim. Acta* **2014**, *181*, 935–940.

(104) Pakapongpan, S.; Mensing, J. P.; Phokharatkul, D.; Lomas, T.; Tuantranont, A. Highly Selective Electrochemical Sensor for Ascorbic Acid Based on a Novel Hybrid Graphene-Copper Phthalocyanine-Polyaniline Nanocomposites. *Electrochim. Acta* **2014**, *133*, 294–301.

(105) Nezamzadeh-Ejehieh, A.; Pouladsaz, P. Voltammetric Determination of Riboflavin Based on Electrocatalytic Oxidation at Zeolite-

Modified Carbon Paste Electrodes. *J. Ind. Eng. Chem.* **2014**, *20*, 2146–2152.

(106) Baghizadeh, A.; Karimi-Maleh, H.; Khoshnama, Z.; Hassankhani, A.; Abbasghorbani, M. A Voltammetric Sensor for Simultaneous Determination of Vitamin C and Vitamin B6 in Food Samples Using ZrO<sub>2</sub> Nanoparticle/Ionic Liquids Carbon Paste Electrode. *Food Anal. Methods* **2015**, *8*, 549–557.

(107) Pang, P.; Liu, Y.; Zhang, Y.; Gao, Y.; Hu, Q. Electrochemical Determination of Luteolin in Peanut Hulls Using Graphene and Hydroxyapatite Nanocomposite Modified Electrode. *Sens. Actuators, B* **2014**, *194*, 397–403.

(108) Zhang, D.; Zhang, Y.; He, L. Sensitive Voltammetric Determination of Baicalein at Thermally Reduced Graphene Oxide Modified Glassy Carbon Electrode. *Electroanalysis* **2013**, *25*, 2136–2144.

(109) Wu, D.; Guo, A.; Guo, Z.; Xie, L.; Wei, Q.; Du, B. Simultaneous electrochemical Detection of Cervical Cancer Markers Using Reduced Graphene Oxide-Tetraethylene Pentamine as Electrode Materials and Distinguishable Redox Probes as Labels. *Biosens. Bioelectron.* **2014**, *54*, 634–639.

(110) Newman, J. D.; Turner, A. P. F. Home Blood Glucose Biosensors: A Commercial Perspective. *Biosens. Bioelectron.* **2005**, *20*, 2435–2453.

(111) Wang, J. Electrochemical Glucose Biosensors. *Chem. Rev.* **2008**, *108*, 814–825.

(112) Zhang, X.; Liu, D.; Li, L.; You, T. Direct Electrochemistry of Glucose Oxidase on Novel Free-Standing Nitrogen-Doped Carbon Nanospheres@Carbon Nanofibers Composite Film. *Sci. Rep.* **2015**, *5*, 9885.

(113) Zhou, X.; Tan, B.; Zheng, X.; Kong, D.; Li, Q. Interfacial Electron Transfer of Glucose Oxidase on Poly(Glutamic Acid)-Modified Glassy Carbon Electrode and Glucose Sensing. *Anal. Biochem.* **2015**, *489*, 9–16.

(114) O'Malley, J. J.; Ulmer, R. W. Thermal Stability of Glucose Oxidase and its Admixtures with Synthetic Polymers. *Biotechnol. Bioeng.* **1973**, *15*, 917–925.

(115) Gougis, M.; Tabet-Aoul, A.; Ma, D.; Mohamedi, M. Laser Synthesis and Tailor-Design of Nanosized Gold onto Carbon Nanotubes for Non-Enzymatic Electrochemical Glucose Sensor. *Sens. Actuators, B* **2014**, *193*, 363–369.

(116) Bright, H. J.; Appleby, M. The pH Dependence of the Individual Steps in the Glucose Oxidase Reaction. *J. Biol. Chem.* **1979**, *244*, 3625–3634.

(117) Zhu, Z.; Garcia-Gancedo, L.; Flewitt, A. J.; Xie, H.; Moussy, F.; Milne, W. I. A Critical Review of Glucose Biosensors Based on Carbon Nanomaterials: Carbon Nanotubes and Graphene. *Sensors* **2012**, *12*, 5996–6022.

(118) Goornavar, V.; Jeffers, R.; Biradar, S.; Ramesh, G. T. Utilization of Highly Purified Single Wall Carbon Nanotubes Dispersed in Polymer Thin Films for an Improved Performance of an Electrochemical Glucose Sensor. *Mater. Sci. Eng., C* **2014**, *40*, 299–307.

(119) Liu, D.; Zhang, X.; You, T. Electrochemical Performance of Electrospun Free-Standing Nitrogen-Doped Carbon Nanofibers and Their Application for Glucose Biosensing. *ACS Appl. Mater. Interfaces* **2014**, *6*, 6275–6280.

(120) Wang, Y.; Joshi, P. P.; Hobbs, K. L.; Johnson, M. B.; Schmidtke, D. W. Nanostructured Biosensors Built by Layer-by-Layer Electrostatic Assembly of Enzyme-Coated Single-Walled Carbon Nanotubes and Redox Polymers. *Langmuir* **2006**, *22*, 9776–9783.

(121) Kang, Z.; Yan, X.; Zhang, Y.; Pan, J.; Shi, J.; Zhang, X.; et al. Single-Stranded DNA functionalized Single-Walled Carbon Nanotubes for Microbiosensors via Layer-by-Layer Electrostatic Self-Assembly. *ACS Appl. Mater. Interfaces* **2014**, *6*, 3784–3789.

(122) Hyun, K.; Han, S. W.; Koh, W.-G.; Kwon, Y. Direct Electrochemistry of Glucose Oxidase Immobilized on Carbon Nanotube for Improving Glucose Sensing. *Int. J. Hydrogen Energy* **2015**, *40*, 2199–2206.

(123) Liu, Y.; Dolidze, T. D.; Singhal, S.; Khoshtariya, D. E.; Wei, J. New Evidence for a Quasi-Simultaneous Proton-Coupled Two-

Electron Transfer and Direct Wiring for Glucose Oxidase Captured by the Carbon Nanotube-Polymer Matrix. *J. Phys. Chem. C* **2015**, *119*, 14900–14910.

(124) Lin, K. C.; Hung, Y. T.; Chen, S. M. Facile Preparation of a Highly Sensitive Nonenzymatic Glucose Sensor Based on Multiwalled Carbon Nanotubes Decorated with Electrodeposited metals. *RSC Adv.* **2015**, *5*, 2806–2812.

(125) Zhang, Y.; Zhou, E.; Li, Y.; He, X. A Novel Nonenzymatic Glucose Sensor Based on Magnetic Copper Ferrite Immobilized on Multiwalled Carbon Nanotubes. *Anal. Methods* **2015**, *7*, 2360–2366.

(126) Guo, C.; Li, H.; Zhang, X.; Huo, H.; Xu, C. 3D porous CNT/MnO<sub>2</sub> Composite Electrode for High-Performance Enzymeless Glucose Detection and Supercapacitor Application. *Sens. Actuators, B* **2015**, *206*, 407–414.

(127) Sedghi, R.; Pezeshkian, Z. Fabrication of Non-Enzymatic Glucose Sensor Based on Nanocomposite of MWCNTs-COOH-Poly(2-aminothiophenol)-Au NPs. *Sens. Actuators, B* **2015**, *219*, 119–124.

(128) Veeramani, V.; Madhu, R.; Chen, S.-M.; Veerakumar, P.; Hung, C.-T.; Liu, S.-B. Heteroatom-Enriched Porous Carbon/Nickel Oxide Nanocomposites Asenzyme-Free Highly Sensitive Sensors for Detection of Glucose. *Sens. Actuators, B* **2015**, *221*, 1384–1390.

(129) Li, L.; et al. Ultrasensitive Electrospun Nickel-Doped Carbon Nanofibers Electrode for Sensing Paracetamol and Glucose. *Electrochim. Acta* **2015**, *152*, 31–37.

(130) Choi, T.; et al. Synthesis of Carbon Nanotube–Nickel Nanocomposites Using Atomic Layer Deposition for High-Performance Non-Enzymatic Glucose Sensing. *Biosens. Bioelectron.* **2015**, *63*, 325–330.

(131) Alizadeh, T.; Mirzagholidpur, S. An Outstandingly Sensitive Enzyme-Free Glucose Sensor Prepared by Co-Deposition of Nano-Sized Cupric Oxide and Multi-Walled Carbon Nanotubes on Glassy Carbon Electrode. *Biochem. Eng. J.* **2015**, *97*, 81–91.

(132) Gao, W.; Tjiu, W. W.; Wei, J.; Liu, T. Highly Sensitive Nonenzymatic Glucose and H<sub>2</sub>O<sub>2</sub> Sensor Based on Ni(OH)<sub>2</sub>/Electroreduced Graphene Oxide–Multiwalled Carbon Nanotube Film Modified Glass Carbon Electrode. *Talanta* **2014**, *120*, 484–490.

(133) Liu, Y.; Yu, D.; Zeng, C.; Miao, Z.; Dai, L. Biocompatible Graphene Oxide-Based Glucose Biosensors. *Langmuir* **2010**, *26*, 6158–6160.

(134) Wang, Z.; Zhou, X.; Zhang, J.; Boey, F.; Zhang, H. Direct Electrochemical Reduction of Single-Layer Graphene Oxide and Subsequent Functionalization with Glucose Oxidase. *J. Phys. Chem. C* **2009**, *113*, 14071–14075.

(135) Kemp, K. C.; Seema, H.; Saleh, M.; Le, N. H.; Mahesh, K.; Chandra, V.; Kim, K. S. Environmental Applications Using Graphene Composites: Water Remediation and Gas Adsorption. *Nanoscale* **2013**, *5*, 3149–3171.

(136) Acik, M.; Lee, G.; Mattevi, C.; Pirkle, A.; Wallace, R. M.; Chhowalla, M.; et al. The Role of Oxygen during Thermal Reduction of Graphene Oxide Studied by Infrared Absorption Spectroscopy. *J. Phys. Chem. C* **2011**, *115*, 19761–19781.

(137) Fernández-Merino, M. J.; Guardia, L.; Paredes, J. I.; Villar-Rodil, S.; Solís-Fernández, P.; Martínez-Alonso, A.; Tascón, J. M. D. Vitamin C Is an Ideal Substitute for Hydrazine in the Reduction of Graphene Oxide Suspensions. *J. Phys. Chem. C* **2010**, *114*, 6426–6432.

(138) Teymourian, H.; Salimi, A.; Firoozi, S. A High Performance Electrochemical Biosensing Platform for Glucose Detection and IgE Aptasensing Based on Fe<sub>3</sub>O<sub>4</sub>/Reduced Graphene Oxide Nanocomposite. *Electroanalysis* **2014**, *26*, 129–138.

(139) Bai, X.; Shiu, K. K. J. Investigation of the Optimal Weight Contents of Reduced Graphene Oxide–Gold Nanoparticles Composites and their Application in Electrochemical Biosensors. *Electroanal. Chem.* **2014**, *720–721*, 84–91.

(140) Hasan, K.; Asif, M. H.; Hassan, M. U.; Sandberg, M. O.; Nur, O.; Willander, M.; Fagerholm, S.; Strålfors, P. A Miniature Graphene-based Biosensor for Intracellular Glucose Measurements. *Electrochim. Acta* **2015**, *174*, 574–580.

(141) Chia, J. S. Y.; Tan, M. T. T.; Khiew, P. S.; Chin, J. K.; Siong, C. W. A Bio-Electrochemical Sensing Platform for Glucose Based Onirreversible, Non-Covalent Pi–Pi Functionalization of Graphene-produced via a Novel, Green Synthesis Method. *Sens. Actuators, B* **2015**, *210*, 558–565.

(142) Fang, Y.; Zhang, D.; Guo, Y.; Guo, Y.; Chen, Q. Simple One-Pot Preparation of Chitosan-Reduced Graphene Oxide-Au Nanoparticles Hybrids for Glucose Sensing. *Sens. Actuators, B* **2015**, *221*, 265–272.

(143) Ye, Y.; Ding, S.; Ye, Y.; Xu, H.; Cao, X.; Liu, S.; Sun, H. Enzyme-Based Sensing of Glucose Using a Glassy Carbon Electrode Modified with a One-Pot Synthesized Nanocomposite Consisting of Chitosan, Reduced Graphene Oxide and Gold Nanoparticles. *Microchim. Acta* **2015**, *182*, 1783–1789.

(144) Wang, L.; Lu, X.; Ye, Y.; Sun, L.; Song, Y. Nickel-Cobalt Nanostructures Coated Reduced Graphene Oxide Nanocomposite Electrode for Nonenzymatic Glucose Biosensing. *Electrochim. Acta* **2013**, *114*, 484–493.

(145) Subramanian, P.; Niedziółka-Jönsson, J.; Lesniewski, A.; Wang, Q.; Li, M.; Boukherroub, R.; Szunerits, S. J. Preparation of Reduced Graphene Oxide–Ni(OH)<sub>2</sub> Composites by Electrophoretic Deposition: Application for Non-Enzymatic Glucose Sensing. *J. Mater. Chem. A* **2014**, *2*, 5525–5533.

(146) Hu, Y.; He, F.; Ben, A.; Chen, C. Synthesis of Hollow Pt–Ni–Graphene Nanostructures for Nonenzymatic Glucose Detection. *J. Electroanal. Chem.* **2014**, *726*, 55–61.

(147) Tian, Y.; Liu, Y.; Wang, W.; Zhang, X.; Peng, W. CuO Nanoparticles on Sulfur-Doped Graphene for Nonenzymatic Glucose Sensing. *Electrochim. Acta* **2015**, *156*, 244–251.

(148) Yang, S.; Liu, L.; Wang, G.; Li, G.; Deng, D.; Qu, D. One-pot Synthesis of Mn<sub>3</sub>O<sub>4</sub> Nanoparticles Decorated with Nitrogen-Doped Reduced Graphene Oxide for Sensitive Nonenzymatic Glucose Sensing. *J. Electroanal. Chem.* **2015**, *755*, 15–21.

(149) Hoa, L. T.; Chung, J. S.; Hur, S. H. A Highly Sensitive Enzyme-Free Glucose Sensor Based on Co<sub>3</sub>O<sub>4</sub> Nanoflowers and 3D Graphene Oxide Hydrogel Fabricated Viahydrothermal Synthesis. *Sens. Actuators, B* **2016**, *223*, 76–82.

(150) Zhang, X.; Liao, Q.; Liu, S.; Xu, W.; Liu, Y.; Zhang, Y. CuNiO Nanoparticles Assembled on Graphene as an Effective Platform for Enzyme-Free Glucose Sensing. *Anal. Chim. Acta* **2015**, *858*, 49–54.

(151) Dhara, K.; Thiagarajan, R.; Nair, B. G.; Thekkedath, G. S. B. Highly Sensitive and Wide-Range Nonenzymatic Disposable Glucose Sensor Based on a Screen Printed Carbon Electrode Modified with Reduced Graphene Oxide and Pd-CuO Nanoparticles. *Microchim. Acta* **2015**, *182*, 2183–2192.

(152) Chang, G.; Shu, H.; Huang, Q.; Oyama, M.; Ji, K.; Liu, X.; He, Y. Synthesis of Highly Dispersed Pt Nanoclusters Anchored Graphene Composites and their Application for Non-Enzymatic Glucose Sensing. *Electrochim. Acta* **2015**, *157*, 149–157.

(153) Hoa, L. T.; Sun, K. G.; Hur, S. H. Highly Sensitive Non-Enzymatic Glucose Sensor Based on Pt nanoparticle Decorated Graphene Oxide Hydrogel. *Sens. Actuators, B* **2015**, *210*, 618–623.

(154) Wang, Q.; Wang, Q.; Li, M.; Szunerits, S.; Boukherroub, R. Preparation of Reduced Graphene Oxide/Cu Nanoparticle Composites through Electrophoretic Deposition: Application for Nonenzymatic Glucose Sensing. *RSC Adv.* **2015**, *5*, 15861–15869.

(155) Ghanemi, A. Schizophrenia and Parkinson's Disease: Selected Therapeutic Advances beyond the Dopaminergic Etiologies. *Alex. J. Med.* **2013**, *49*, 287–291.

(156) Li, Y.; Ran, G.; Yi, W. J.; Luo, H. Q. A Glassy Carbon Electrode Modified with Graphene and Poly(Acridine Red) for Sensing Uric Acid. *Microchim. Acta* **2012**, *178*, 115–121.

(157) Block, W. D.; Geib, N. C. An Enzymatic Method for the Determination of Uric Acid in Whole Blood. *J. Biol. Chem.* **1947**, *168*, 747–756.

(158) Noroozifar, M.; Khorasani-Motlagh, M.; Jahromi, F.-Z.; Rostami, S. Sensitive and Selective Determination of Uric Acid in Real Samples by Modified Glassy Carbon Electrode with Holmium



Fluoride Nps/Multi-Walled Carbon Nanotube as a New Biosensor. *Sens. Actuators, B* **2013**, *188*, 65–72.

(159) Özcan, A.; Şahin, Y. Preparation of Selective and Sensitive Electrochemically Treated Pencil Graphite Electrodes for the Determination of Uric Acid in Urine and Blood Serum. *Biosens. Bioelectron.* **2010**, *25*, 2497–2502.

(160) Numnuam, A.; Thavarungkul, P.; Kanatharana, P. An Amperometric Uric Acid Biosensor Based on Chitosan-Carbon Nanotubes Electrospun Nanofiber on Silver Nanoparticles. *Anal. Bioanal. Chem.* **2014**, *406*, 3763–3772–3772.

(161) Kaur, B.; Pandiyan, T.; Satpati, B.; Srivastava, R. Simultaneous and Sensitive Determination of Ascorbic Acid, Dopamine, Uric Acid, And Tryptophan with Silver Nanoparticles-Decorated Reduced Graphene Oxide Modified Electrode. *Colloids Surf, B* **2013**, *111*, 97–106.

(162) Zhang, Z.; Yin, J. Sensitive Detection of Uric Acid on Partially Electro-Reduced Graphene Oxide Modified Electrodes. *Electrochim. Acta* **2014**, *119*, 32–37.

(163) Aneesh, P. K.; Nambiar, S. R.; Rao, T. P.; Ajayaghosh, A. Electrochemically Synthesized Partially Reduced Graphene Oxide Modified Glassy Carbon Electrode for Individual and Simultaneous Voltammetric Determination of Ascorbic Acid, Dopamine and Uric Acid. *Anal. Methods* **2014**, *6*, 5322–5330.

(164) Mazloum-Ardakani, M.; Ahmadi, S. H.; Mahmoudabadi, Z. S.; Heydar, K. T.; Mirjalili, B. F. Electrochemical Behavior of Dopamine at a [1,1'-Binaphthalene]-4,4'-Diol-Modified Carbon Nanotube Paste Electrode and the Simultaneous Determination of Dopamine, Folic Acid and Uric Acid. *Anal. Methods* **2013**, *5*, 6982–6989.

(165) Mazloum-Ardakani, M.; Naser-Sadrabadi, A.; Sheikh-Mohseni, M. A.; Benvidi, A.; Naeimi, H.; Karshenas, A. An Electrochemical Sensor Based on Carbon Nanotubes and a New Schiff Base for Selective Determination of Dopamine in the Presence of Uric Acid, Folic Acid, and Acetaminophen. *Ionics* **2013**, *19*, 1663–1671.

(166) Fei, X.; Luo, J.; Liu, R.; Liu, J.; Liu, X.; Chen, M. Multiwalled Carbon Nanotubes Noncovalently Functionalized by Electro-Active Amphiphilic Copolymer Micelles for Selective Dopamine Detection. *RSC Adv.* **2015**, *5*, 18233–18241.

(167) Mercante, L. A.; et al. Electrospun Polyamide 6/Poly-(Allylamine Hydrochloride) Nanofibers Functionalized with Carbon Nanotubes for Electrochemical Detection of Dopamine. *ACS Appl. Mater. Interfaces* **2015**, *7*, 4784–4790.

(168) Cheng, H.; Qiu, H.; Zhu, Z.; Li, M.; Shi, Z. Investigation of the Electrochemical Behavior of Dopamine at Electrodes Modified with Ferrocene-Filled Double-Walled Carbon Nanotubes. *Electrochim. Acta* **2012**, *63*, 83–88.

(169) Cheng, H.; Guan, L.; Shi, Z.; Zhu, Z.; Gu, Z.; Li, M. Bi-Directional Electrocatalytic Detection of Dopamine at an Electrode Modified with Ferrocene-Filled Carbon Nanotube Peapods. *Electroanalysis* **2013**, *25*, 2041–2044.

(170) Karuppiah, C.; Devasenathipathy, R.; Chen, S.-M.; Arulraj, D.; Palanisamy, S.; Mani, V.; Vasantha, V. S. Fabrication of Nickel Tetrasulfonated Phthalocyanine Functionalized Multiwalled Carbon Nanotubes on Activated Glassy Carbon Electrode for the Detection of Dopamine. *Electroanalysis* **2015**, *27*, 485–493.

(171) Figueiredo-Filho, L. C. S.; Silva, T. A.; Vicentini, F. C.; Fatibello-Filho, O. Simultaneous Voltammetric Determination of Dopamine and Epinephrine in Human Body Fluid Samples Using a Glassy Carbon Electrode Modified with Nickel Oxide Nanoparticles and Carbon Nanotubes within a Dihexadecylphosphate Film. *Analyst* **2014**, *139*, 2842–2849.

(172) Vinoth, V.; Wu, J. J.; Asiri, A. M.; Anandan, S. Simultaneous Detection of Dopamine and Ascorbic Acid Using Silicate Network Interlinked Gold Nanoparticles and Multi-Walled Carbon Nanotubes. *Sens. Actuators, B* **2015**, *210*, 731–741.

(173) Tsierekzos, N. G.; Ritter, U.; Thaha, Y. N.; Downing, C.; Szroeder, P.; Scharff, P. Multi-Walled Carbon Nanotubes Doped with Boron as an Electrode Material for Electrochemical Studies on Dopamine, Uric Acid, And Ascorbic Acid. *Microchim. Acta* **2015**, DOI: 10.1007/s00604-015-1585-6.

(174) Ammari, R.; Lopez, C.; Fiorentino, H.; Gonon, F.; Hammond, C. A Mouse Juvenile or Adult Slice with Preserved Functional Nigro-Striatal Dopaminergic Neurons. *Neuroscience* **2009**, *159*, 3–6.

(175) Exley, R.; Clements, M. A.; Hartung, H.; McIntosh, J. M.; Cragg, S. J.  $\alpha 6$ -Containing Nicotinic Acetylcholine Receptors Dominate the Nicotine Control of Dopamine Neurotransmission in Nucleus Accumbens. *Neuropsychopharmacology* **2008**, *33*, 2158–2166.

(176) Petkovic, M.; Ferguson, J. L.; Gunaratne, H. Q. N.; Ferreira, R.; Leitão, M. C.; Seddon, K. R.; et al. Novel Biocompatible Cholinium-Based Ionic Liquids—Toxicity and Biodegradability. *Green Chem.* **2010**, *12*, 643–649.

(177) Hough, W. L.; Smiglak, M.; Rodríguez, H.; Swatloski, R. P.; Spear, S. K.; Daly, D. T.; et al. The Third Evolution of Ionic Liquids: Active Pharmaceutical Ingredients. *New J. Chem.* **2007**, *31*, 1429–1436.

(178) Noroozifar, M.; Khorasani-Motlagh, M.; Parizi, M. B.; Akbari, R. Highly Sensitive Electrochemical Detection of Dopamine and Uric Acid on a Novel Carbon Nanotube-Modified Ionic Liquid-Nanozeolite Paste Electrode. *Ionics* **2013**, *19*, 1317–1327.

(179) Li, Y.; et al. Non-Enzymatic Sensing of Uric Acid Using a Carbon Nanotube Ionic-Liquid Paste Electrode Modified with Poly(B-Cyclodextrin). *Microchim. Acta* **2015**, *182*, 1877–1884.

(180) Bhakta, A. K.; et al. Iron Nanoparticles Decorated Multi-Wall Carbon Nanotubes Modified Carbon Paste Electrode as an Electrochemical Sensor for the Simultaneous Determination of Uric Acid in the Presence of Ascorbic Acid, Dopamine and L-Tyrosine. *Mater. Sci. Eng., C* **2015**, *57*, 328–337.

(181) Sun, X.; Wu, J.; Chen, Z.; Su, X.; Hinds, B. J. Fouling Characteristics and Electrochemical Recovery of Carbon Nanotube Membranes. *Adv. Funct. Mater.* **2013**, *23*, 1500–1506.

(182) Celik, E.; Park, H.; Choi, H.; Choi, H. Carbon Nanotube Blended Polyethersulfone Membranes for Fouling Control in Water Treatment. *Water Res.* **2011**, *45*, 274–282.

(183) Yang, H.; Li, Y.; Liu, Y.; Zhang, Y.; Zhao, Y.; Zhao, M. One-Pot Chemical Blasting Synthesis of the Bamboo-Like Multiwalled Carbon Nanotubes/Graphene Oxide Nanocomposite and its Application in Electrochemical Detection of Dopamine. *J. Solid State Electrochem.* **2015**, *19*, 145–152.

(184) Shieh, Y.; Jiang, H. F. Graphene Oxide-Assisted Dispersion of Carbon Nanotubes in Sulfonated Chitosan-Modified Electrode for Selective Detections of Dopamine, Uric Acid, And Ascorbic Acid. *J. Electroanal. Chem.* **2015**, *736*, 132–138.

(185) Cheemalapati, S.; Palanisamy, S.; Mani, V.; Chen, S. M. Simultaneous Electrochemical Determination of Dopamine and Paracetamol on Multiwalled Carbon Nanotubes/Graphene Oxide Nanocomposite-Modified Glassy Carbon Electrode. *Talanta* **2013**, *117*, 297–304.

(186) Li, H.; Wang, Y.; Ye, D.; Luo, J.; Su, B.; Zhang, S.; et al. An Electrochemical Sensor for Simultaneous Determination of Ascorbic Acid, Dopamine, Uric Acid and Tryptophan Based on Mwnts Bridged Mesocellular Graphene Foam Nanocomposite. *Talanta* **2014**, *127*, 255–261.

(187) Yang, Y. J.; Li, W. CTAB Functionalized Graphene Oxide/Multiwalled Carbon Nanotube Composite Modified Electrode for the Simultaneous Determination of Ascorbic Acid, Dopamine, Uric Acid and Nitrite. *Biosens. Bioelectron.* **2014**, *56*, 300–306.

(188) Ramakrishnan, S.; Pradeep, K. R.; Raghul, A.; Senthilkumar, R.; Rangarajan, M.; Kothurkar, N. K. One-step Synthesis of Pt-Decorated Graphene–Carbon Nanotubes for the Electrochemical Sensing of Dopamine, Uric Acid and Ascorbic Acid. *Anal. Methods* **2015**, *7*, 779–786.

(189) Wang, S.; Zhang, W.; Zhong, X.; Chai, Y.; Yuan, R. Simultaneous Determination of Dopamine, Ascorbic Acid and Uric Acid Using a Multi-Walled Carbon Nanotube and Reduced Graphene Oxide Hybrid Functionalized by PAMAM and Au Nanoparticles. *Anal. Methods* **2015**, *7*, 1471–1477.

(190) Yang, L.; Liu, D.; Huang, J.; You, T. Simultaneous Determination of Dopamine, Ascorbic Acid and Uric Acid at

Electrochemically Reduced Graphene Oxide Modified Electrode. *Sens. Actuators, B* **2014**, *193*, 166–172.

(191) Yang, B.; Wang, H.; Du, J.; Fu, Y.; Yang, P.; Du, Y. Direct Electrodeposition of Reduced Graphene Oxide on Carbon Fiber Electrode for Simultaneous Determination of Ascorbic Acid, Dopamine and Uric Acid. *Colloids Surf., A* **2014**, *456*, 146–152.

(192) Nancy, T. E. M.; Anithakumary, V.; Swamy, B. E. K. Solar Graphene Modified Glassy Carbon Electrode for the Voltammetric Resolution and Detection of Dopamine, Ascorbic Acid and Uric Acid. *J. Electroanal. Chem.* **2014**, *720–721*, 107–114.

(193) Gao, F.; Cai, X.; Wang, X.; Gao, C.; Liu, S.; Gao, F.; et al. Highly Sensitive and Selective Detection of Dopamine in the Presence of Ascorbic Acid at Graphene Oxide Modified Electrode. *Sens. Actuators, B* **2013**, *186*, 380–387.

(194) Bagherzadeh, M.; Heydari, M. Electrochemical Detection of Dopamine Based on Pre-Concentration by Graphene Nanosheets. *Analyst* **2013**, *138*, 6044–6051.

(195) Qi, S.; Zhao, B.; Tang, H.; Jiang, X. Determination of Ascorbic Acid, Dopamine, and Uric Acid by a Novel Electrochemical Sensor Based on Pristine Graphene. *Electrochim. Acta* **2015**, *161*, 395–402.

(196) Dong, X. C.; Wang, X. W.; Wang, L. H.; Song, H.; Zhang, H.; Huang, W.; Chen, P. 3D Graphene Foam as a Monolithic and Macroporous Carbon Electrode for Electrochemical Sensing. *ACS Appl. Mater. Interfaces* **2012**, *4*, 3129–3133.

(197) Li, S. M.; Yang, S. Y.; Wang, Y. S.; Lien, C. H.; Tien, H. W.; Hsiao, S. T.; et al. Controllable Synthesis of Nitrogen-Doped Graphene and its Effect on the Simultaneous Electrochemical Determination of Ascorbic Acid, Dopamine, and Uric Acid. *Carbon* **2013**, *59*, 418–429.

(198) Manivel, P.; Dhakshnamoorthy, M.; Balamurugan, A.; Ponpandian, N.; Mangalaraj, D.; Viswanathan, C. Conducting Polyaniline-Graphene Oxide Fibrous Nanocomposites: Preparation, Characterization and Simultaneous Electrochemical Detection of Ascorbic Acid, Dopamine and Uric Acid. *RSC Adv.* **2013**, *3*, 14428–14437.

(199) Liu, X.; Zhang, L.; Wei, S.; Chen, S.; Ou, X.; Lu, Q. Overoxidized Polyimidazole/Graphene Oxide Copolymer Modified Electrode for the Simultaneous Determination of Ascorbic Acid, Dopamine, Uric Acid, Guanine and Adenine. *Biosens. Bioelectron.* **2014**, *57*, 232–238.

(200) Weng, X.; Cao, Q.; Liang, L.; Chen, J.; You, C.; Ruan, Y.; Lin, H.; Wu, L. Simultaneous Determination of Dopamine And Uric acid Using Layer-By-Layer Graphene and Chitosan Assembled Multilayer Films. *Talanta* **2013**, *117*, 359–365.

(201) Zhang, H.; Gai, P.; Cheng, R.; Wu, L.; Zhang, X.; Chen, J. Self-Assembly Synthesis of a Hierarchical Structure Using Hollow Nitrogen-Doped Carbon Spheres as Spacers to Separate the Reduced Graphene Oxide for Simultaneous Electrochemical Determination of Ascorbic Acid, Dopamine and Uric Acid. *Anal. Methods* **2013**, *5*, 3591–3600.

(202) Nancy, T. E. M.; Kumary, V. A. Synergistic Electrocatalytic Effect of Graphene/Nickel Hydroxide Composite for the Simultaneous Electrochemical Determination of Ascorbic Acid, Dopamine and Uric Acid. *Electrochim. Acta* **2014**, *133*, 233–240.

(203) Zeng, Y.; Zhou, Y.; Kong, L.; Zhou, T.; Shi, G. A Novel Composite of SiO<sub>2</sub>-Coated Graphene Oxide and Molecularly Imprinted Polymers for Electrochemical Sensing Dopamine. *Biosens. Bioelectron.* **2013**, *45*, 25–33.

(204) Qiu, Y. C.; Zhang, X. F.; Yang, S. H. High Performance Supercapacitors Based on Highly Conductive Nitrogen-Doped Graphene Sheets. *Phys. Chem. Chem. Phys.* **2011**, *13*, 12554–12558.

(205) Jeon, I. Y.; Yu, D. S.; Bae, S. Y.; Choi, H. J.; Chang, D. W.; Dai, L. M.; et al. Formation of Large-Area Nitrogen-Doped Graphene Film Prepared from Simple Solution Casting of Edge-Selectively Functionalized Graphite and its Electrocatalytic Activity. *Chem. Mater.* **2011**, *23*, 3987–3992.

(206) Shao, Y. Y.; Zhang, S.; Engelhard, M. H.; Li, G. S.; Shao, G. C.; Wang, Y.; et al. Nitrogen-Doped Graphene and its Electrochemical Applications. *J. Mater. Chem.* **2010**, *20*, 7491–7496.

(207) Chen, L.; Zheng, J.; Wang, A.; Wu, L.; Chen, J.; Feng, J. Facile Synthesis of Porous Bimetallic Alloyed PdAg Nanoflowers Supported on Reduced Graphene Oxide for Simultaneous Detection of Ascorbic Acid, Dopamine, and Uric Acid. *Analyst* **2015**, *140*, 3183–3192.

(208) Liu, Y.; She, P.; Gong, J.; Wu, W.; Xu, S.; Li, J.; Zhao, K.; Deng, A. A Novel Sensor Based on Electrodeposited Au–Pt Bimetallicnanoclusters Decorated on Graphene Oxide (GO)–Electrochemically-reduced GO for Sensitive Detection of Dopamine and Uric Acid. *Sens. Actuators, B* **2015**, *221*, 1542.

(209) Yang, Y. J. One-Pot Synthesis of Reduced Graphene Oxide/Zinc Sulfide Nanocomposite at Room Temperature for Simultaneous Determination of Ascorbic Acid, Dopamine and Uric Acid. *Sens. Actuators, B* **2015**, *221*, 750–759.

(210) Pruneanu, S.; Biris, A. R.; Pogacean, F.; Socaci, C.; Coros, M.; et al. The Influence of Uric and Ascorbic Acid on the Electrochemical Detection of Dopamine Using Graphene-Modified Electrodes. *Electrochim. Acta* **2015**, *154*, 197–204.

(211) Li, S.; Wang, Y.; Hsiao, S.; Liao, W.; Lin, C.; Yang, S.; Tien, H.; Ma, C. M.; Hu, C. Fabrication of a Silver Nanowire-Reduced Graphene Oxide-Based Electrochemical Biosensor and its Enhanced Sensitivity in the Simultaneous Determination of Ascorbic Acid, Dopamine, and Uric Acid. *J. Mater. Chem. C* **2015**, *3*, 9444–9453.

(212) Zou, H. L.; Li, B. L.; Luo, H. Q.; Li, N. B. A Novel Electrochemical Biosensor Based on Hemin Functionalized Graphene Oxide Sheets for Simultaneous Determination of Ascorbic Acid, Dopamine and Uric Acid. *Sens. Actuators, B* **2015**, *207*, 535–541.

(213) Zhang, W.; Zheng, J.; Shi, J.; Lin, Z.; Huang, Q.; Zhang, H.; Wei, C.; et al. Nafion Covered Core–Shell Structured Fe<sub>3</sub>O<sub>4</sub>@ Graphene Nanospheres Modified Electrode for Highly Sensitive Detection of Dopamine. *Anal. Chim. Acta* **2015**, *853*, 285–290.

(214) Salamon, J.; Sathishkumar, Y.; Ramachandran, K.; Lee, Y. S.; Yoo, D. J.; Kim, A. R.; Kumar, G. G. One-Pot Synthesis of Magnetite Nanorods/Graphene Composites and its Catalytic Activity Toward Electrochemical Detection of Dopamine. *Biosens. Bioelectron.* **2015**, *64*, 269–276.

(215) Shumyantseva, V. V.; Suprun, E. V.; Bulko, T. V.; Archakov, A. Electrochemical Methods for Detection of Post-Translational Modifications of Proteins. *Biosens. Bioelectron.* **2014**, *61*, 131–139.

(216) Shen, G.; Zhang, X.; Shen, Y.; Zhang, S.; Fang, L. L. One-Step Immobilization of Antibodies for  $\alpha$ -1-Fetoprotein Immunosensor Based on Dialdehyde Cellulose/Ionic Liquid Composite. *Anal. Biochem.* **2015**, *471*, 38–43.

(217) Jiang, L.; Han, J.; Li, F.; Gao, J.; Li, Y.; Dong, Y.; Wei, Q. A Sandwich-Type Electrochemical Immunosensor Based on Multiple Signal Amplification for  $\alpha$ -Fetoprotein Labeled by Platinum Hybrid Multiwalled Carbon Nanotubes Adhered Copper Oxide. *Electrochim. Acta* **2015**, *160*, 7–14.

(218) Schindler, M.; Assaf, Y.; Sharon, N. D.; Chipman, M. Mechanism of Lysozyme Catalysis - Role of Ground-State Strain in Subsite D in Hen Eggwhite and Human Lysozymes. *Biochemistry* **1977**, *16*, 423–431.

(219) Gorbenko, G. P.; Ioffe, V. M.; Kinnunen, P. K. J. Binding of Lysozyme to Phospholipid Bilayers: Evidence for Protein Aggregation upon Membrane Association. *Biophys. J.* **2007**, *93*, 140–153.

(220) Revenis, M. E.; Kaliner, M. A. J. Lactoferrin and Lysozyme Deficiency in Airway Secretions: Association with the Development of Bronchopulmonary Dysplasia. *J. Pediatr.* **1992**, *121*, 262–270.

(221) Bai, Y. H.; Xu, J. J.; Chen, H. Y. Selective Sensing of Cysteine on Manganese Dioxide Nanowires and Chitosan Modified Glassy Carbon Electrodes. *Biosens. Bioelectron.* **2009**, *24*, 2985–2990.

(222) Yosypchuk, B.; Novotny, I. Cathodic Stripping Voltammetry of Cysteine Using Silver and Copper Solid Amalgam Electrodes. *Talanta* **2002**, *56*, 971–976.

(223) Wring, S. A.; Hart, J. P.; Birch, B. J. Determination of Glutathione in Human Plasma Using High-Performance Liquid Chromatography with Electrochemical Detection with a Carbon-Epoxy Resin Composite Electrode Chemically Modified with Cobalt Phthalocyanine. *Analyst* **1989**, *114*, 1571–1573.



- (224) Dale, Y.; Mackey, V.; Mushi, R.; Nyanda, A.; Maleque, M.; Ike, J. Simultaneous Measurement of Phenylalanine and Tyrosine in Phenylketonuric Plasma and Dried Blood by High-Performance Liquid Chromatography. *J. Chromatogr. B: Anal. Technol. Biomed. Life Sci.* **2003**, *788*, 1–8.
- (225) Tang, X.; Liu, Y.; Hou, H.; You, T. Electrochemical Determination of L-Tryptophan, L-Tyrosine and L-Cysteine Using Electrospun Carbon Nanofibers Modified Electrode. *Talanta* **2010**, *80*, 2182–2186.
- (226) Silva, F. A. S.; da Silva, M. G. A.; Lima, P. R.; Meneghetti, M. R.; Kubota, L. T.; Goulart, M. O. F. A Very Low Potential Electrochemical Detection of L-cysteine Based on a Glassy Carbon Electrode Modified with Multi-Walled Carbon Nanotubes/Gold Nanorods. *Biosens. Bioelectron.* **2013**, *50*, 202–209.
- (227) Madrakian, T.; Haghshenas, E.; Afkhami, A. Simultaneous Determination of Tyrosine, Acetaminophen and Ascorbic Acid Using Gold Nanoparticles/Multiwalled Carbon Nanotube/Glassy Carbon Electrode by Differential Pulse Voltammetric Method. *Sens. Actuators, B* **2014**, *193*, 451–460.
- (228) Wald, N.; Stone, R.; Cuckle, H. S.; Grudzinskas, J. G.; Barkai, G.; Brambati, B.; et al. First Trimester Concentrations of Pregnancy Associated Plasma Protein A and Placental Protein 14 in Down's Syndrome. *Br. Med. J.* **1992**, *305*, 28.
- (229) Li, J.; Liu, G.; Zhang, W.; Cheng, W.; Xu, H.; Ding, S. Competitive Detection of Pregnancy-Associated Plasma Protein-A in Serum Using functional Single Walled Carbon Nanotubes/Chitosan-Based Electrochemical Immunosensor. *J. Electroanal. Chem.* **2013**, *708*, 95–101.
- (230) Feng, D.; Lu, X.; Dong, X.; Ling, Y.; Zhang, Y. Label-Free Electrochemical Immunosensor for the Carcinoembryonic Antigen Using a Glassy Carbon Electrode Modified with Electrodeposited Prussian Blue, a Graphene and Carbon Nanotube Assembly and an Antibody Immobilized on Gold Nanoparticles. *Microchim. Acta* **2013**, *180*, 767–774.
- (231) Xu, W.; He, J.; Gao, L.; Zhang, J.; Yu, C. Immunoassay for Netrin 1 via a Glassy Carbon Electrode Modified with Multi-Walled Carbon Nanotubes, Thionine and Gold Nanoparticles. *Microchim. Acta* **2015**, *182*, 2115–2122.
- (232) Silva, M. M. S.; Dias, A. C. M. S.; Silva, B. V. M.; Gomes-Filho, S. L. R.; et al. Electrochemical Detection of Dengue Virus NS1 Protein with a Poly(Allylamine)/Carbon Nanotube Layered Immuno Electrode. *J. Chem. Technol. Biotechnol.* **2015**, *90*, 194–200.
- (233) Shi, X.; Gu, W.; Li, B.; Chen, N.; Zhao, K.; Xian, Y. Enzymatic Biosensors Based on the use of Metal Oxide Nanoparticles. *Microchim. Acta* **2014**, *181*, 1–22.
- (234) Majid, S. M.; Teymourian, H.; Salimi, A. Fabrication of an Electrochemical L-Cysteine Sensor Based on Graphene Nanosheets Decorated Manganese Oxide Nanocomposite Modified Glassy Carbon Electrode. *Electroanalysis* **2013**, *25*, 2201–2210.
- (235) Shen, G.; Hu, X.; Zhang, S. A Signal-Enhanced Electrochemical Immunosensor based on Dendrimer Functionalized-Graphene as a Label for the Detection of  $\alpha$ -1-Fetoprotein. *J. Electroanal. Chem.* **2014**, *717–718*, 172–176.
- (236) Erdem, A.; Eksin, E.; Muti, M. Chitosan–Graphene Oxide Based Aptasensor for the Impedimetric Detection of Lysozyme. *Colloids Surf., B* **2014**, *115*, 205–211.
- (237) Wang, Q.; Zhou, Z.; Zhai, Y.; Zhang, L.; Hong, W.; Zhang, Z.; Dong, S. Label-Free Aptamer Biosensor for Thrombin Detection Based on Functionalized Graphene Nanocomposites. *Talanta* **2015**, *141*, 247–252.
- (238) Xue, Q.; Liu, Z.; Guo, Y.; Guo, S. Cyclodextrin Functionalized Graphene–Goldnanoparticle Hybrids with Strong Supramolecular Capability for Electrochemical Thrombin Aptasensor. *Biosens. Bioelectron.* **2015**, *68*, 429–436.
- (239) Wayu, M. B.; King, J. E.; Johnson, J. A.; Chusuei, C. C. A Zinc Oxide Carbon Nanotube Based Sensor for *in situ* Monitoring of Hydrogen Peroxide in Swimming Pools. *Electroanalysis* **2015**, *500187*.
- (240) Deng, S. Y.; Zhang, G. Y.; Shan, D.; Liu, Y. H.; Wang, K.; Zhang, X. J. Pyrocatechol Violet-Assisted *in situ* Growth of Copper Nanoparticles on Carbon Nanotubes: The Synergic Effect for Electrochemical Sensing of Hydrogen Peroxide. *Electrochim. Acta* **2015**, *155*, 78–84.
- (241) Liu, D.; Guo, Q.; Zhang, X.; Hou, H.; You, T. PdCo Alloy Nanoparticle–Embedded Carbon Nanofiber for Ultrasensitive Non-enzymatic Detection of Hydrogen Peroxide and Nitrite. *J. Colloid Interface Sci.* **2015**, *450*, 168–173.
- (242) Li, J.; Jiang, Y.; Zhai, Y.; Liu, H.; Li, L. Prussian Blue/Reduced Graphene Oxide Composite for the Amperometric Determination of Dopamine and Hydrogen Peroxide. *Anal. Lett.* **2015**, *48*, 2786–2798.
- (243) Sheng, Q.; Zhang, D.; Wu, Q.; Zheng, J.; Tang, H. Electrodeposition of Prussian Blue Nanoparticles on Polyaniline Coated Halloysite Nanotubes for Nonenzymatic Hydrogen Peroxide Sensing. *Anal. Methods* **2015**, *7*, 6896–6903.
- (244) Clausen, D. N.; Duarte, E. H.; Sartori, E. R.; Pereira, A. C.; Tarley, C. R. T. Evaluation of a Multi-Walled Carbon Nanotube-Hemin Composite for the Voltammetric Determination of Hydrogen Peroxide in Dental Products. *Anal. Lett.* **2014**, *47*, 750–754.
- (245) Zhang, Y.; Xia, Z.; Liu, H.; Yang, M.; Lin, L.; Li, Q. Hemin-Graphene Oxide-Pristine Carbon Nanotubes Complexes with Intrinsic Peroxidase-Like Activity for the Detection of H<sub>2</sub>O<sub>2</sub> and Simultaneous Determination for Trp, AA, DA, and UA. *Sens. Actuators, B* **2013**, *188*, 496–501.
- (246) Lin, K. C.; Huang, J. Y.; Chen, S. M. Enhancing Electrodeposition and Electrocatalytic Properties of Poly(Neutral Red) and FAD to Determine NADH and H<sub>2</sub>O<sub>2</sub> Using Amino-Functionalized Multi-Walled Carbon Nanotubes. *RSC Adv.* **2013**, *3*, 25727–25734.
- (247) Butwong, N.; Zhou, L.; Ng-eontae, W.; Burakkham, R.; Moore, E.; et al. A Sensitive Nonenzymatic Hydrogen Peroxide Sensor Using Cadmium Oxide Nanoparticles/Multiwall Carbon Nanotube Modified Glassy Carbon Electrode. *Electroanal. Chem.* **2014**, *717–718*, 41–46.
- (248) Jia, X.; Hu, G.; Nitze, F.; Barzegar, H. R.; Sharif, T.; Tai, C. W.; et al. Synthesis of Palladium/Helical Carbon Nanofiber Hybrid Nanostructures and Their Application for Hydrogen Peroxide and Glucose Detection. *ACS Appl. Mater. Interfaces* **2013**, *5*, 12017–12022.
- (249) Pannopard, P.; Boonyuen, C.; Warakulwit, C.; Hoshikawa, Y.; Kyotani, T.; Limtrakul, J. Size-Tailored Synthesis of Gold Nanoparticles and Their Facile Deposition on AAO-Templated Carbon Nanotubes via Electrostatic Self-Assembly: Application to H<sub>2</sub>O<sub>2</sub> Detection. *Carbon* **2015**, *94*, 836–844.
- (250) Lorestani, F.; Shahnava, Z.; Mn, P.; Alias, Y.; Manan, N. S. A. One-Step Hydrothermal Green Synthesis of Silver Nanoparticle-Carbon Nanotube Reduced-Graphene Oxide Composite and its Application as Hydrogen Peroxide Sensor. *Sens. Actuators, B* **2015**, *208*, 389–398.
- (251) Kumar, G. G.; Babu, K. J.; Nahm, K. S.; Hwang, Y. J. A Facile One-Pot Green Synthesis of Reduced Graphene Oxide and its Composites for Non-Enzymatic Hydrogen Peroxide Sensor Applications. *RSC Adv.* **2014**, *4*, 7944–7951.
- (252) Liu, M.; Liu, R.; Chen, W. Graphene Wrapped Cu<sub>2</sub>O nanocubes: Non-Enzymatic Electrochemical Sensors for the Detection of Glucose and Hydrogen Peroxide with Enhanced Stability. *Biosens. Bioelectron.* **2013**, *45*, 206–212.
- (253) Nalini, S.; Nandini, S.; Shanmugam, S.; Neelagund, S. E.; Melo, J. S.; Suresh, G. S. Amperometric Hydrogen Peroxide and Cholesterol Biosensors Designed by Using Hierarchical Curtailed Silver Flowers Functionalized Graphene and Enzymes Deposits. *J. Solid State Electrochem.* **2014**, *18*, 685–701.
- (254) Sun, W.; Gong, S.; Deng, Y.; Li, T.; Cheng, Y.; Wang, W.; et al. Electrodeposited Nickel Oxide and Graphene Modified Carbon Ionic Liquid Electrode for Electrochemical Myoglobin Biosensor. *Thin Solid Films* **2014**, *562*, 653–658.
- (255) Fan, Z.; Lin, Q.; Gong, P.; Liu, B.; Wang, J.; Yang, S. A New Enzymatic Immobilization Carrier Based on Graphene Capsule for Hydrogen Peroxide Biosensors. *Electrochim. Acta* **2015**, *151*, 186–194.
- (256) Yang, S.; Li, G.; Wang, G.; Zhao, J.; Hu, M.; Qu, L. A Novel Nonenzymatic H<sub>2</sub>O<sub>2</sub> Sensor Based on Cobalt Hexacyanoferrate nanoparticles and Graphene Composite Modified Electrode. *Sens. Actuators, B* **2015**, *208*, 593–599.



- (257) Tian, Y.; Liu, Y.; Wang, W.; Zhang, X.; Peng, W. Sulfur-Doped Graphene-Supported Ag Nanoparticles for Nonenzymatic Hydrogen Peroxide Detection. *J. Nanopart. Res.* **2015**, *17*, 193.
- (258) Xue, C.; Kung, C. C.; Gao, M.; Liu, C. C.; Dai, L.; Urbas, A.; Li, Q. Facile Fabrication of 3D Layer-by-Layer Graphene-Gold Nanorod Hybrid Architecture for Hydrogen Peroxide Based Electrochemical Biosensor. *Sens. Bio-Sens. Res.* **2015**, *3*, 7–11.
- (259) Liu, J.; Bo, X.; Zhao, Z.; Guo, L. Highly Exposed Pt Nanoparticles Supported on Porous Graphene for Electrochemical Detection of Hydrogen Peroxide in Living Cells. *Biosens. Bioelectron.* **2015**, *74*, 71–77.
- (260) Mani, V.; Devasenathipathy, R.; Chen, S.; Wang, S.; Devi, P.; Tai, Y. Electrodeposition of Copper Nanoparticles Using Pectin Scaffold at Graphene Nanosheets for Electrochemical Sensing of Glucose and Hydrogen Peroxide. *Electrochim. Acta* **2015**, *176*, 804–810.
- (261) Min, S. K.; Cho, Y.; Mason, D. R.; Lee, J.; Kim, K. S. Theoretical Design of Nanomaterials and Nanodevices: Nanolensing, Supermagneto Resistance, and Ultrafast DNA Sequencing. *J. Phys. Chem. C* **2011**, *115*, 16247–16257.
- (262) Thomas, S.; Rajan, A. C.; Rezapour, M. R.; Kim, K. S. In Search of a Two Dimensional Material for DNA Sequencing. *J. Phys. Chem. C* **2014**, *118*, 10855–10858.
- (263) Rezapour, M. R.; Rajan, A. C.; Kim, K. S. Molecular Sensing Using Armchair Graphene Nanoribbon. *J. Comput. Chem.* **2014**, *35*, 1916–1920.
- (264) Benvidi, A.; Rajabzadeh, N.; Mazloum-Ardakani, M.; Heidari, M. M. Comparison of Impedimetric Detection of DNA Hybridization Onchemically and Electrochemically Functionalized Multi-Wall Carbon Nanotubes Modified Electrode. *Sens. Actuators, B* **2015**, *207*, 673–682.
- (265) Liu, L.; Jiang, S.; Wang, L.; Zhang, Z.; Xie, G. Direct Detection of microRNA-126 at a Femtomolar Level Using a Glassy Carbon Electrode Modified with Chitosan, Graphene Sheets, and a Poly-(Amidoamine) Dendrimer Composite with Gold and Silver Nanoclusters. *Microchim. Acta* **2015**, *182*, 77–84.
- (266) Li, J.; Lee, E.-C. Carbon Nanotube/Polymer Composite Electrodes for Flexible, Attachable Electrochemical DNAsensors. *Biosens. Bioelectron.* **2015**, *71*, 414–419.
- (267) Zhang, Y.; Geng, X.; Ai, J.; Gao, Q.; Qi, H.; Zhang, C. Signal Amplification Detection of DNA Using a Sensor Fabricated by One-Step Covalent Immobilization of Amino-Terminated Probe DNA onto the Polydopamine-Modified Screen-Printed Carbon Electrode. *Sens. Actuators, B* **2015**, *221*, 1535.
- (268) Kashanian, S.; Khodaei, M. M.; Roshanfekr, H.; Peyman, H. DNA Interaction of [Cu(dmp) (phen-dion)] (dmp = 4,7 and 2,9 dimethyl phenanthroline, phen-dion = 1,10-phenanthroline-5,6-dion) Complexes and DNA-Based Electrochemical Biosensor Using Chitosan–Carbon Nanotubes Composite Film. *Spectrochim. Acta, Part A* **2013**, *114*, 642–649.
- (269) Huang, K. J.; Liu, Y. J.; Wang, H. B.; Wang, Y. Y.; Liu, Y. M. Sub-Femtomolar DNA Detection Based on Layered Molybdenum Disulfide/Multi-Walled Carbon Nanotube Composites, Au Nanoparticle and Enzyme Multiple Signal Amplification. *Biosens. Bioelectron.* **2014**, *55*, 195–202.
- (270) Miodek, A.; Mejri, N.; Gomgnimbou, M.; Sola, C.; Korri-Youssoufi, H. E-DNA Sensor of Mycobacterium tuberculosis Based on Electrochemical Assembly of Nanomaterials (MWCNTs/PPy/PAMAM). *Anal. Chem.* **2015**, *87*, 9257–9264.
- (271) Li, F.; Peng, J.; Wang, J.; Tang, H.; Tan, L.; Xie, Q.; Yao, S. Carbon Nanotube-Based Label-Free Electrochemical Biosensor for Sensitive Detection of miRNA-24. *Biosens. Bioelectron.* **2014**, *54*, 158–164.
- (272) Li, F.; Peng, J.; Zheng, Q.; Guo, X.; Tang, H.; Yao, S. Carbon Nanotube-Polyamidoamine Dendrimer Hybrid-Modified Electrodes for Highly Sensitive Electrochemical Detection of MicroRNA24. *Anal. Chem.* **2015**, *87*, 4806–4813.
- (273) Zhang, Z.; Liu, S.; Zhang, Y.; Kang, M.; He, L.; Feng, X.; Peng, D.; Wang, P. Easy Amino-Group Modification of Graphene Using Intermolecular Forces for DNA Biosensing. *RSC Adv.* **2014**, *4*, 16368–16373.
- (274) Du, D.; Guo, S.; Tang, L.; Ning, Y.; Yao, Q.; Zhang, G. J. Graphene-Modified Electrode for DNA Detection via PNA–DNA Hybridization. *Sens. Actuators, B* **2013**, *186*, 563–570.
- (275) Sun, W.; Lu, Y.; Wu, Y.; Zhang, Y.; Wang, P.; Chen, Y.; Li, G. Electrochemical Sensor for Transgenic Maize MON810 Sequence with Electrostatic Adsorption DNA on Electrochemically Reduced Graphene Modified Electrode. *Sens. Actuators, B* **2014**, *202*, 160–166.
- (276) Tian, T.; Li, Z.; Lee, E. C. Sequence-Specific Detection of DNA Using Functionalized Graphene as an Additive. *Biosens. Bioelectron.* **2014**, *53*, 336–339.
- (277) Cao, X. Ultra-sensitive Electrochemical DNA Biosensor Based on Signal Amplification Using Gold Nanoparticles Modified with Molybdenum Disulfide, Graphene and Horseradish Peroxidase. *Microchim. Acta* **2014**, *181*, 1133–1141.
- (278) Huang, K. J.; Liu, Y. J.; Wang, H. B.; Gan, T.; Liu, Y. M.; Wang, L. L. Signal Amplification for Electrochemical DNA Biosensor Based on Two-Dimensional Graphene Analogue Tungsten Sulfide–Graphene Composites and Gold Nanoparticles. *Sens. Actuators, B* **2014**, *191*, 828–836.
- (279) Wang, J.; Shi, A.; Fang, X.; Han, X.; Zhang, Y. An Ultrasensitive Electrochemical DNA Biosensor Based on Graphene/Au Nanorod/Polythionine for Human Papillomavirus DNA Detection. *Anal. Biochem.* **2015**, *469*, 71–75.
- (280) Pan, H.; Yu, H.; Wang, N.; Zhang, Z.; Wan, G.; Liu, H.; Guan, X.; Chang, D. Electrochemical DNA Biosensor Based on a Glassy Carbon Electrode Modified with Gold Nanoparticles and Graphene for Sensitive Determination of Klebsiella Pneumoniae Carbapenemase. *J. Biotechnol.* **2015**, *214*, 133–138.
- (281) Peng, H.; Hu, Y.; Liu, P.; Deng, Y.; Wang, P.; Chen, W.; Liu, A.; Chen, Y.; Lin, X. Label-Free Electrochemical DNA Biosensor for Rapid Detection of Multidrug Resistance Gene Based on Au Nanoparticles/Toluidine Blue–Graphene Oxide Nanocomposites. *Sens. Actuators, B* **2015**, *207*, 269–276.
- (282) Wang, J.; Shi, A.; Fang, X.; Han, X.; Zhang, Y. An Ultrasensitive Supersandwich Electrochemical DNA Biosensor Based on Gold Nanoparticles Decorated Reduced Graphene Oxide. *Anal. Biochem.* **2015**, *469*, 71–75.
- (283) Huang, K. J.; Liu, Y. J.; Wang, H. B.; Wang, Y. Y. A Sensitive Electrochemical DNA Biosensor Based on Silver Nanoparticles-Polydopamine@Graphene Composite. *Electrochim. Acta* **2014**, *118*, 130–137.
- (284) Zheng, X.; Wang, L. Direct Electrocatalytic Oxidation and Simultaneous Determination of 5-Methylcytosine and Cytosine at Electrochemically Reduced Graphene Modified Glassy Carbon Electrode. *Electroanalysis* **2013**, *25*, 1697–1705.
- (285) Akhavan, O.; Ghaderi, E.; Rahighi, R. Toward Single-DNA Electrochemical Biosensing by Graphene Nanowalls. *ACS Nano* **2012**, *6*, 2904–2916.
- (286) Li, C.; Qiu, X.; Ling, Y. Electrocatalytic Oxidation and the Simultaneous Determination of Guanine and Adenine on (2,6-Pyridinedicarboxylic Acid)/Graphene Composite Film Modified Electrode. *J. Electroanal. Chem.* **2013**, *704*, 44–49.
- (287) Yang, T.; Kong, Q.; Li, Q.; Wang, X.; Chen, L.; Jiao, K. One-step Electropolymerization of Xanthurenic Acid–Graphene Film Prepared by a Pulse Potentiostatic Method for Simultaneous Detection of Guanine and Adenine. *Polym. Chem.* **2014**, *5*, 2214–2218.
- (288) Yang, T.; Kong, Q.; Li, Q.; Wang, X.; Chen, L.; Jiao, K. Highly Sensitive and Synergistic Detection of Guanine and Adenine Based on Poly(xanthurenic acid)-Reduced Graphene Oxide Interface. *ACS Appl. Mater. Interfaces* **2014**, *6*, 11032–11037.
- (289) Zheng, Q.; Wu, H.; Shen, Z.; Gao, W.; Yu, Y.; Ma, Y.; Guang, W.; Guo, Q.; Yan, R.; Wang, J.; Ding, K. An Electrochemical DNA Sensor Based on Polyaniline/Graphene: High Sensitivity to DNA Sequences in a Wide Range. *Analyst* **2015**, *140*, 6660–6670.
- (290) Jafari, S.; Faridbod, F.; Norouzi, P.; Dezfouli, A. S.; Ajloo, D.; Mohammadpanah, F.; Ganjali, M. R. Detection of Aeromonas

Hydrophila DNA Oligonucleotide Sequence Using a Biosensor Design Based on Ceria Nanoparticles Decorated Reduced Graphene Oxide and Fast Fourier Transform Square Wave Voltammetry. *Anal. Chim. Acta* **2015**, *895*, 80–88.

(291) Congur, G.; Eksin, E.; Erdem, A. Impedimetric Detection of microRNA at Graphene Oxide Modified Sensors. *Electrochim. Acta* **2015**, *172*, 20–27.

(292) Hu, T.; Zhang, L.; Wen, W.; Zhang, X.; Wang, S. Enzyme Catalytic Amplification of miRNA-155 Detection with Graphene Quantum Dot-Based Electrochemical Biosensor. *Biosens. Bioelectron.* **2015**, *77*, 451–456, <http://dx.doi.org/10.1016/j.bios.2015.09.068>.

(293) Azimzadeh, M.; Rahaie, M.; Nasirizadeh, N.; Ashtari, K.; Naderi-Manesh, H. An Electrochemical Nanobiosensor for Plasma miRNA-155, Based on Graphene Oxide and Gold Nanorod, for Early Detection of Breast Cancer. *Biosens. Bioelectron.* **2016**, *77*, 99–106.

(294) Cheemalapati, S.; Palanisamy, S.; Chen, S. M. A Simple and Sensitive Electroanalytical Determination of Anxiolytic Buspirone Hydrochloride Drug Based on Multiwalled Carbon Nanotubes Modified Electrode. *J. Appl. Electrochem.* **2014**, *44*, 317–323.

(295) Primo, E. N.; Oviedo, M. B.; Sánchez, C. G.; Rubianes, M. D.; Rivas, G. A. Bioelectrochemical Sensing of Promethazine with Bamboo-Type Multiwalled Carbon Nanotubes Dispersed in Calf-Thymus Double Stranded DNA. *Bioelectrochemistry* **2014**, *99*, 8–16.

(296) Satyanarayana, M.; Goud, K. Y.; Reddy, K. K.; Gobi, K. V. Biopolymer Stabilized Nanogold Particles on Carbon Nanotube Support as Sensing Platform for Electrochemical Detection of 5-Fluorouracil *in vitro*. *Electrochim. Acta* **2015**, *178*, 608–616.

(297) Mao, A.; Li, H.; Jin, D.; Yu, L.; Hu, X. Fabrication of Electrochemical Sensor for Paracetamol Based on Multi-Walled Carbon Nanotubes and Chitosan–Copper Complex by Self-Assembly Technique. *Talanta* **2015**, *144*, 252–257.

(298) Afkhami, A.; Kafrahi, F.; Madrakian, T. Electrochemical Determination of Levodopa in the Presence of Ascorbic Acid by Polyglycine/ZnO Nanoparticles/Multi-Walled Carbon Nanotubes-Modified Carbon Paste Electrode. *Ionics* **2015**, *21*, 2937–2947.

(299) Xiang, L.; Yu, P.; Hao, J.; Zhang, M.; Zhu, L.; Dai, L.; et al. Vertically Aligned Carbon Nanotube-Sheathed Carbon Fibers as Pristine Microelectrodes for Selective Monitoring of Ascorbate *in vivo*. *Anal. Chem.* **2014**, *86*, 3909–3914.

(300) Nigović, B.; Sadiković, M.; Jurić, S. Electrochemical Sensing of Mesalazine and its N-Acetylated Metabolite in Biological Samples Using Functionalized Carbon Nanotubes. *Talanta* **2016**, *147*, 50–58.

(301) Madrakian, T.; Soleimani, M.; Afkhami, A. Electrochemical Determination of Fluvoxamine on Mercury Nanoparticle Multi-Walled Carbon Nanotube Modified Glassy Carbon Electrode. *Sens. Actuators, B* **2015**, *210*, 259–266.

(302) Zhang, W.; Zhang, X.; Zhang, L.; Chen, G. Fabrication of Carbon Nanotube-Nickel Nanoparticle Hybrid Paste Electrodes for Electrochemical Sensing of Carbohydrates. *Sens. Actuators, B* **2014**, *192*, 459–466.

(303) Xin, X.; Sun, S.; Li, H.; Wang, M.; Jia, R. Electrochemical Bisphenol A Sensor Based on Core–Shell Multiwalled Carbon Nanotubes/Graphene Oxide Nanoribbons. *Sens. Actuators, B* **2015**, *209*, 275–280.

(304) Jain, U.; Narang, J.; Rani, K.; Dekha, B.; Dhayia, S.; Chauhan, N. Synthesis of Cadmium Oxide and Carbon Nanotube Based Nanocomposites and Their Use as a Sensing Interface for Xanthine Detection. *RSC Adv.* **2015**, *5*, 29675–29683.

(305) Pavinatto, A.; Mercante, L. A.; Leandro, C. S.; Mattoso, L. H. C.; Correa, D. S. Layer-by-Layer assembled films of Chitosan and Multi-Walled Carbon Nanotubes for the Electrochemical Detection of 17 $\alpha$ -Ethinylestradiol. *J. Electroanal. Chem.* **2015**, *755*, 215–220.

(306) Li, Y.; Ali, M. A.; Chen, S. M.; Yang, S. Y.; Lou, B. S.; Al-Hemaid, F. M. A. Poly(basic red 9) Doped Functionalized Multi-Walled Carbon Nanotubes as Composite Films for Neurotransmitters Biosensors. *Colloids Surf., B* **2014**, *118*, 133–139.

(307) Cesarino, I.; Galesco, H. V.; Machado, S. A. S. Determination of Serotonin on Platinum Electrode Modified with Carbon Nano-

tubes/Polypyrrole/Silver Nanoparticles Nanohybrid. *Mater. Sci. Eng., C* **2014**, *40*, 49–54.

(308) Domisse, C. S.; Vane, C. L. D. Buspirone: A New Type of Anxiolytic. *Intell. Clin. Pharm.* **1985**, *19*, 624–628.

(309) Parfitt, K.; Sweetman, S. C.; Blake, P. S.; Parsons, A. V. *Martindale—The Extra Pharmacopoeia*; Pharmaceutical Press: London, 1999.

(310) Martínez-Perinán, E.; et al. Insulin Sensor Based on Nanoparticle-Decorated Multiwalled Carbonnanotubes Modified Electrodes. *Sens. Actuators, B* **2016**, *222*, 331–338.

(311) Madrakian, T.; Soleimani, M.; Afkhami, A. Simultaneous Determination of Mycophenolate Mofetil and its Active Metabolite, Mycophenolic Acid, by Differential Pulse Voltammetry Using Multi-Walled Carbon Nanotubes Modified Glassy Carbon Electrode. *Mater. Sci. Eng., C* **2014**, *42*, 38–45.

(312) Stamford, J. A.; Isaac, D.; Hicks, C. A.; Ward, M. A.; Osborne, D. J.; O'Neill, M. J. Ascorbic Acid is Neuroprotective Against Global Ischaemia in Striatum but not Hippocampus: Histological and Voltammetric Data. *Brain Res.* **1999**, *835*, 229–240.

(313) Shekarchizadeh, H.; Ensafi, A.; Kadivar, M. Selective Determination of Sucrose Based on Electropolymerized Molecularly Imprinted Polymer Modified Multiwall Carbon Nanotubes/Glassy Carbon Electrode. *Mater. Sci. Eng., C* **2013**, *33*, 3553–3561.

(314) Pilehvar, S.; Rather, J. A.; Dardenne, F.; Robbens, J.; Blust, R.; De Wael, K. Carbon Nanotubes Based Electrochemical Aptasensing Platform for the Detection of Hydroxylated Polychlorinated Biphenyl in Human Blood Serum. *Biosens. Bioelectron.* **2014**, *54*, 78–84.

(315) Sun, D.; Zheng, X.; Yang, W.; Xie, X.; Yang, X. Electrochemical Immunosensor for CD8+ T-Cells Based on a Functionalized Multi-Walled Carbon Nanotubes-Modified Electrode. *Anal. Methods* **2013**, *5*, 5248–5252.

(316) Jain, R.; Shrivastava, S. A. Graphene-Polyaniline-Bi<sub>2</sub>O<sub>3</sub> Hybrid Film Sensor for Voltammetric Quantification of Anti-Inflammatory Drug Etodolac. *J. Electrochem. Soc.* **2014**, *161*, H189–H194.

(317) Liu, G. T.; Chen, H. F.; Lin, G. M.; Ye, P. P.; Wang, X. P.; Jiao, Y. Z.; Guo, X. Y.; Wen, Y.; Yang, H. F. One-Step Electrodeposition of Graphene Loaded Nickel Oxides Nanoparticles for Acetaminophen Detection. *Biosens. Bioelectron.* **2014**, *56*, 26–32.

(318) Yu, S.; Wei, Q.; Du, B.; Wu, D.; Li, H.; Yan, L.; et al. Label-free Immunosensor for the Detection of Kanamycin Using Ag@Fe<sub>3</sub>O<sub>4</sub> Nanoparticles and Thionine Mixed Graphene Sheet. *Biosens. Bioelectron.* **2013**, *48*, 224–229.

(319) Zeng, L.; Wang, R.; Zhu, L.; Zhang, J. Graphene and CdS nanocomposite: A facile Interface for Construction of DNA-Based Electrochemical Biosensor and its Application to the Determination of Phenformin. *Colloids Surf., B* **2013**, *110*, 8–14.

(320) Wang, M. Y.; Huang, J. R.; Wang, M. W.; Zhang, D. E.; Chen, J. Electrochemical Nonenzymatic Sensor Based on CoO Decorated Reduced Graphene Oxide for the Simultaneous Determination of Carbofuran and Carbaryl in Fruits and Vegetables. *Food Chem.* **2014**, *151*, 191–197.

(321) Eissa, S.; Ng, A.; Siaj, M.; Zourob, M. Label-Free Voltammetric Aptasensor for the Sensitive Detection of Microcystin-LR Using Graphene-Modified Electrodes. *Anal. Chem.* **2014**, *86*, 7551–7557.

(322) Wang, Z.; Han, Q.; Xia, J.; Xia, L.; Bi, S.; Shi, G.; et al. A Novel Phosphomolybdic Acid–Polypyrrole/Graphene Composite Modified Electrode for Sensitive Determination of Folic Acid. *J. Electroanal. Chem.* **2014**, *726*, 107–111.

(323) Antiochia, R.; Gorton, L. A New Osmium-Polymer Modified Screen-Printed Graphene Electrode for Fructose Detection. *Sens. Actuators, B* **2014**, *195*, 287–293.

(324) Jiang, L.; Ding, Y.; Jiang, F.; Li, L.; Mo, F. Electrodeposited Nitrogen-Doped Graphene/Carbon Nanotubes Nanocomposite as Enhancer for Simultaneous and Sensitive Voltammetric Determination of Caffeine and Vanillin. *Anal. Chim. Acta* **2014**, *833*, 22–28.

(325) Yang, G.; Zhao, F.; Zeng, B. Facile Fabrication of a Novel Anisotropic Gold Nanoparticle-Chitosan-Ionic Liquid/Graphene Modified Electrode for the Determination of Theophylline and Caffeine. *Talanta* **2014**, *127*, 116–122.

- (326) Luo, J. H.; Li, B. L.; Li, N. B.; Luo, H. Q. Sensitive Detection of Gallic Acid Based on Polyethyleneimine-Functionalized Graphene Modified Glassy Carbon Electrode. *Sens. Actuators, B* **2013**, *186*, 84–89.
- (327) Filik, H.; Çetintaş, G.; Avan, A. A.; Aydar, S.; Koç, S. N.; Boz, I. Square-Wave Stripping Voltammetric Determination of Caffeic Acid on Electrochemically Reduced Graphene Oxide–Nafion Composite Film. *Talanta* **2013**, *116*, 245–250.
- (328) Liu, L.; Gou, Y.; Gao, X.; Zhang, P.; Chen, W.; Feng, S.; et al. Electrochemically Reduced Graphene Oxide-Based Electrochemical Sensor for the Sensitive Determination of Ferulic Acid in A. Sinensis and Biological Samples. *Mater. Sci. Eng., C* **2014**, *42*, 227–233.
- (329) Li, Y.; Zhao, X.; Li, P.; Huang, Y.; Wang, J.; Zhang, J. Highly Sensitive Fe<sub>3</sub>O<sub>4</sub> Nanobeads/Graphene-Based Molecularly Imprinted Electrochemical Sensor for 17 $\beta$ -Estradiol in Water. *Anal. Chim. Acta* **2015**, *884*, 106–113.
- (330) Yola, M. L.; Eren, T.; Atar, N. A Sensitive Molecular Imprinted Electrochemical Sensor Based on Goldnanoparticles Decorated Graphene Oxide: Application to Selective Determination of Tyrosine in Milk. *Sens. Actuators, B* **2015**, *210*, 149–157.
- (331) Chen, Z.; Zhang, C.; Li, X.; Ma, H.; Wan, C.; Li, K.; Lin, Y. Aptasensor for Electrochemical Sensing of Angiogenin Based on Electrode Modified by Cationic Polyelectrolyte-Functionalized Graphene/Goldnanoparticles Composites. *Biosens. Bioelectron.* **2015**, *65*, 232–237.
- (332) Singhal, R.; Orynbayeva, Z.; Sundaram, R. V. K.; Niu, J. J.; Bhattacharyya, S.; Vitol, E. A.; et al. Multifunctional Carbon-Nanotube Cellular Endoscopes. *Nat. Nanotechnol.* **2011**, *6*, 57–64.
- (333) Loo, A. H.; Bonanni, A.; Pumera, M. Inherently Electroactive Graphene Oxide Nanoplatelets as Labels for Specific Protein-Target Recognition. *Nanoscale* **2013**, *5*, 7844–7848.
- (334) Bonanni, A.; Chua, C. K.; Zhao, G. J.; Sofer, Z.; Pumera, M. Inherently Electroactive Graphene Oxide Nanoplatelets as Labels for Single Nucleotide Polymorphism Detection. *ACS Nano* **2012**, *6*, 8546–8555.
- (335) Feng, L.; Zhang, Z.; Ren, J.; Qu, X. Functionalized Graphene as Sensitive Electrochemical Label in Target-Dependent Linkage of Split Aptasensor for Dual Detection. *Biosens. Bioelectron.* **2014**, *62*, 52–58.